

INVESTIGATING CARBON MONOXIDE (CO) CONSUMPTION IN THE MARINE  
BACTERIUM *SILICIBACTER POMEROYI* (DSS3) WITH *COXL* GENE EXPRESSION

by

Elizabeth Adair Johnson

(Under the Direction of William Miller)

ABSTRACT

The main sink for photochemically produced carbon monoxide is bacterial consumption. Understanding bacterial CO consumption is critical for evaluation of the oceanic CO cycle. *Silicibacter pomeroyi* (DSS3) is a marine bacterium that consumes CO as an energy source. Genomic analysis of *S. pomeroyi* reveals the presence of two operons encoding aerobic carbon monoxide dehydrogenase, the enzyme mediating oxidation of CO to CO<sub>2</sub>. Here we describe gene expression of the large subunit (*coxL*) in response to varying CO concentration, the CO oxidation rate of *S. pomeroyi*, and the oceanic significance of CO consumption. Gene expression was examined in *S. pomeroyi* inoculated into seawater media with and without CO. Various primer sets were designed and screened through reverse transcription polymerase chain reaction and gel electrophoresis. An oxidation rate was calculated based on cell numbers and the consumption of CO over time. Bacterial impact on oceanic [CO] was modeled based on this CO oxidation rate constant. Initial results suggest that expression of *coxL* by *S. pomeroyi* may be constitutive.

INDEX WORDS: Carbon Monoxide Oxidation, *Silicibacter pomeroyi*, Marine Photochemistry, CoxL, Gene Expression

INVESTIGATING CARBON MONOXIDE (CO) CONSUMPTION IN THE MARINE  
BACTERIUM *SILICIBACTER POMEROYI* (DSS3) WITH *COXL* GENE EXPRESSION.

by

ELIZABETH ADAIR JOHNSON

B.A., Wake Forest University, 2004

A Thesis Submitted to the Graduate Faculty of The University of Georgia in Partial Fulfillment of  
the Requirements for the Degree

MASTER OF SCIENCE

ATHENS, GEORGIA

2007

© 2007

Elizabeth Adair Johnson

All Rights Reserved

INVESTIGATING CARBON MONOXIDE (CO) CONSUMPTION IN THE MARINE  
BACTERIUM *SILICIBACTER POMEROYI* (DSS3) WITH *COXL* GENE EXPRESSION.

by

ELIZABETH ADAIR JOHNSON

Major Professor: William Miller  
Committee: Mary Ann Moran  
Patricia Yager

Electronic Version Approved:

Maureen Grasso  
Dean of the Graduate School  
The University of Georgia  
August 2007

## DEDICATION

For my grandmother, Adele Johnson, who loved the ocean.

## ACKNOWLEDGEMENTS

I would like to thank all of those who have helped me along the way. Thank you to Drs. William Miller, Mary Ann Moran, and Patricia Yager for all of their guidance and suggestions; to the entire Moran lab for countless hours of teaching me how to be a microbiologist, especially Erin Beirs, Erinn Howard, Wendy Ye, and Helmut Bürgmann; to the Miller lab for teaching me how to be a chemical oceanographer, especially Cedric Fichot and Heather Reader; and to my parents, Neil and Beth Johnson, for their constant support.

## TABLE OF CONTENTS

	Page
ACKNOWLEDGEMENTS.....	v
LIST OF TABLES.....	viii
LIST OF FIGURES.....	ix
CHAPTER	
1 INTRODUCTION.....	1
1.1 Marine Carbon Monoxide Measurements.....	2
1.2 Photochemical Carbon Monoxide Production.....	4
1.3 Bacterial CO Consumption.....	8
1.4 Genetics of Carbon Monoxide Oxidation.....	9
1.5 <i>Silicibacter pomeroyi</i> .....	9
1.6 Global Cycling of CO and Microbial CO Oxidation.....	13
1.7 Thesis Objectives.....	16
2 METHODS.....	17
2.1 General Information.....	17
2.2 Bacterial Growth.....	17
2.3 CO Kettle Incubations.....	18
2.4 Gas Chromatography.....	21
2.5 Preparing RNA for Gene Expression Analysis.....	29
2.6 Bacterial Counts Using DAPI.....	33
3 RESULTS.....	35
3.1 Measurements of Carbon Monoxide Concentration.....	35
3.2 CO Oxidation by <i>Silicibacter pomeroyi</i> .....	35

3.3	DAPI Bacterial Counts .....	44
3.4	Carbon Monoxide Oxidation Rate.....	44
3.5	Optimization of Temperature Gradients for Designed Primers .....	47
3.6	<i>coxL</i> Gene Expression in <i>Silicibacter pomeroyi</i> .....	51
3.7	Impact of <i>Silicibacter pomeroyi</i> on Marine CO Concentration .....	64
4	DISCUSSION .....	72
4.1	CO Oxidation by <i>Silicibacter pomeroyi</i> .....	72
4.2	CO Oxidation Rate .....	72
4.3	<i>coxL</i> Gene Expression in <i>Silicibacter pomeroyi</i> .....	73
4.4	Modeled Impact of CO Oxidizing Bacteria.....	76
5	CONCLUSION .....	78
5.1	Concluding Statements .....	78
5.2	Future Research.....	79
	REFERENCES .....	80
	APPENDICES.....	85
A	Extended Materials and Methods .....	85
B	Calculating the Carbon Monoxide Concentration in Water.....	98
C	Calculating the Bunsen Coefficient for Carbon Monoxide .....	100
D	Calculating Bacterial Cells from DAPI Counts.....	101
E	Calculating the Cell Normalized CO Oxidation Rate.....	102

## LIST OF TABLES

	Page
Table 1.1: Estimated global CO Sea to air fluxes in units of tera grams CO per year.....	3
Table 2.1: Typical variation in standard CO gas samples.....	26
Table 2.2: Primer sets used to amplify the <i>coxL</i> genes.....	30
Table 2.3: Degeneracy table of base pairs used in primer design.....	32
Table 3.1: Control experiments for CO oxidation by <i>Silicibacter pomeroyi</i> .....	36
Table 3.2: Control experiments for CO oxidation by <i>Silicibacter pomeroyi</i> .....	37
Table 3.3: Experiments for CO oxidation by <i>Silicibacter pomeroyi</i> .....	40
Table 3.4: Experiments for CO oxidation by <i>Silicibacter pomeroyi</i> .....	42
Table 3.5: DAPI bacterial counts performed with fluorescence microscopy.....	45
Table 3.6: Carbon monoxide oxidation rate by <i>S. pomeroyi</i> .....	46
Table 3.7: Carbon monoxide oxidation rate calculated per cell of <i>S. pomeroyi</i> .....	49
Table 3.8: CO Impact model.....	67

## LIST OF FIGURES

	Page
Figure 1.1: The upper ocean carbon cycle.....	6
Figure 1.2: Average headspace consumption of CO by cultures of <i>S. pomeroyi</i> .....	10
Figure 1.3: Phylogenetic tree of 16S rRNA gene sequences.....	12
Figure 1.4: Neighbor-joining phylogenetic analysis for the CoxL sequences. ....	14
Figure 2.1: Flow chart of the methods. ....	19
Figure 2.2: Schematic of the kettle container. ....	20
Figure 2.3: Diagram of the SRI Gas Chromatograph.....	22
Figure 2.4: Schematic of the valve in “Load”.....	23
Figure 2.5: Schematic of the valve in “Inject”.....	24
Figure 2.6: Typical standard curve for CO.....	27
Figure 3.1: Kettle Reaction bubble with CO free Schutze Air in Controls 1 & 2. ....	39
Figure 3.2: Kettle reaction bubbled with CO for Experiments 1 & 2.....	43
Figure 3.3: Carbon monoxide oxidation rate by <i>S. pomeroyi</i> .....	48
Figure 3.4: Temperature gradients with the first primer set.....	50
Figure 3.5: Temperature gradient with the second primer set.....	52
Figure 3.6: Control 1 CO-free air. ....	53
Figure 3.7: Control 1 CO-free air. ....	54
Figure 3.8: Control 2 CO-free air. ....	56
Figure 3.9: Control 2 CO-free air. ....	57
Figure 3.10: Experiment 1 with elevated CO.....	59

Figure 3.11: Experiment 1 with CO.....	60
Figure 3.12: Experiment 1 with CO, CoxL1 and CoxL 2. ....	62
Figure 3.13: Experiment 2 with CO, CoxL1 and CoxL 2. ....	63
Figure 3.14: Colored dissolved organic matter and apparent quantum yield spectra. ....	66
Figure 3.15: CO Photoproduction vs. Bacterial Consumption. ....	68
Figure 3.16: CO Photoproduction vs. Bacterial Consumption. ....	69

## CHAPTER 1

### INTRODUCTION

Carbon monoxide concentrations in the ocean are in a constant flux through a cycle of photochemical production and microbial consumption. Important marine microbial CO consumers belong to the Roseobacter clade. *Silicibacter pomeroyi* is a cultured member of the Roseobacter clade that appears to utilize CO as an energy source by oxidizing it to carbon dioxide (Moran, 2004). Limited information exists about the processes and reasons behind the use of carbon monoxide as an energy source by marine bacteria. It is thought that the supplemental energy gained by *S. pomeroyi* and other Roseobacters is a strategy for coping with a nutrient poor ocean (Moran, 2004). CO consumption by marine heterotrophs is significant, however with microbial activity by Silicibacter-like lithoheterotrophs representing a microbial CO sink in the surface ocean with CO representing a significant source of metabolized carbon (King, 2003; Moran, 2004). This sink may represent an important part of the global carbon cycle, providing a rationale for further investigation of microbial CO consumption.

Here I specifically examine the gene expression of the large subunit of the carbon monoxide dehydrogenase (*coxL*) in *S. pomeroyi*. These studies address the regulation of CO oxidation activity in this model organism, and specifically whether gene expression is constitutive or turned on and off by some environmental or physiological regulator. Because CO concentrations in ocean surface waters vary on a diel basis, I specifically tested CO concentration as a possible regulatory mechanism for gene expression.

## 1.1 Marine Carbon Monoxide Measurements

Carbon monoxide (CO), an important gas in atmospheric chemistry, exists at supersaturated concentrations in the oceans' surface waters. This supersaturation with respect to the partial pressure of carbon monoxide in the atmosphere forms a concentration gradient that results in a net flux of CO from the ocean into the atmosphere (Swinnerton, et al., 1970; Erickson, 1989). Consequently, the ocean may be the largest known natural global source of carbon monoxide with an estimated flux of 15-80 Tg CO y<sup>-1</sup> (Table 1.1) (Swinnerton, et al., 1970; Zafiriou, et al., 2003).

Although CO is not a greenhouse gas, it has an important effect on the radiative balance of the atmosphere through its enhancement of the buildup of methane, ozone, and other radiatively important trace gases (Valentine and Zepp, 1993). CO is also a useful tracer key for constraining multiprocess surface ocean models that integrate photochemistry, biology, gas exchange, optics, and mixing to test our understanding of mixed layer processes (Zafiriou, et al 2003).

Because CO is readily exchanged between the ocean and atmosphere, the simultaneously occurring processes of production and loss control CO concentration in surface water of the oceans (Conrad, et al., 1982). CO concentrations have been shown to exhibit a maximum in the early afternoon and a minimum in the morning, correlating with the pattern of solar radiation intensity. In the water column of the equatorial Pacific, CO concentration decreased as depth increased, approaching a constant low concentration in waters below 70 m (Ohta, 1997). Due to the marked diurnal variations in CO concentrations in surface waters, *in situ* biological CO oxidation by marine bacteria was thought to be controlled by CO consumers (Conrad, and Seiler, 1980; Swinnerton, et al., 1970). It was thought that in areas of low production where microbial

Table 1.1: Estimated global CO Sea to air fluxes in units of tera grams CO per year.

<b>Table 1.1 Marine Carbon Monoxide Sea to Air Flux Estimates (Tg CO y<sup>-1</sup>)</b>		
<b>Region</b>	<b>Value</b>	<b>References</b>
Global	9	<i>Swinnerton et al. [1970]</i>
Global	10-120	<i>Seiler [1978]</i>
Global	10-180	<i>Conrad et al. [1982]</i>
N. and S. Atlantic	4.3-47	<i>Conrad et al. [1982]</i>
Global	165±80	<i>Erickson[1989]</i>
N. and S. Atlantic	71±34	<i>Erickson[1989]</i>
Global	15-80	<i>Zafiriou et al. [2003]</i>

processes proceed slowly, such as the Sargasso Sea, the CO removal process is driven largely by the air-sea exchange. In areas of high production, the oxidation of CO by microbial activity is the driving force in CO removal (Ohta, 1997). A time lag of 2-3 hours has also been noted for these diurnal patterns. Conrad et al., [1982] contributed this time lag to a reaction mechanism of CO production in which the reaction is initiated by light and releases CO through multi-step photosensitized or photochemical reactions over a period of time. These diurnal variations and productive/consumptive processes work to vary the overall CO concentration in the world's oceans.

The concentration of dissolved CO in the open ocean's surface waters has been found to range widely from maximum values of 4-5 ppm to minimum values of 0.07-0.10 ppm (Conrad, et al., 1982). Other measurements of dissolved CO concentrations typical of sunlit coastal surface waters average 12 ppm, while open ocean surface waters for the Atlantic and Pacific average less than 2 ppm (Jones and Amador 1993 and Zafiriou, et al., 1993). For example Jones and Amador [1993] found that surface CO concentrations ranged from 0.9 nM near the Mona Passage (open ocean) to 4.9 nM near the mouth of the Orinoco River (coastal) during the spring. Although reported as both parts per million (ppm) and nanomolar (nM) in field and lab studies, CO concentrations can be readily interconverted with 1.21 ppm being equivalent to 0.97 nM.

## **1.2 Photochemical Carbon Monoxide Production**

Since surface waters are typically supersaturated with CO, there must be a source in the ocean to create such high concentrations. Originally the source was thought to be biological, however research by Conrad et al, [1980] dispelled this theory and photochemistry was suspected to be the source. Now it is known that CO in the ocean is produced through

photochemical reactions, specifically from the photooxidation of dissolved organic material (DOM) (Conrad and Seiler, 1980). Photochemical degradation of marine DOM gives rise to gaseous species including carbon monoxide, COS, and CO<sub>2</sub> as well as non-gaseous low molecular weight (LMW) carbonyl compounds (Mopper and Kieber, 2000). CO is one of the more abundant photoproducts of DOM and is produced at rates greater than any of the LMW compounds (Mopper et al., 1991). Carbon dioxide is produced about 15-20 times faster than CO but is not available for heterotrophic microbial use, leaving CO as the most abundant microbial substrate produced from photochemistry.

The first law of photochemistry, attributed to Grotthus and Draper in the early 1800's, states that for a photochemical reaction to take place a chemical substance must absorb light (Miller, 1999). Simply stated, if no light is absorbed, then no photochemistry occurs. The absorption of sunlight by humic substances initiates photochemical reactions in natural waters that impact the ocean carbon cycle. Traditionally, physical and biological processes such as air-sea CO<sub>2</sub> exchange, surface mixing, deep seawater venting, carbon fixation, respiration, calcium carbonate formation, and sedimentation are thought to be the most important factors affecting the carbon cycle in the ocean (Mopper and Kieber, 2000). Recent studies have shown that photochemical processes at the ocean's surface also strongly impact the carbon cycle (Figure 1.1).

Evidence that CO is produced from photochemistry is that CO has been observed to increase in sterile controls (without cells) that were incubated in the light, suggesting that these gases might be produced from dissolved organic carbon (DOC) (Wilson, et al., 1970). Ohta

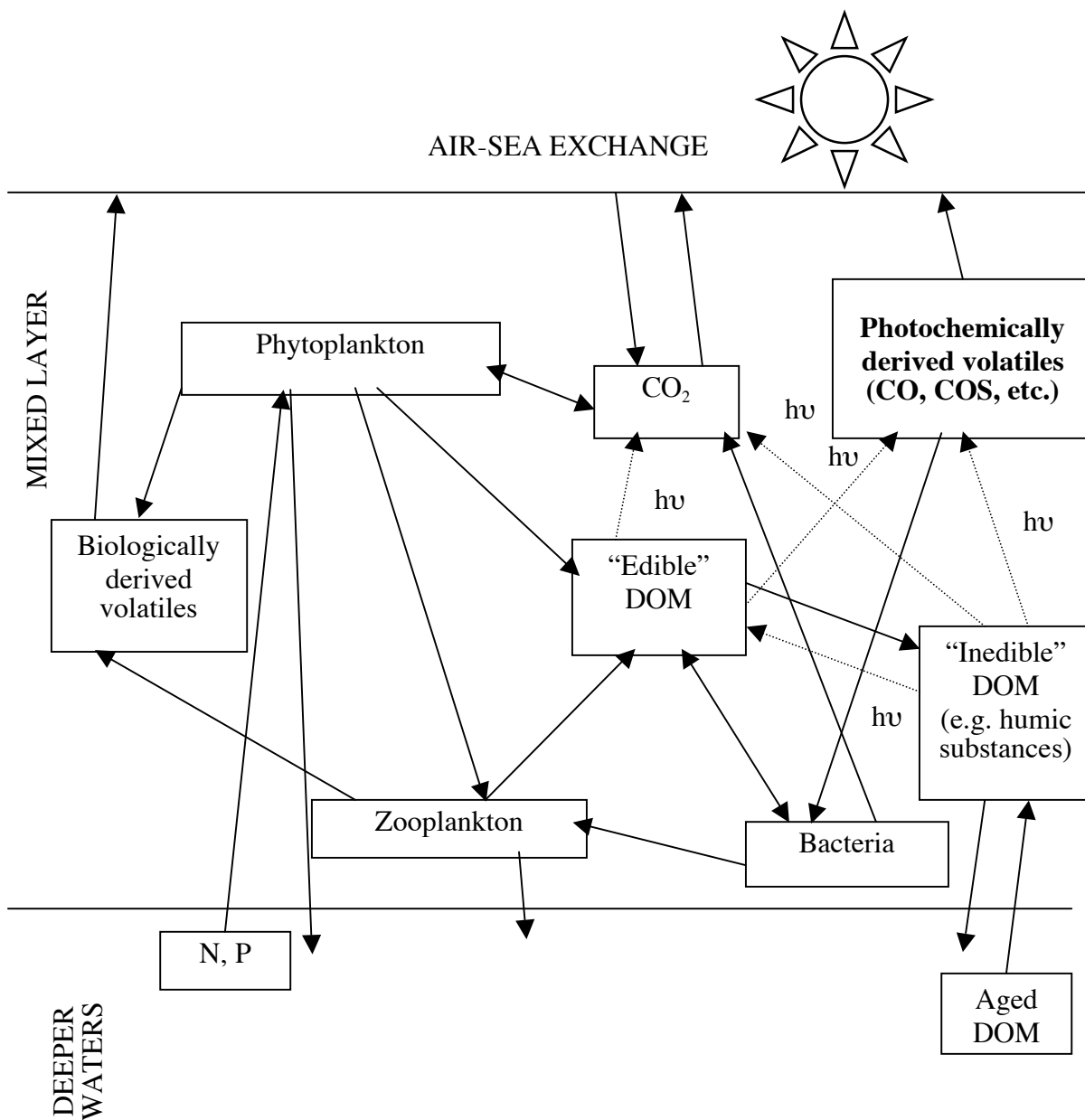


Figure 1.1: The upper ocean carbon cycle. The traditional view of the carbon cycle is shown along with a reservoir of photochemically produced DOM (adapted from Mopper and Kieber, 2000).

[1997] also made an observation in which CO concentrations revealed marked diurnal variations with patterns resembling those of solar radiation. This supports the conclusion that CO production is dependent on light intensity and led to the proposal that CO was a photochemical product formed in seawater when sunlight oxidizes marine dissolved organic matter (Zafiriou et al., 2003).

Photochemical processes play a number of important roles in biogeochemical cycles involving dissolved organic matter (DOM) in natural waters, affecting water optical properties, biological processes, and trace element distributions (Miller and Moran, 1997). Larger molecules are degraded by exposure to sunlight into smaller photoproducts. When DOM absorbs sunlight, the average molecular weight (MW) is reduced and many photoproducts form (Moran and Zepp, 1997). The smaller photoproducts fall into four categories 1) low-molecular-weight organic compounds (e.g. carbonyl compounds with a MW of <200); 2) carbon gases (e.g. CO); 3) unidentified bleached organic matter; and 4) nitrogen and phosphorus-rich compounds (e.g.  $\text{NH}_4^+$  and  $\text{PO}_4^{3-}$ ).

These smaller photoproducts are then removed from the DOM pool by direct volatilization of carbon gases (carbon monoxide and dissolved inorganic carbon) and through microbial consumption of labile photoproducts (Miller and Moran 1997). Carbon monoxide and dissolved inorganic carbon (DIC) make up the dominant gaseous photoproducts. Photochemical degradation of DOM has important effects on the biological productivity in many carbon or nitrogen-limited aquatic ecosystems (Moran and Zepp 1997). In addition to the production of CO by photochemical reactions, microorganisms such as green algae may also produce CO, but the more significant role of microorganisms is as a carbon monoxide consumer (Conrad, R. and W. Seiler 1980).

### 1.3 Bacterial CO Consumption

Microbial consumption of CO by various forms of marine bacteria is an important process for the balance of the carbon monoxide cycle (Conrad and Seiler, 1980). Accordingly, consumption rates in seawater should depend on bacterial population density, species composition, supply of organic substrates and inorganic nutrients, temperature, and pH (Xie, et al., 2005). *Silicibacter*-like lithoheterotrophs are some of these CO consumers, and might act as a significant microbial sink in the surface ocean (Moran, 2004).

The open ocean is considered one of the most extreme environments for marine organisms with respect to permanently low nutrient concentrations (Hirsch et al., 1979). In such an oligotrophic environment, marine Roseobacters like *S. pomeroyi* have had to develop a strategy for coping with limited nutrient availability. The growth-limiting nutrients for many oligotrophic microbes are organic carbon substrates that provide an energy and/or carbon source. Carbon monoxide is one example of a constant but very low source of oxidizable carbon (Conrad and Seiler, 1982). Different microorganisms and modes of metabolism may be involved in the consumption of low CO concentrations (Conrad and Seiler, 1982). The possible mode that *S. pomeroyi* employs is specific (utilitarian, profitable) meaning they gain an advantage from the oxidation of CO for growth or maintenance. The advantage may be the profitable use of CO as an additional energy source or as an additional electron donor allowing the microorganism to attain a higher growth yield on other organic substrates (Conrad and Seiler, 1982).

## 1.4 Genetics of Carbon Monoxide Oxidation

Carbon monoxide dehydrogenase (CODH) is the key enzyme for the oxidation of carbon monoxide. The CODHs of aerobic organisms are O<sub>2</sub> –stable, three-subunit hydroxylases, often CO inducible, that catalyze the oxidation of CO to CO<sub>2</sub> (Kerby, et al., 1992). The three non-identical subunits (*CoxL*, *CoxM*, and *CoxS*) are named for the large, medium, and small size of the protein subunits (Kang and Kim, 1999). The redox reaction equation of the oxidation of carbon monoxide to carbon dioxide is:



Two operons encoding aerobic carbon monoxide dehydrogenase are present in and at least one is shown to function in the *S. pomeroyi* genome (*coxSML*) (Moran, 2004). Genetic evidence for CO oxidation has been found in six of the major *Roseobacter* sub-lineages thus far.

Consumption of CO in the headspace of *S. pomeroyi* cultures was measured by Moran et al. [2004] to demonstrate CO oxidation by the bacterium (Figure 1.2). Initial headspace CO concentrations were approximately 10 ppm and subsequently drawn down exponentially by *S. pomeroyi* to ~ 0.13 ppm after 50 hrs. of incubation. This drawdown experiment shows that *S. pomeroyi* can consume/oxidize CO.

## 1.5 *Silicibacter pomeroyi*

*Silicibacter pomeroyi* (DSS3) is a gram-negative, rod-shaped aerobic bacterium that provided the first genome sequence from any major heterotrophic marine bacteria clade (Moran et al., 2004). The genome consists of a chromosome (4,109,422 base pairs) and megaplasmid

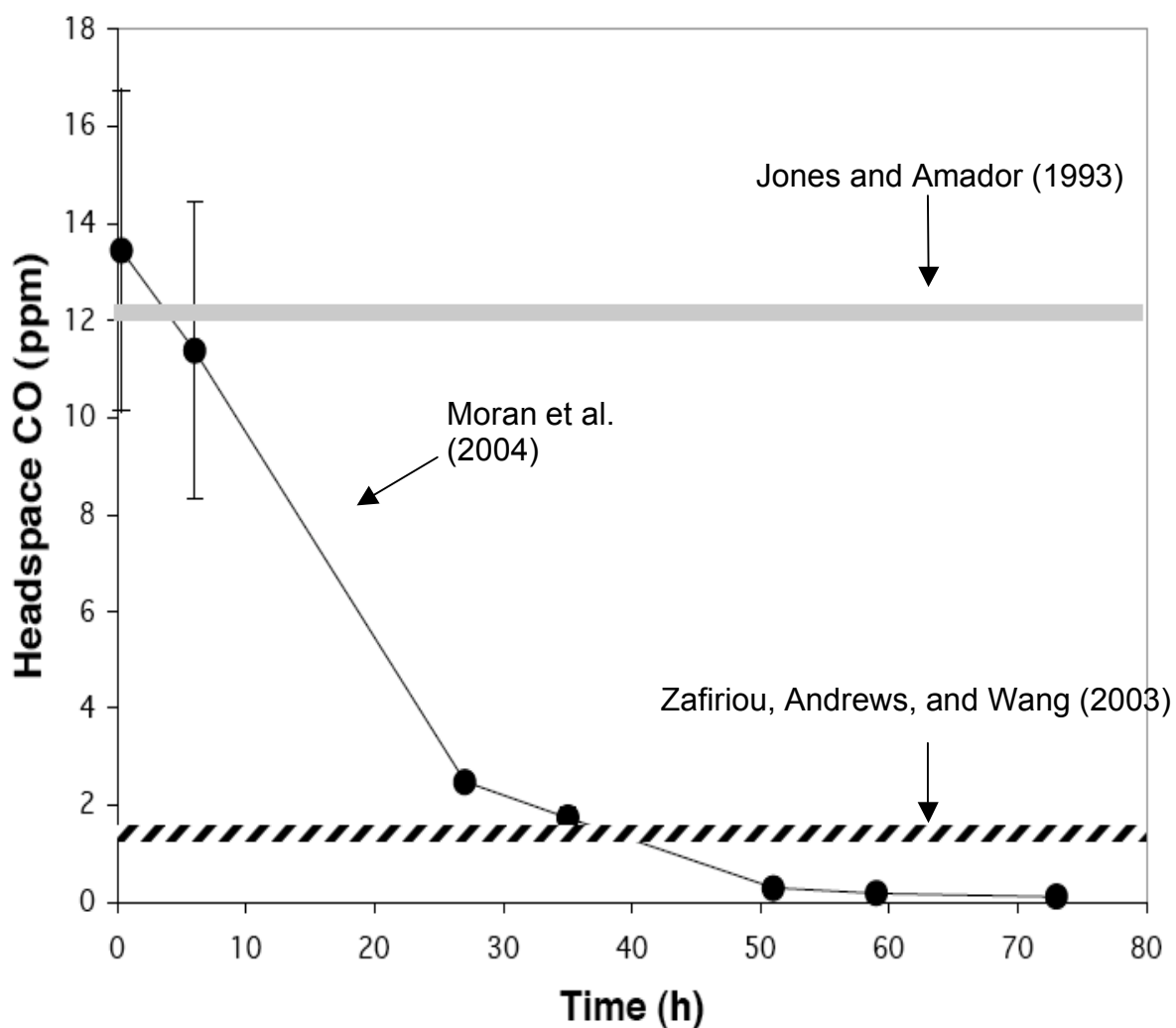


Figure 1.2: Average headspace consumption of CO by cultures of *S. pomeroyi* determined by Moran et al. (2004). Measurements of CO concentration in the coastal ocean surface waters determined by Jones and Amador (1993). Measurements of open ocean surface water determined by Zafiriou, Andrews, and Wang (2003). Headspace CO concentrations are equivalent to equilibrium dissolved CO concentrations typical of sunlit coastal ocean surface waters and of open ocean surface waters. This figure is taken from Moran et al., 2004 and slightly modified.

(491,611 base pairs). *S. pomeroyi*, as a member of the marine Roseobacter clade (Figure 1.3), represents an important group of bacteria, comprising 10-20% of coastal and oceanic mixed-layer bacterioplankton. The *Roseobacter* clade is one of the major marine groups and is well represented across diverse marine habitats, from coastal to open oceans and from sea ice to sea floor (Buchan et al., 2005). While exploring the physiologies of the *Roseobacter* clade, some of the members including *S. pomeroyi* were implicated in the consumption of carbon monoxide. Evidence that clade members are participating in biological CO oxidation in the ocean includes the demonstration that strains can oxidize CO in culture and that *S. pomeroyi* harbors two CO oxidation (*cox*) operons in its genome. The presence of CO dehydrogenase genes in the genome suggests that Roseobacters may utilize CO as a source of energy, but not as a carbon source for biomass (Moran et al., 2004). *S. pomeroyi* has been shown to oxidize CO at concentrations typically measured in coastal and open ocean surface waters (12 nM and 2 nM, respectively) (Jones and Amador 1993 and Zafiriou, et al., 1993). It differs from previously characterized non-marine CO oxidizers in that it does not grow autotrophically and instead uses CO as a supplementary energy source during heterotrophic growth (Moran 2004). Members of the *Roseobacter* clade shown to oxidize CO to CO<sub>2</sub>, including *S. pomeroyi*, respire organic substrates resulting in the release of CO<sub>2</sub> counter to the traditional “CO<sub>2</sub> sink” of the upper oceans (Swingley, 2007). Members of this widespread lineage that oxidize CO may therefore influence the global carbon cycle (Buchan, 2005).

CO dehydrogenase genes (*cox*) analyzed by King [2003] using amino acid sequences for the *coxL* gene were found to make up two closely related but phylogenetically distinct clades,

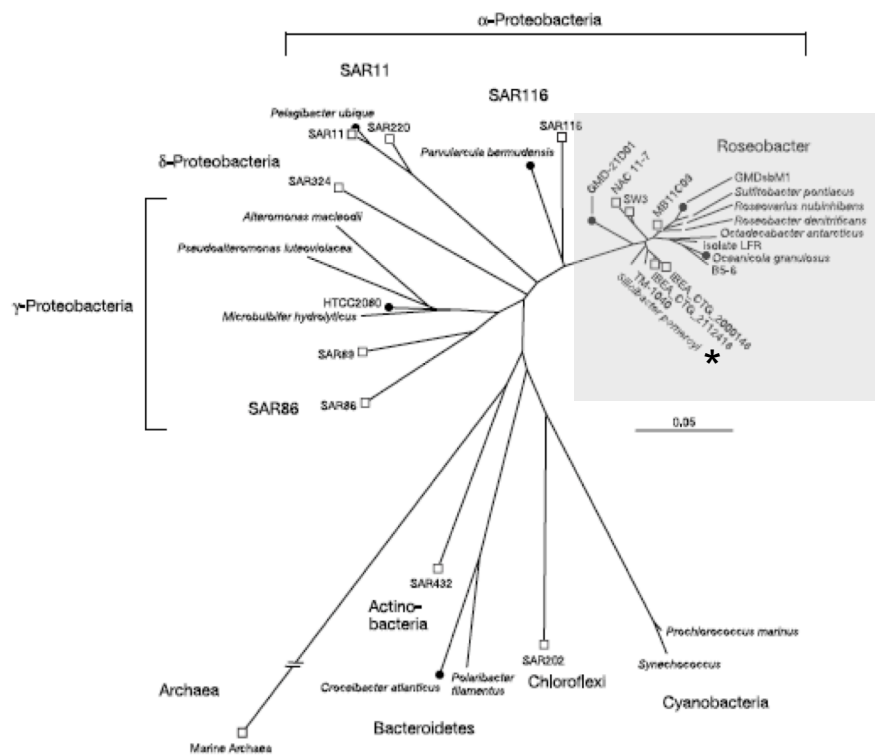


Figure 1.3: Phylogenetic tree of 16S rRNA gene sequences from typical marine bacterial groups. Shows the members of the Roseobacter clade including *Silicibacter pomeroyi* (from Moran et al., 2004). The asterisk indicates the location of *S. pomeroyi* on the tree.

OMP and BMS (Figure 1.4). The OMP clade contains several well-known carboxydrotrophs plus newly identified CO oxidizers. Carboxydrotrophic bacteria constitute a small but diverse group of aerobes, primarily within the  $\alpha$ -*Proteobacteria*, that utilize CO as sole carbon and energy sources at high concentrations while expressing relatively low- affinity CO uptake systems. The BMS clade contrastingly is dominated by newly documented CO oxidizers and characterized by putative *coxL* for which inferred amino acid sequences are about 70% similar to OMP sequences (King 2003). While some isolates contain only BMS or OMP genes, several contain both, including *S. pomeroyi*. The *coxL1* gene of *Silicibacter pomeroyi* falls under the BMS clade of previously unidentified CO oxidizers while the *coxL2* gene falls under the OMP clade of previously known CO oxidizers. Each sequence is roughly 2400 bp and is found on the *S. pomeroyi* chromosome. The co- occurrence of BMS and OMP *coxL* sequences raises questions about the expression and physiological and ecological roles of CO dehydrogenases. Whether both are expressed in the same organism and under what conditions are not known. However, a combination of BMS and OMP *coxL* may affect whole-cell affinities for CO (King, 2003).

## 1.6 Global Cycling of CO and Microbial CO Oxidation

Examining the global emissions of CO to the atmosphere, Khalil and Rasmussen [1990] estimated the annual input to be about  $2,600 \pm 600$  Tg. They attribute ~60% to be from anthropogenic activities such as the burning of fossil fuels and oxidation of hydrocarbons and ~40% to be from natural processes (primarily the oxidation of hydrocarbons but also from plants and the oceans; Khalil and Rasmussen, 1990). Major atmospheric CO sinks are believed to be

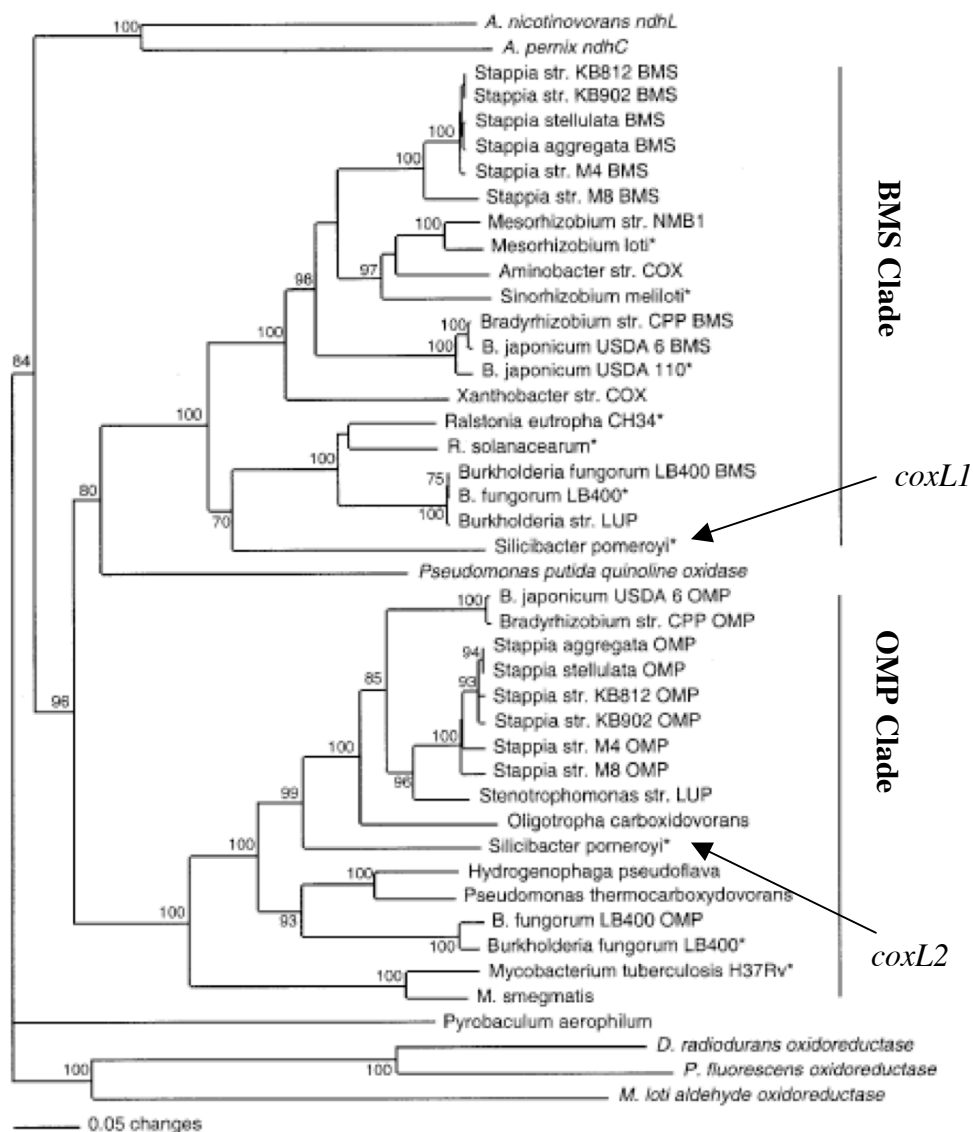


Figure 1.4: Neighbor-joining phylogenetic analysis for the *CoxL* sequences (from King, 2003). The analysis, based on for the amino acid sequences, divides into two clades, BMS and OMP. *S. pomeroyi* has two *coxL* genes that lie in each clade. The clade separation of *coxL1* and *coxL2* is indicated on the figure.

reactions with OH radicals removing CO from the atmosphere and balancing the flux in the global cycle of carbon monoxide. A small increase of CO concentration of 1% per year attributed to human activities, however, is causing an imbalance in the CO flux (Khalil and Rasmussen 1990). This increase, though slight, may have larger implications for the global CO cycle and indirect effects on global climate and atmospheric chemistry.

Zafiriou et al. [2003] balanced the marine CO sources and sinks to confirm the global ocean estimate of CO flux. In looking at the source of photochemical production and microbial consumption, Zafiriou et al. [2003] assumed that a balance exists in which the sum of the current known CO sources is approximately equal to the sum of the CO sinks. These findings led them to conclude that the global marine CO flux to the atmosphere is within the range of ~15-80 Tg CO y<sup>-1</sup>.

CO consumption by marine heterotrophs like *S. pomeroyi* is significant because microbial activity represents an important CO sink in the oceans and because CO may represent a significant source of metabolized carbon (King, 2003). Should substantial oceanic CO be released to the atmosphere in regions far from fossil fuel and CH<sub>4</sub> oxidation sources, the oceanic CO flux may be intimately tied to the tropospheric cycles of ozone, OH, CO<sub>2</sub>, and related climate reactive compounds (Erickson, 1989). Recent oceanographic studies have further implied that CO may occupy a key position in oceanic carbon cycling as an intermediate in the photochemical mineralization of marine DOM that is otherwise resistant to direct biological decomposition (Zuo, and Jones, 1995).

## 1.7 Thesis Objectives

The purpose of this study was to better understand the fate of photochemically produced CO due to bacterial utilization in the ocean. This was accomplished through the examination of seawater [CO] and the cellular process of microbial CO consumption using a representative marine bacterium, *Silicibacter pomeroyi*. The potential regulator for CO gene expression explored in this study was carbon monoxide concentration. The specific objectives of this thesis were to determine if *coxL* was constitutively expressed in the model organism *S. pomeroyi* or if seawater [CO] regulated gene expression. Because of the two apparent *cox* operons, I also investigated differences in expression between the *coxL1* and *coxL2* CO genes of *S. pomeroyi*. Based on CO drawdown experiments, I calculated a CO oxidation rate and cell-normalized rate constant for this organism. This rate constant was used as the basis for a simple model to examine the potential impact of organisms with similar physiologies to *Silicibacter pomeroyi* on oxidation of coastal oceanic [CO].

## CHAPTER 2

### METHODS

#### 2.1 General Information

Sampling and bacterial growth was carried out between May 2005 and March 2007. The bacterium used during this research was *Silicibacter pomeroyi* strain DSS-3. *S. pomeroyi* is a marine bacterium that was isolated from the coast of Georgia in 1998. Cultured isolates of *S. pomeroyi* were obtained from Dr. Mary Ann Moran. For an extended description of the methods see Appendix A.

#### 2.2 Bacterial Growth

*Silicibacter pomeroyi* were inoculated on plates with ½ YTSS medium consisting of 1.25g tryptone, 2g yeast extract, 10g sea salts, 7.5g agar, and 500 ml Deionized (DI) H<sub>2</sub>O. The inoculated plates were incubated at 30°C for 2-3 days. A single cell colony of *S. pomeroyi* was taken from the agar plate and inoculated into 10 ml ½ liquid YTSS growth medium (See above; agar was omitted). The inoculated ½ liquid YTSS was incubated overnight at 30°C in a shaking incubator. It was then used to inoculate 1000 ml of Marine Basal Media (MBM). The MBM was prepared from four separate recipe stocks and combined after autoclaving and sterile filtration. FeEDTA Stock Solution was prepared with 50 mg FeEDTA (Ethylenediamine tetraacetic acid; ferric-sodium salt, Sigma) and 100 ml DI H<sub>2</sub>O. The Basal Medium was prepared with 150 ml 1M Tris HCl buffer (pH 7.5), 87 mg K<sub>2</sub>HPO<sub>4</sub>, 1.5 g NH<sub>4</sub>Cl, and 375 ml DI

H<sub>2</sub>O. For the Sea Salt Stock Solution 20 g of Sigma Sea Salts were combined with 700 ml DI H<sub>2</sub>O. The three solutions were combined as follows: 700 ml Sea Salt Solution, 250 ml Basal Media, 50 ml FeEDTA stock, 1  $\mu$ M glucose (as a carbon substrate), and 0.1% vitamin supplement. The vitamin supplement contained (per 100 ml) 2 mg biotin, 2 mg folic acid, 10 mg pyridoxine-HCl, 5 mg riboflavin, 5 mg thiamine, 5 mg nicotinic acid, 5 mg pantothenic acid, 0.1 cyanocobalamin, and 5 mg p-aminobenzoic acid. The carbon substrate was added by sterile filtration after the medium was autoclaved. The MBM was incubated overnight in a shaker incubator at 30°C.

### **2.3 CO Kettle Incubations**

Carbon monoxide drawdown was examined using a sealed 2000 ml Pyrex® glass reaction kettle (Figure 2.1). Its cover had four openings that held a thermometer, repipet dispenser, bubbling stick, and CO-free air vent. Cover and kettle were clamped together to form a gas tight seal. Room air was pumped through polyethylene drying tubes filled with Leco® Schutze Reagent to create CO-free air and driven through a three-valve flowmeter for mixing with a 51.8 ppm  $\pm$  5% Scotty® Specialty Gases CO tank. Mixed gas from the flowmeter was directed through a DI water humidifier flask and into the reaction kettle. The reaction kettles were allowed to reach equilibrium and set up either with or without cultures of *Silicibacter pomeroyi* in Marine Basal Medium (Figure 2.2). To remove CO from the MBM CO-free air was bubbled through the kettle for a minimum of 90 minutes. After initial experiments, the CO drawdown

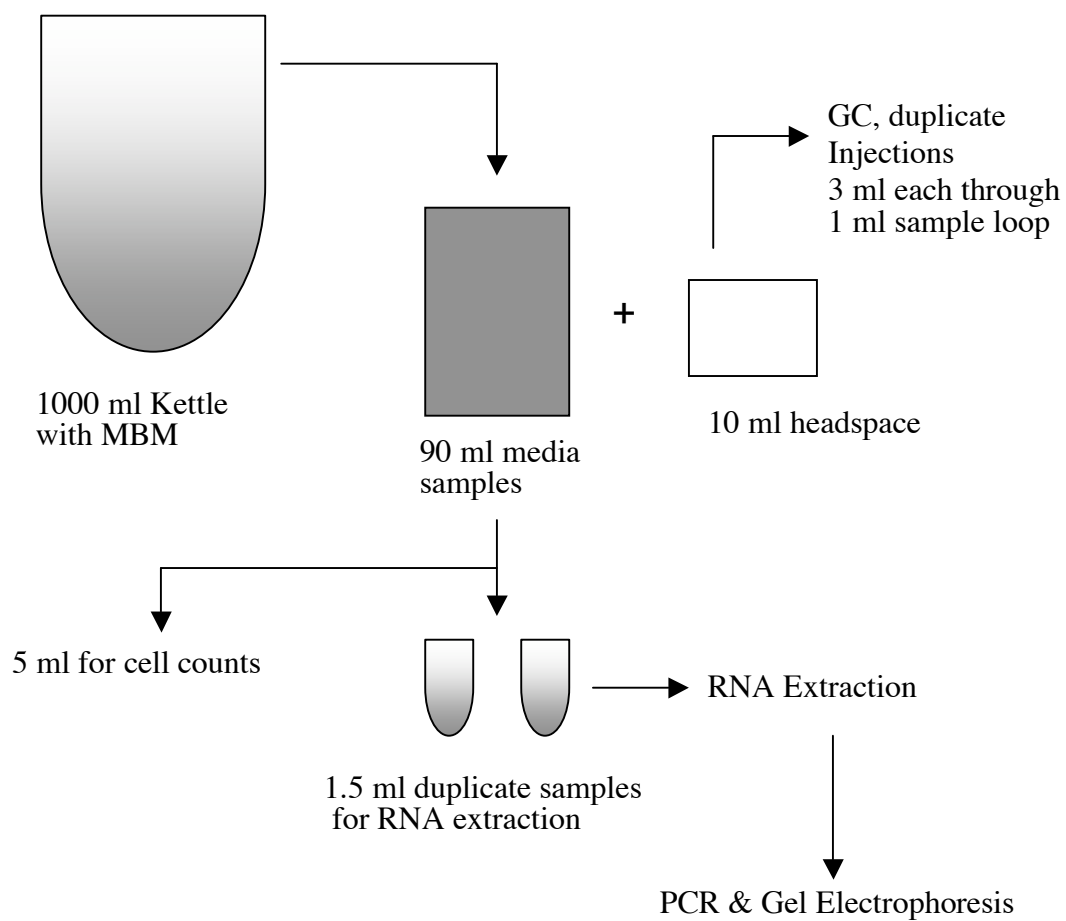


Figure 2.1: Flow chart of methods. The chart shows the steps and volumes from the kettle reaction, headspace injections into the GC, bacterial samples for RNA extraction, PCR, and gel electrophoresis.

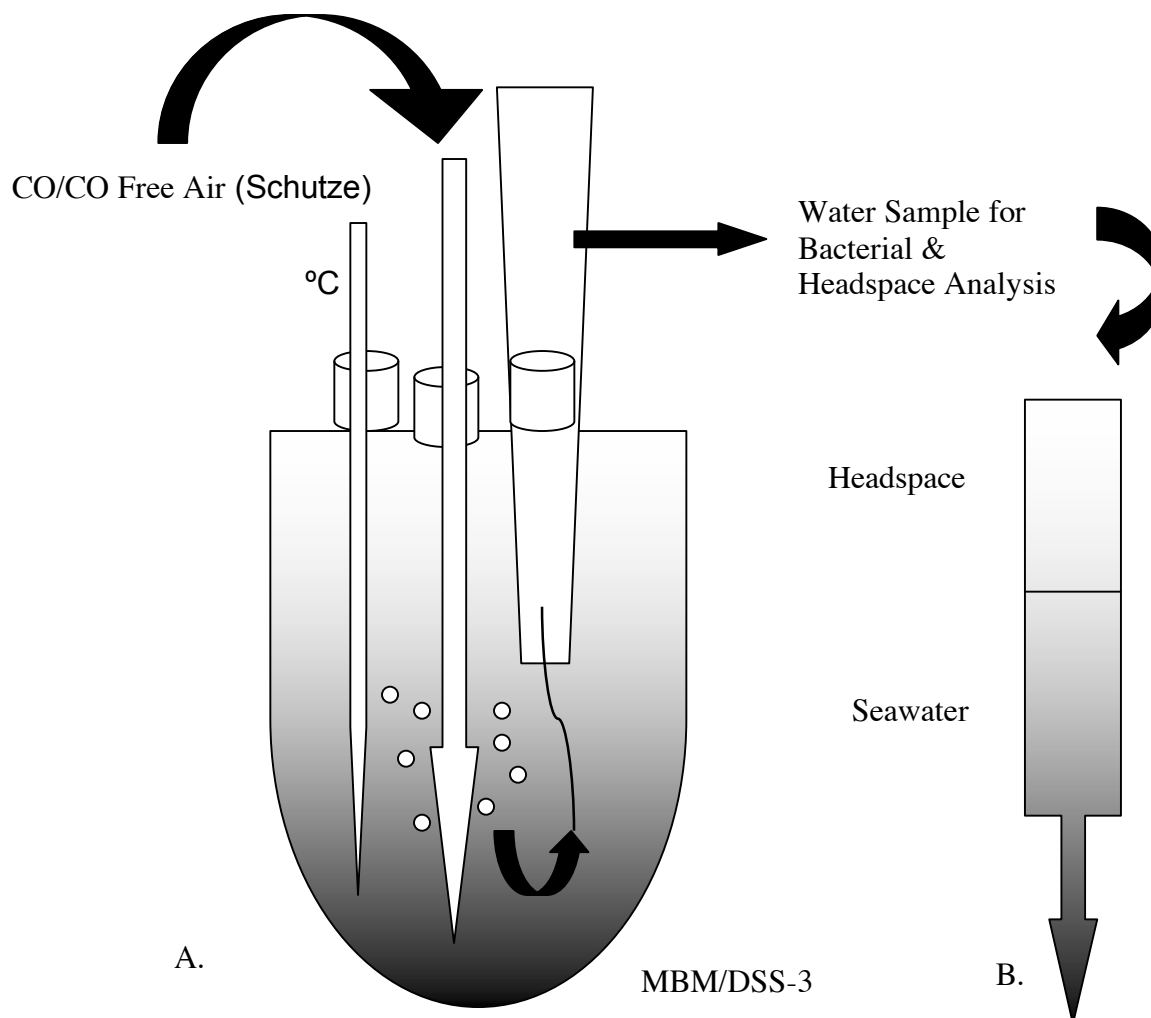


Figure 2.2: Schematic of the kettle container. Either CO or CO-free air was bubbled into the kettle. The temperature was monitored throughout each experiment, an air mixture was bubbled through a bubbling stick in the middle of the container, and media/bacteria samples were drawn off with a dispensing pipettor.

method was modified so that *S. pomeroyi* was grown up in identical conditions in 1000 ml of MBM overnight and the cells were spun down by centrifugation and collected. They were then resuspended into 1000 ml cell-free MBM that was previously bubbled to the desired CO concentration ([CO]) before the drawdown experiment was initiated by reintroducing the cells. Gas samples were analyzed over time and [CO] in the headspace was measured using a Reduced Gas Detector, Gas Chromatograph (RGD-GC) (See below). Microbial samples were taken from the media in correlation with the gas sampling time points.

## 2.4 Gas Chromatography

To measure [CO] in incubation samples (Figure 2.3), a known volume of seawater (90 ml) was extracted via a gas tight syringe at various time points and CO-free air was pulled into the syringe through a Schutze Reagent column to create a known volume of headspace (10 ml). The syringe was shaken by hand for approximately 30 s to 1 minute to equilibrate the headspace and seawater, a procedure previously found to be sufficient for the two phases in the glass syringe to equilibrate (Conrad, et al., 1982). The headspace was then injected into a 1 ml sample loop of a SRI (RGD-GC) (Figures 2.4 and 2.5). The GC's temperature and pressure settings were set as follows: nitrogen carrier gas, 20 psi; reactor cell, 290°C; reduced gas detector cell, 170°C; column oven, 110°C. Passing the sample sequentially through a 30" Unibeads® 1S 60/80 column and a 30" molecular sieve 5A column separated the CO for analysis. The CO then

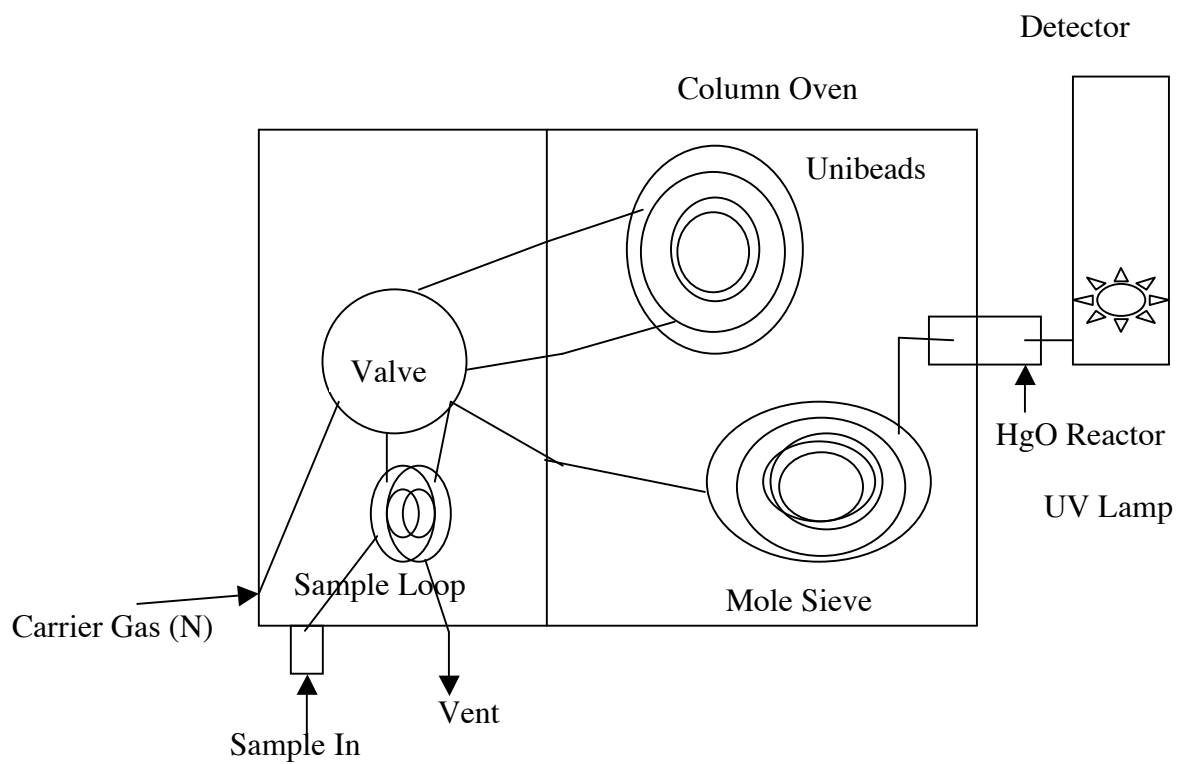


Figure 2.3: Diagram of the SRI Gas Chromatograph. The Reduced Gas Detector GC was used for the analysis of CO concentration. For valve details see Figures 2.4 & 2.5.

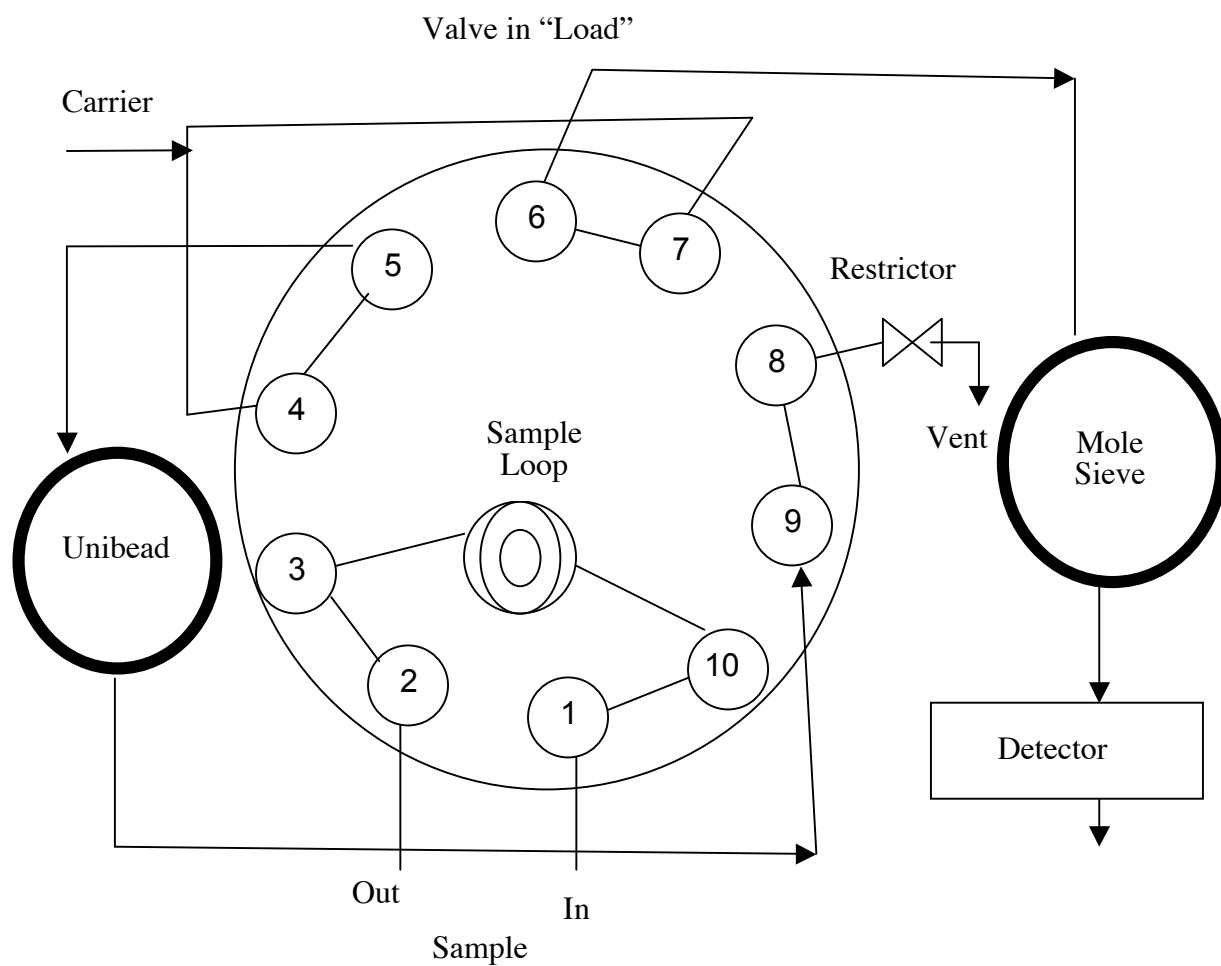


Figure 2.4: Schematic of the valve in "Load". The valve in the GC was used to load and inject gas samples into the gas chromatograph. The valve is depicted in the load position and shows the sample held in the sample loop.

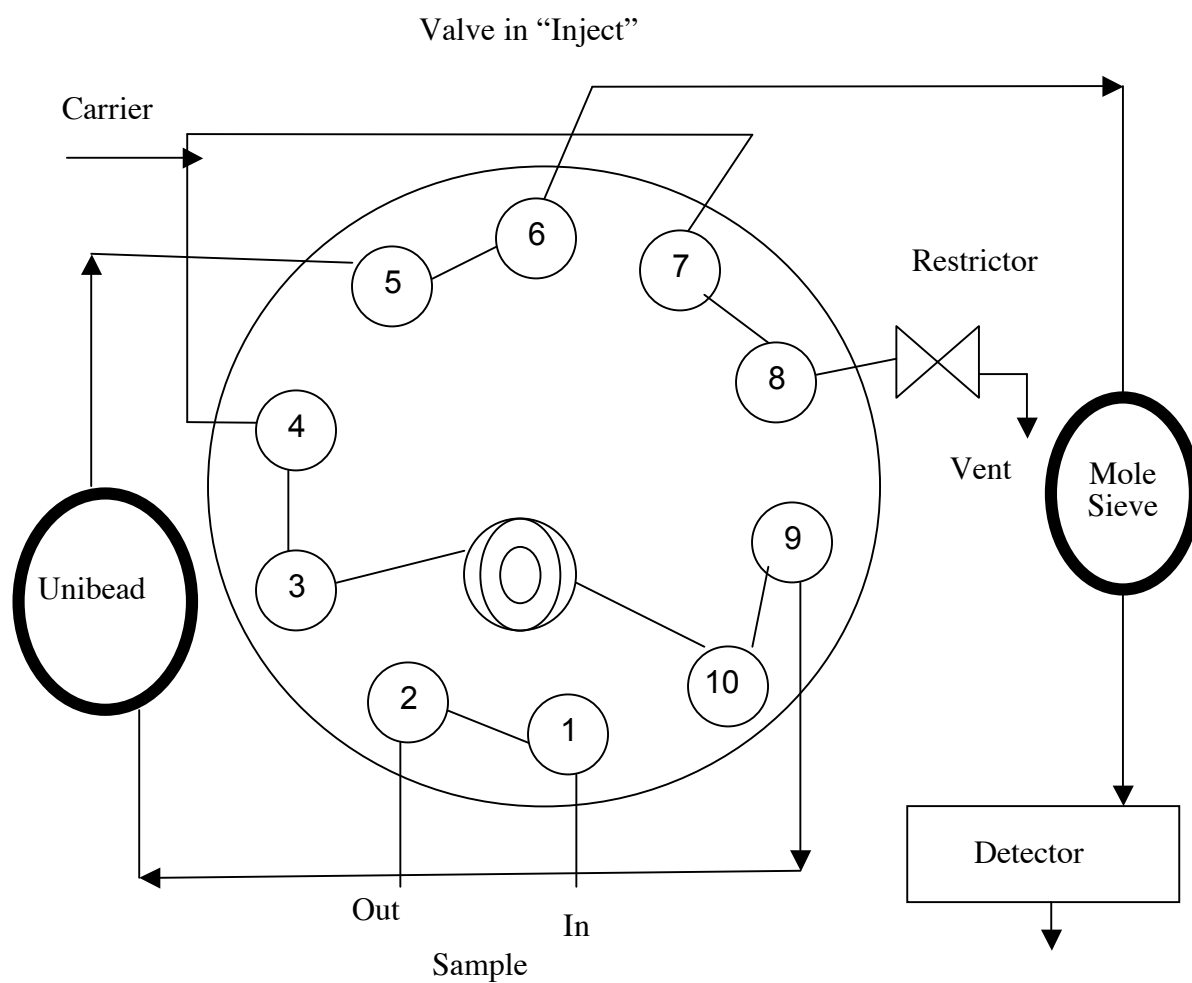


Figure 2.5: Schematic of the valve in “Inject”. The valve in the GC was used to load and inject gas samples into the gas chromatograph. The valve is depicted in the inject position. From the sample loop the gas enters the Unibeads column, the Molecular Sieve column, and the detector.

passed through a heated mercuric oxide (HgO) reactor, reducing the mercuric oxide to mercury vapor as the CO was oxidized as in the following equation:



The CO concentration was detected using the resulting reduction of mercuric oxide to mercury vapor and detected by ultraviolet (UV) absorbance producing sample peaks analyzed using Peak Simple® v. 3.29 chromatography software. The resultant peak areas were compared to peaks from a standard curve produced by dilutions of a 1 ppm NIST primary CO standard (Table 2.1, Figure 2.6).

#### 2.4.1 Calculating CO Concentration in an Aqueous Solution

To calculate the CO concentration in the aqueous solution a multi-part calculation was used that accounted for salinity, air to volume ratio in the syringe, and the water temperature (Additional details for the calculation are in Appendix B). Peak areas were converted into CO concentrations in the aqueous solution (nmol) using a set of equations by Xie et al, [2002] (ppmv, part per million by volume) as follows:

$$\{CO\}_w = 10^{-6} \beta m_a p \quad (2.2)$$

$$m_a (\text{ppmv}) = \frac{PA * \text{std}(\text{ppm})}{\text{std}PA} \quad (2.3)$$

$$\{CO\}_{aq} = (\{CO\}_w V_w + 10^{-6} m_a V_a) / V_w \quad (2.4)$$

$$\{CO\}_{aq} = 10^{-6} m_a (\beta p V_w + V_a) / V_w \quad (2.5)$$

$$[CO]_{aq} = \frac{10^9 * p \{CO\}_{aq}}{(RT)} \quad (2.6)$$

where  $\{CO\}_w$  is the dissolved CO concentration (ml CO/ml),  $\beta$  is the Bunsen solubility coefficient of CO (ml CO/ml), and  $p$  is atmospheric pressure (atm) of dry air.  $PA$  is the peak

Table 2.1: Typical variation in standard CO gas samples. The standard samples were run through the GC. A 1 ppm CO gas standard was diluted with CO free Schutze air to attain various [CO] for the standard curve. The injections represent five different mixtures from the standard CO. The standard deviation represents the difference in integrateable peaks as found by using manual integration through Peak Simple®.

	Peak Area (mV)						
[CO] ppm	Trial 1	Trial 2	Trial 3	Trial 4	Trial 5	Average	SD
1	952.261	952.667	944.154	928.265	945.844	944.638	9.904
0.5	543.552	542.563	535.635	540.548	535.124	539.484	3.905
0.25	236.784	248.433	232.900	248.539	334.3505	260.201	42.031
0.125	130.424	163.896	118.152	157.640	167.109	147.444	21.846

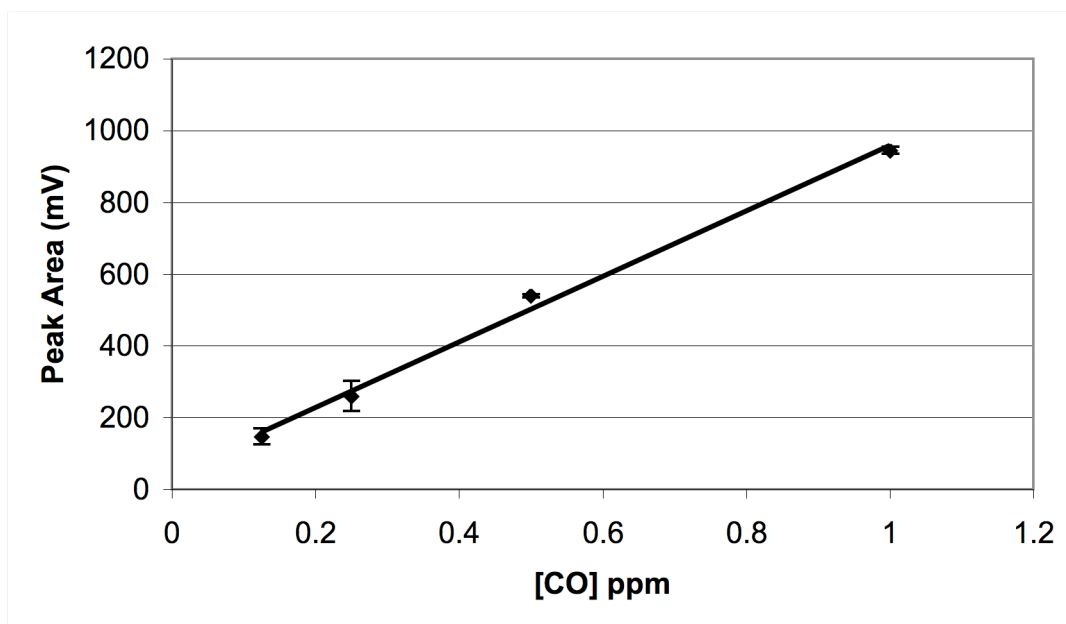


Figure 2.6: Typical standard curve for CO. Various known concentrations from the 1 ppm CO standard gas tank were used.  $y=915.13x + 43.973$ ,  $R^2=0.9949$ . The vertical error bars for each point from left to right are  $\pm 21.846$  mV,  $\pm 42.031$  mV,  $\pm 3.905$  mV, and  $\pm 9.904$  mV.

area measured for a gas sample (mV),  $std$  (ppm) is the CO concentration of the standard (ppmv),  $stdPA$  is the measured standard peak area (millions of counts),  $\{CO\}_{aq}$  is the initial concentration of CO in seawater (ml CO/ml), and  $V_w$  is the water sample volume (ml).  $V_a$  is the volume of equilibrated headspace air (ml),  $[CO]_{aq}$  is the concentration of CO in the collected seawater sample in nM,  $R$  is the gas constant ( $0.08206 \text{ atm l mol}^{-1} \text{ K}^{-1}$ ), and  $T$  is temperature (K).

#### 2.4.2 The Limit of Detection

The limit of detection (LOD) for CO was determined from a number of standard curves. Since a blank measurement of “Schutze Air” produced no measurable peak from the RGD-GC, the LOD was calculated as the x-intercept of the standard curve when a linear best fit line was not constrained to pass through the origin. This value was equated with a carbon monoxide concentration, averaged, and standard deviations were calculated. The limit of detection (LOD) was determined using methods from Greenberg et al. [1992], by multiplying the standard deviation of twelve standard curve x-intercept values by 3.290. The LOD defined in this way represents the amount of CO that produces a signal sufficiently large that 99% of the trials with that amount will produce a detectable signal. To reduce the probability of a false detection to 5%, the standard deviation (s) was multiplied by 1.645 from a cumulative normal probability table. Also, to reduce the probability of false nondetection to 5%, this amount was doubled to 3.290. This was then defined as the LOD and measured in parts per million (ppm) (Greenberg et al., 1992).

## 2.5 Preparing RNA for Gene Expression Analysis

### 2.5.1 RNA Extraction

Bacteria samples were collected for RNA extraction at time points coincident with the headspace analysis of [CO] in the kettle. To obtain the desired cell number ( $2 \times 10^9$  cells) for analysis, 1.5 ml of culture was added to 2.0 ml centrifuge tubes. 10% stop solution of phenol in ethanol was added to the tubes (150  $\mu$ L/1.5 ml) to preserve the expression for the desired time point. This was centrifuged for 10 minutes at 4°C at 5000 rpm. The supernatant was decanted and the pellet stored at -80°C until RNA was extracted using an RNA extraction protocol (RiboPure™-Bacteria Kit) and checked on a nanodrop spectrophotometer for RNA quantity and quality. The extracted RNA was treated with Turbo DNA-free™, to remove any DNA before the reverse transcription step and stored at -80°C. The SuperScript™ III RT protocol was followed for reverse transcription creating complementary DNA (cDNA) for polymerase chain reaction (PCR). The products from the PCR were then analyzed using Gel Electrophoresis.

### 2.5.2 Primer Design

Primers were designed specifically for the *coxL* gene in *Silicibacter pomeroyi*. Three different primers were designed based on the two known CO oxidizing clades, OMP and BMS (Table 2.2). These clades refer to two specific *coxL* genes within the *S. pomeroyi* genome. The primer sets were named as follows: CoxLf and CoxLr, CoxL1f and CoxL1r, and CoxL2f and CoxL2r (f=forward, r=reverse). The primers targeted the *coxL1* and *coxL2* genes individually as well as an overall CoxL primer designed to target both. The *coxL1* & 2 gene sequences were obtained from Roseobase (<http://roseobase.org>) and aligned using BioEdit®. For the overall CoxL primer, the *coxL1* and *coxL2* sequences, were aligned through selected conserved regions

Table 2.2: Primer sets used to amplify the *coxL* genes. Primer sets were designed for the *coxL*, *coxL1*, and *coxL2* genes in *Silicibacter pomeroyi*. The first set represents the first primers designed to look at carbon monoxide gene expression. After multiple bands were produced by the first set of primers, a modified second set was designed for the same genes. The CoxL and CoxL1 primer sets were redesigned while the CoxL2 was kept the same throughout.

<b>Forward Primers</b>		
	<b>First Set</b>	<b>Second Set</b>
CoxLf	CGGYMTGGGCACCTATGGWT	CGGYMTGGGCACCTATGGWT
CoxL1f	GAGCCGGGCCATCCGGTCCT	TTTGCTATGACTGGGGCTTC
CoxL2f	ACAATCACATCTTCACATGG	ACAATCACATCTTCACATGG
<b>Reverse Primers</b>		
	<b>First Set</b>	<b>Second Set</b>
CoxLr	TCCAGCCCCGGCTCGAT	KCYTCCAGCCCCGGCTCGAT
CoxL1r	CCAGCTCCAGCGTGGTGACA	CGCCTCCGACCGCGACGAGG
CoxL2r	GTTGTCCATCCGGTCTTCGA	GTTGTCCATCCGGTCTTCGA

of around 20 bp for the forward and reverse primers. To find primer sets for CoxL1 and CoxL2 the gene sequences were manually searched for areas of conservation that did not overlap. Degeneracies were used for base pairs specifically in the CoxL primer set that when aligned, did not share the same base pair (Table 2.3). All three primer sets were checked for primer dimers and hairpins in AutoDimer™ and using a Basic Local Alignment Search Tool (BLAST) to make sure they did not amplify with anything other than *Silicibacter pomeroyi*.

After the initial primer sets were designed, multiple amplicon bands were detected in the temperature gradients using gel electrophoresis. Specifically, double bands were present in the primer sets for the overall CoxL and individual CoxL1. The initial sets designed for *coxL2* did not produce multiple bands in the temperature gradients. New primer sets were then designed for the overall *coxL* and *coxL1* genes while primer sets for the *coxL2* gene were not redesigned.

The primers were reconstituted into a stock solution and distributed into working solutions for further gene expression analysis using PCR. A 100  $\mu$ M concentration stock solution was made by dilution with DEPC (Diethylprocarbonate) water. The original oligonucleotide was in concentrations of nM. Working solutions were made for each primer set used from the stock primer solutions of 100  $\mu$ l (10  $\mu$ M) in 0.5 ml microcentrifuge tubes.

The primer sets were optimized to find the best melting temperature ( $T_m$ ) for the set. The optimization temperature range was calculated from the lowest  $T_m$  in the primer set, subtracting 8°C from the lower range and then adding 2°C to the upper range so that the gradient range covered 10°C. (ex: CoxL f=59.7, CoxL r=65.4, giving a range of 52-62°C). The PCR was set up for a gradient of temperatures and approximately five temperatures were picked for each primer set. Each of the 12 columns of wells in the gradient thermal cycler were set at a specific temperature. The temperatures for each primer set were recorded and the final PCR was run on a

Table 2.3: Degeneracy table of bases used in primer design. Degenerate bases allow the primers to have a number of options in the sequence to anneal and amplify a variety of related sequences and were used in areas of primer sets that did not have the same base. Using a degenerate base reduces primer specificity.

<b>Original Base Pair</b>	<b>Degenerate Symbol</b>
Purine (A or G)	R
Pyrimidine (C or T)	Y
A or T	W
G or C	S
A or C	M
G or T	K
A or T or C	H
G or C or T	B
G or A or C	V
G or A or T	D
G or A or T or C	N

gel to look for the optimum temperature. The optimum temperature for each primer set was determined by the best presence of the amplicon bands without non-specific bands. The amplicon size for the first primer sets were 230 bp for *coxL*, 360 bp for *coxL1*, and 379 bp for *coxL2*. For the redesigned second primer sets for *coxL* and *coxL1*, the amplicon sizes were 251 and 294 bp respectively. The primer sets were also run at the new optimum temperatures.

## **2.6 Bacterial Counts Using DAPI**

At time points corresponding to samples taken for [CO] and RNA extraction, 5 ml of MBM with *Silicibacter pomeroyi* (DSS-3) was preserved in 6% buffered formalin, and stored in the dark at 4°C. The cells were later filtered and stained with 4',6-diamidino-2-phenylindole (DAPI) for counting. A 16 mm filtration column was used to vacuum filter the appropriate volume of diluted culture onto a 0.2 µm pore size, black membrane Poretics® polycarbonate filter. The filter was kept on the filter holder while a working DAPI solution was added to just cover the cells. The working DAPI solution was prepared by adding 25 µL of the 5 mg/ml stock solution to 50 ml of filtered DI water giving a final concentration of 2.5 µg/ml. The tower was covered with aluminum foil and the cells incubated with DAPI for 5 minutes. The remaining liquid was pulled through the filter column by vacuum and the column was rinsed with DI water to remove excess DAPI and loose cells. The filter was placed onto a slide, a drop of immersion oil was added, and covered with a coverslip. The slides were stored in the dark at 4° prior to immediate counting or at -20°C for a more permanent storage of the samples. They were then counted using a fluorescence microscope with a DAPI light filter. The cells were counted in a 10

x 10 grid for at least 10 fields of view. The number of cells counted in each sample was then extrapolated using the column volume and sample volume; these bacterial counts allowed calculation of cell concentration in experimental samples.

## CHAPTER 3

### RESULTS

#### **3.1 Measurements of Carbon Monoxide Concentration**

The concentrations of carbon monoxide used in these experiments were selected based on previous *in situ* data collected from coastal and open ocean samples by Jones and Amador (1993) and Zafiriou et al (2003). The average value for coastal carbon monoxide concentration was assumed to be 12 nM while the average open ocean concentration was assumed to be 1.4 nM. These values are used for relevance throughout presentation of the data as solid lines in the graphs, aiding in evaluation of the experimental results in terms of environmental CO concentration.

#### **3.2 CO Oxidation by *Silicibacter pomeroyi***

In Controls 1 & 2 after 90 minutes of degassing, [CO] was measured at  $0.94 \text{ nM} \pm 0.06 \text{ nM}$  and  $0.81 \text{ nM} \pm 0.07$  (Table 3.1 and 3.2). Continuous bubbling throughout only reduced [CO] to a minimum of  $0.51 \text{ nM} \pm 0.01 \text{ nM}$  and  $0.59 \text{ nM} \pm 0.01 \text{ nM}$ , never reaching an undetectable concentration of CO. The concentrations, however, were below that of the low-end measurements for [CO] in the open ocean ( $\sim 1.4 \text{ nM}$ , Zafiriou et al. 2003).

Originally when media inoculated with *S. pomeroyi* was bubbled with CO, drawdown rates were too fast to allow significant [CO] to be established in the kettle, with *S. pomeroyi* taking the CO out of the water at about the same rate as CO was bubbled into the kettle. To

Table 3.1: Control experiments for CO oxidation by *Silicibacter pomeroyi*. Within Control 1 (a) and (b) represent duplicate headspace injections from a single time point. The temperature and salinity were kept constant at 22°C and 28. The sample volume for CO concentration measurements was 90 ml with a headspace of 10 ml of CO-free air.  $m_a$  is the measured concentration of CO in the equilibrated headspace in ppmv.

<b>Control: 1 (a) CO Free-Air DSS3/MBM in 1000 ml with 300 ml/min</b>			
Time (hrs.)	Peak Area (mV)	$m_a$	[CO] aq (nM)
0	149.4	0.18	0.99
0.25	125.2	0.15	0.83
0.5	75	0.09	0.5
1	104.3	0.13	0.69
2	185.2	0.23	1.22
4	183.3	0.22	1.21
<b>Control: 1 (b) CO Free-Air DSS3/MBM in 1000 ml with 300 ml/min</b>			
Time (minutes)	Peak Area (mV)	$m_a$	[CO] aq (nM)
0	134.7	0.16	0.89
0.25	126.5	0.15	0.84
0.5	78	0.1	0.52
1	101.3	0.12	0.67
2	194	0.24	1.28
4	202.3	0.25	1.34
Control 1 (a) & (b) Average $m_a$	Control 1 (a) & (b) Average [CO] (nM)	Control 1 (a) & (b) Standard Deviation $m_a$	Control 1 (a) & (b) Standard Deviation [CO] (nM)
0.17	0.94	0.013	0.068
0.15	0.83	0.001	0.006
0.09	0.51	0.003	0.015
0.13	0.68	0.003	0.014
0.23	1.25	0.008	0.041
0.24	1.27	0.016	0.088

Table 3.2: Control experiments for CO oxidation by *Silicibacter pomeroyi*. Within Control 2 (a) and (b) represent duplicate headspace injections from a single time point. The temperature and salinity were kept constant at 24°C and 27. The sample volume for CO concentration measurements was 90 ml with a headspace of 10 ml of CO-free air.

<b>Control: 2 (a) CO Free-Air DSS3/MBM in 1000 ml with 300 ml/min</b>			
Time (hrs.)	Peak Area (mV)	$m_a$	[CO] aq (nM)
0	145.7	0.16	0.87
0.25	125.4	0.14	0.75
0.5	100.3	0.11	0.6
1	122.4	0.14	0.73
2	225	0.25	1.34
4	110.1	0.12	0.66
<b>Control: 2 (b) CO Free-Air DSS3/MBM in 1000 ml with 300 ml/min</b>			
Time (minutes)	Peak Area (mV)	$m_a$	[CO] aq (nM)
0	127.72	0.14	0.76
0.25	100.88	0.11	0.6
0.5	98.93	0.11	0.59
1	92.66	0.1	0.55
2	196.46	0.22	1.17
4	86.17	0.1	0.51
Control 2 (a) & (b) Average $m_a$	Control 2 (a) & (b) Average [CO] (nM)	Control 2 (a) & (b) Standard Deviation $m_a$	Control 2 (a) & (b) Standard Deviation [CO] (nM)
0.15	0.81	0.013	0.068
0.13	0.67	0.001	0.006
0.11	0.59	0.003	0.015
0.12	0.64	0.003	0.014
0.23	1.25	0.008	0.041
0.11	0.58	0.016	0.088

measure CO drawdown, our method was modified so that *S. pomeroyi* grown in MBM media was resuspended in 1000 ml MBM previously equilibrated to the desired [CO] at which point the drawdown experiment was initiated.

Our limit of detection (LOD) for CO was found to be 0.0865 nM. Twelve replicate standard samples (1 ppm concentration) were measured and the average and standard deviation calculated. To get the LOD the standard deviation of 0.0263 nM was then multiplied by 3.290 (Greenberg et al., 1992). Results for the controls are shown in Figure 3.1. In both controls, a minimum CO concentration occurred at time points three and four. This low CO concentration was achieved after bubbling continuously with Schutze air for an additional 30 minutes to 1 hour. After these time points, the CO concentration rose slightly at time point five. For Control 1, the CO concentration remained slightly higher at time point six while for Control 2 the CO concentration went back down to a minimum value. The pattern of CO concentration showed no apparent trend and most likely reflects variations in analytical procedures caused by experimental setup.

During each kettle experiment, temperature and salinity remained constant. There was, however, a difference between experiments ranging from 22-24°C for the temperature and 25-28 for the salinity. These variations were taken into account when calculating the  $[CO]_{aq}$  through the Bunsen coefficient ( $\beta$ ). The ratio of aqueous sample to CO-free headspace in the sample syringe always remained constant at 9:1.

Higher starting values of CO were used to approximate those found in the coastal ocean (on the order of 12 nM; Jones and Amador 1993). Our initial attempt to establish a higher starting [CO] only reached an upper level of  $4.46 \text{ nM} \pm 0.18 \text{ nM}$  (Table 3.3). Our second

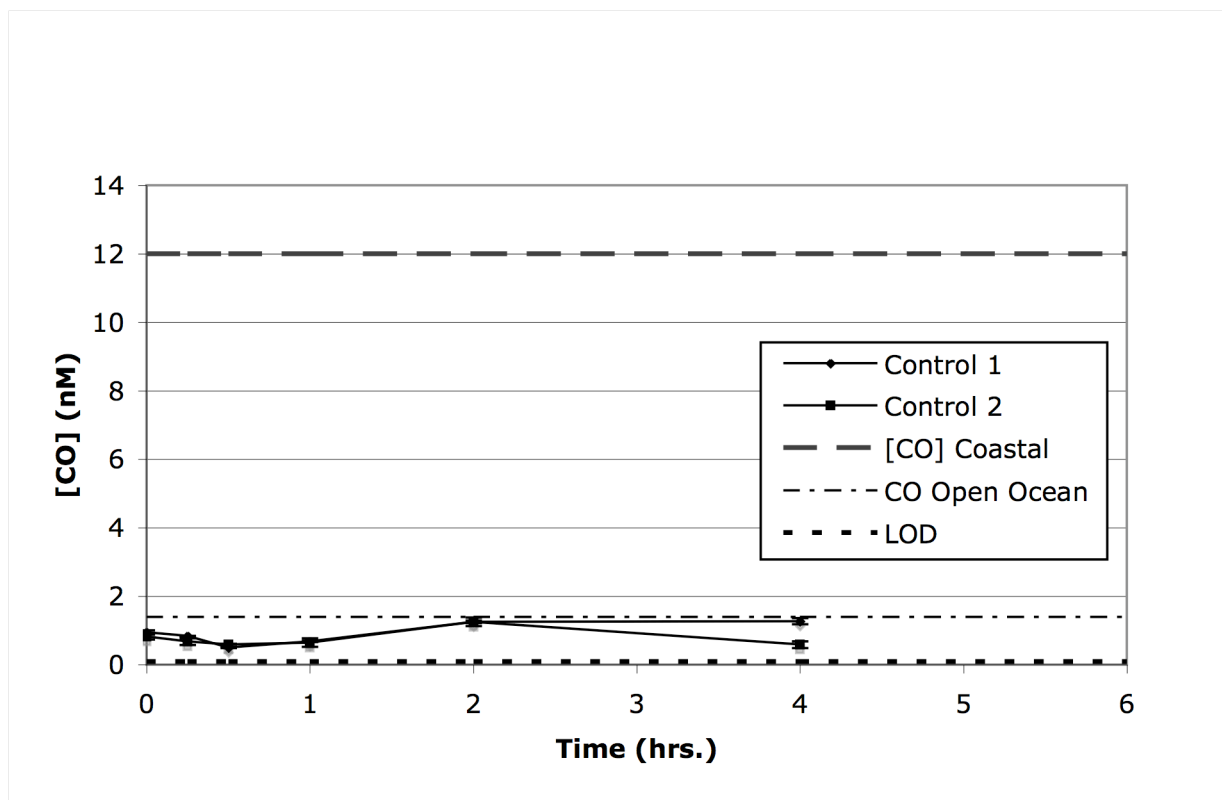


Figure 3.1: Kettle Reaction bubble with CO free Schutze Air in Controls 1 & 2. The figure shows the measured carbon monoxide concentration bubbled with CO-free air (nM) in aqueous solution. The duplicate measurements of a & b for each control have been averaged and the standard deviation taken.

Table 3.3: Experiments for CO oxidation by *Silicibacter pomeroyi*. Within Experiment 1 (a) and (b) represent duplicate headspace injections from a single time point. The temperature and salinity were kept constant at 24°C and 28. The sample volume for CO concentration measurements was 90 ml with a headspace of 10 ml of CO-free air.

<b>Experiment: 1 (a) [CO] DSS3/MBM in 1000 ml with 300 ml/min</b>			
Time (hrs.)	Peak Area (mV)	$m_a$	[CO] aq (nM)
0	557	0.86	4.59
12	70.4	0.11	0.58
23	39.2	0.06	0.32
37	38.1	0.06	0.31
60	32.5	0.05	0.27
<b>Experiment: 1 (b) [CO] DSS3/MBM in 1000 ml with 300 ml/min</b>			
Time (minutes)	Peak Area (mV)	$m_a$	[CO] aq (nM)
0	526.1	0.81	4.34
12	92.1	0.14	0.76
23	38.7	0.06	0.32
37	30.7	0.05	0.25
60	28.4	0.04	0.23
Experiment 1 (a) & (b) Average $m_a$	Experiment 1 (a) & (b) Average [CO] (nM)	Experiment 1 (a) & (b) Standard Deviation $m_a$	Experiment 1 (a) & (b) Standard Deviation [CO] (nM)
0.83	4.46	0.034	0.184
0.13	0.67	0.024	0.127
0.06	0.32	0.001	0.003
0.05	0.28	0.008	0.044
0.05	0.25	0.004	0.024

experiment was performed so that *S. pomeroyi* was introduced through resuspension into MBM that had already been established at a higher [CO]. For this CO drawdown experiment, an equilibrium was established resulting in a water [CO] of  $17.52 \text{ nM} \pm 0.33 \text{ nM}$  (Table 3.4, Figure 3.2). This suggested that in the original setup the bacteria were consuming the CO at rates sufficient to prevent the system from reaching equilibrium with respect to the air-CO mixture, resulting in a steady state [CO] lower than expected.

In Experiment 1, MBM inoculated with DSS-3 was bubbled for 90 minutes with a mixture of 50 ppm Scotty Standard CO gas and CO-free room air to achieve the desired [CO]. After 90 minutes, a CO concentration of  $4.46 \text{ nM} \pm 0.18 \text{ nM}$  was measured and the CO oxidation experiment was allowed to proceed. CO was oxidized over a time period of 60 hours and the concentration was drawn down to  $0.25 \text{ nM} \pm 0.02 \text{ nM}$ . The steepest decline in CO concentration occurred between time point one and time point two, a period of 12 hours. This period of 12 hours was too long to give an accurate measurement of oxidation rates and was reduced to 8 hours for the next experiment to get a more accurate measurement of CO oxidation rates. After the initial rapid decline, the CO concentration was well below the average open ocean measurement where it remained for the entire 60 hour time period.

In Experiment 2, the MBM was bubbled for 90 minutes with the CO gas mixture and *S. pomeroyi* (DSS-3) was then introduced to the CO-enriched media. A CO concentration of  $17.52 \text{ nM} \pm 0.33 \text{ nM}$  was measured and the CO oxidation experiment was allowed to proceed. The kettle was sealed and CO was no longer introduced to the medium. The CO was oxidized over a time period of 139 hours wherein the concentration was reduced to  $1.27 \text{ nM} \pm 0.08 \text{ nM}$ . This concentration was approximately 4 times higher than the previous trial, however the initial concentration was much higher.

Table 3.4: Experiments for CO oxidation by *Silicibacter pomeroyi*. Within Experiment 1 & 2 (a) and (b) represent duplicate headspace injections from a single time point. The temperature and salinity were kept constant at 24°C and 25. The sample volume for CO concentration measurements was 90 ml with a headspace of 10 ml of CO-free air.

<b>Experiment: 2 (a) [CO] DSS3/MBM in 1000 ml with 300 ml/min</b>			
Time (hrs.)	Peak Area (mV)	$m_a$	[CO] aq (nM)
0	2317.4	3.31	17.76
8	1797.3	2.57	13.78
19	1478.3	2.11	11.33
31	1147.4	1.64	8.8
43	941.4	1.35	7.22
67	884.1	1.26	6.78
91	274.9	0.39	2.11
115	209.5	0.3	1.61
139	173.6	0.25	1.33
<b>Experiment: 2 (b) [CO] DSS3/MBM in 1000 ml with 300 ml/min</b>			
Time (minutes)	Peak Area (mV)	$m_a$	[CO] aq (nM)
0	2255	3.23	17.28
8	1754.6	2.51	13.45
19	1504.4	2.15	11.53
31	1072	1.53	8.22
43	908.9	1.3	6.97
67	899.8	1.29	6.9
91	296.1	0.42	2.47
115	218.8	0.31	1.68
139	157.5	0.23	1.21
Experiment 2 (a) & (b) Average $m_a$	Experiment 2 (a) & (b) Average [CO] (nM)	Experiment 2 (a) & (b) Standard Deviation $m_a$	Experiment 2 (a) & (b) Standard Deviation [CO] (nM)
3.27	17.52	0.063	0.338
2.54	13.61	0.043	0.231
2.13	11.43	0.026	0.141
1.59	8.51	0.076	0.409
1.32	7.09	0.033	0.176
1.28	6.84	0.016	0.085
0.41	2.29	0.022	0.257
0.31	1.64	0.009	0.050
0.24	1.27	0.016	0.088

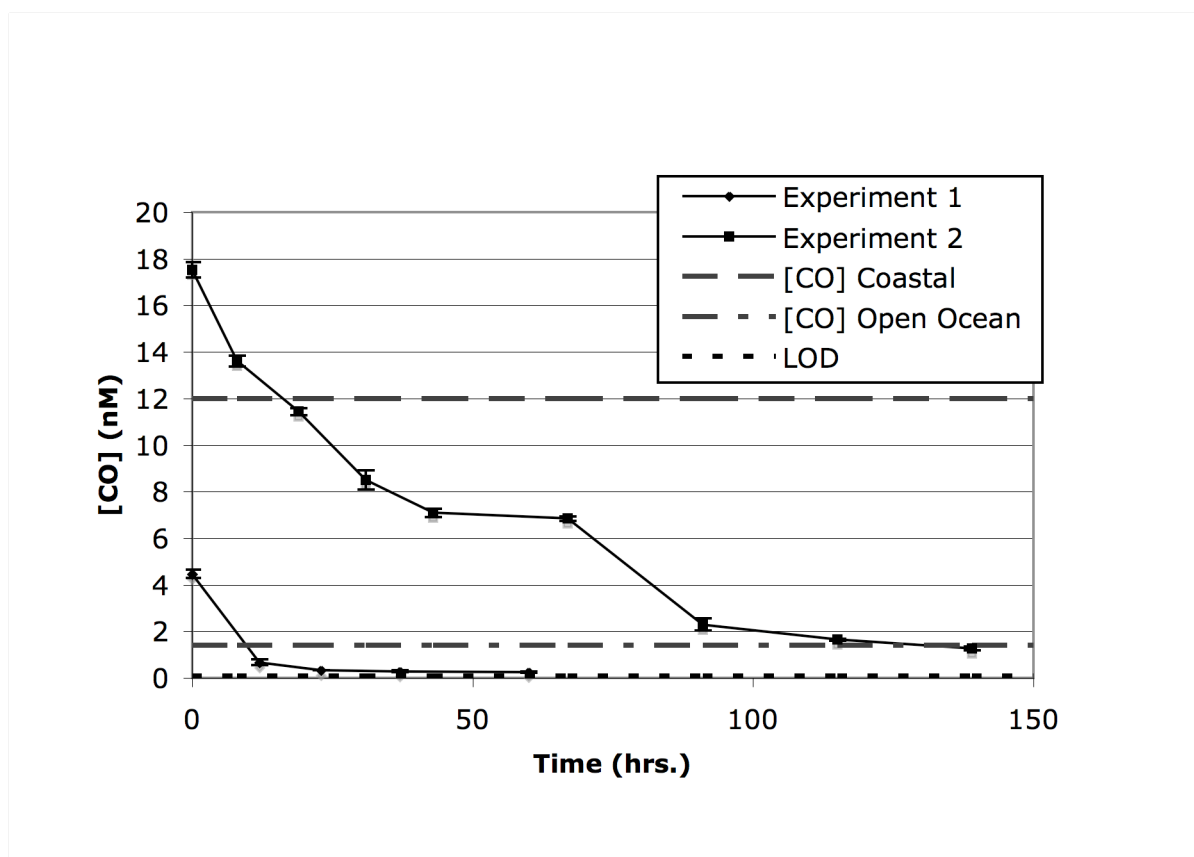


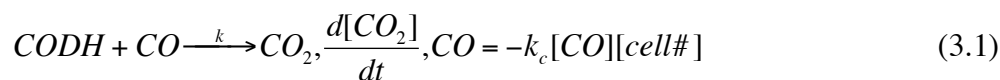
Figure 3.2: Kettle reaction bubbled with CO for Experiments 1 & 2. The figure shows the measured carbon monoxide concentration bubbled with CO (nM) in aqueous solution, CO consumption in Experiments 1 & 2 is plotted with averages and standard deviations taken from the duplicate samples, a & b.

### 3.3 DAPI Bacterial Counts

Bacterial cell counts were carried out using the fluorescent DNA binding stain DAPI to look at the total number of *S. pomeroyi* cells per ml of media. For Experiment 2, cell numbers were relatively constant over 168 hours after the initial 8 hours. The number of *S. pomeroyi* cells ranged from  $19.3 \times 10^7$  cells/ml to  $37.5 \times 10^7$  cells/ml. An average of  $27.4 \times 10^7$  cells/ml  $\pm$   $6.3 \times 10^7$  cells/ml were taken after the initial 8 hours (Table 3.5). The optical density (OD) was also taken for each time point counted. The OD for cell counts ranged from 0.011, taken after incubation overnight at 30°C, to 0.023, at 96 hours at room temperature. There was a significant change in bacterial numbers over the first 8 hours. The growth after this time period was not significant and an average number of bacterial cells from 8 hrs. and beyond were used to calculate the per cell oxidation rate in the kettle by *S. pomeroyi*.

### 3.4 Carbon Monoxide Oxidation Rate

The cell normalized CO oxidation rate was calculated by plotting against time the natural log of [CO] at time  $t$  divided by [CO] at time zero in Experiment 1 and 2 with CO added. Since bacterial growth did not result in a significant change in bacterial number over time after time point 2 (8 hrs.), this can be treated as a pseudo first-order reaction (Table 3.6), with CODH a function of cell number which is a constant:



$$\frac{d[CO]}{dt} = -k[CO] \quad (3.2)$$

Table 3.5: DAPI bacterial counts performed with fluorescence microscopy.

<b>Time (hrs.)</b>	<b>OD</b>	<b>Bacteria/ml (<math>10^6</math>)</b>
0	0.011	72.36
8	0.013	193.52
19	0.016	240.20
31	0.014	241.09
43	0.015	247.99
91	0.012	245.21
115	0.023	375.28
139	0.014	271.38
168	0.016	367.04

Table 3.6: Carbon monoxide oxidation rate by *S. pomeroyi*.

<b>Oxidation Rate</b>		
<b>Experiment 1</b>		
<b>Time (hours)</b>	<b>Average [CO] nM</b>	<b>LN [Co<sub>t</sub>]/[CO<sub>0</sub>]</b>
0	4.463	0
12	0.670	-1.896
23	0.321	-2.633
37	0.284	-2.755
60	0.251	-2.879
<b>Experiment 2</b>		
<b>Time (hours)</b>	<b>Average [CO] nm</b>	<b>LN [Co<sub>t</sub>]/[CO<sub>0</sub>]</b>
0	17.524	0
8	13.613	-0.253
19	11.431	-0.427
31	8.506	-0.723
43	7.091	-0.905
91	6.837	-0.941
115	2.288	-2.036
139	1.455	-2.489

The solution to (3.2) gives

$$[CO]_t = -k[CO]_0 e^{-kt} \quad (3.3)$$

which can be rearranged as:

$$\ln \left[ \frac{CO_t}{CO_o} \right] = -kt \quad (3.4)$$

where  $k$  is the experimental rate constant,  $k_c$  is the cell normalized rate constant, and  $t$  is time. Equation 3.4 was then plotted versus time. The experimental oxidation rate constant  $k$  was then determined from the slope of the best linear fit to the data. It was then divided by the average number of bacterial cells counted per ml, giving a cell normalized CO oxidation rate constant,  $k_c$ , in units of milliliters per cell per hour.  $k$  was found to be  $0.0193 \text{ h}^{-1}$  for Experiment 2 (Figure 3.3). The time points after 8 hours were viewed as the most accurate measurement of  $k$  since they occurred after the initial growth of *S. pomeroyi* in the CO bubbled kettle. Dividing the CO oxidation rate constant by average *S. pomeroyi* cell counts, the cell normalized oxidation rate,  $k_c$ , was found to be  $7.1 \times 10^{-11} \text{ ml cell}^{-1} \text{ h}^{-1}$  (Table 3.7).

### 3.5 Optimization of Temperature Gradients for Designed Primers

In the first primer sets designed for *coxL1*, *coxL2*, and *coxL*, only the *CoxL2* primers showed one band at the appropriate amplicon size, 379 bp. The other two primer sets, *CoxL* and *CoxL1*, showed two or more bands. The predicted amplicon size for *CoxL* and *CoxL1* were 230 bp and 360 bp respectively (Figure 3.4). The optimum temperature for this *CoxL* primer set was never found since a single amplicon band was not produced at any of the temperatures tested, using ranges of  $53.7\text{-}62^\circ\text{C}$  up to of  $82.5\text{-}92.8^\circ\text{C}$  (Figure 3.4). For the *CoxL1* primer set, the optimum temperature was found to be at  $72.8^\circ\text{C}$  (Figure 3.4). The *CoxL2* primer produced

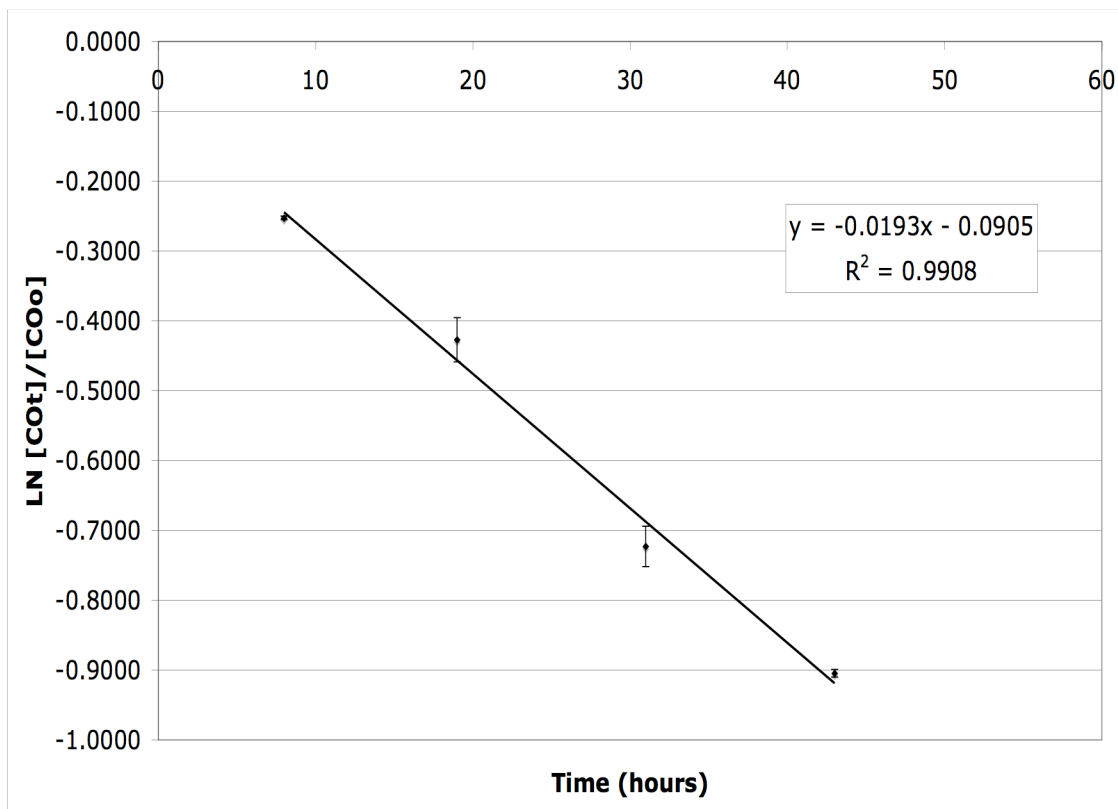


Figure 3.3: Carbon monoxide oxidation rate by *S. pomeroyi*. The rate constant  $k$  was found for Experiment 2 to be the slope of the best-fit line,  $k=0.0193$ .

Table 3.7: Carbon monoxide oxidation rate calculated per cell of *S. pomeroyi*.

<b>Cell Density x10<sup>6</sup> (ml<sup>-1</sup>)</b>	
<b>Average x10<sup>6</sup> (ml<sup>-1</sup>)</b>	<b>SD x 10<sup>6</sup></b>
276.52	63.72
<b>Oxidation Rate Constant (h<sup>-1</sup>)</b>	
<b><i>k</i> (h<sup>-1</sup>)</b>	<b>SD <i>k</i> (h<sup>-1</sup>)</b>
0.0193	0.001
<b>Cell Normalized Oxidation Rate (ml cell<sup>-1</sup> h<sup>-1</sup>)</b>	
<b><i>k</i>/average cell density</b>	<b>SD (<i>k</i>/average cell density)</b>
7.14 x 10 <sup>-11</sup>	2.58 x 10 <sup>-13</sup>

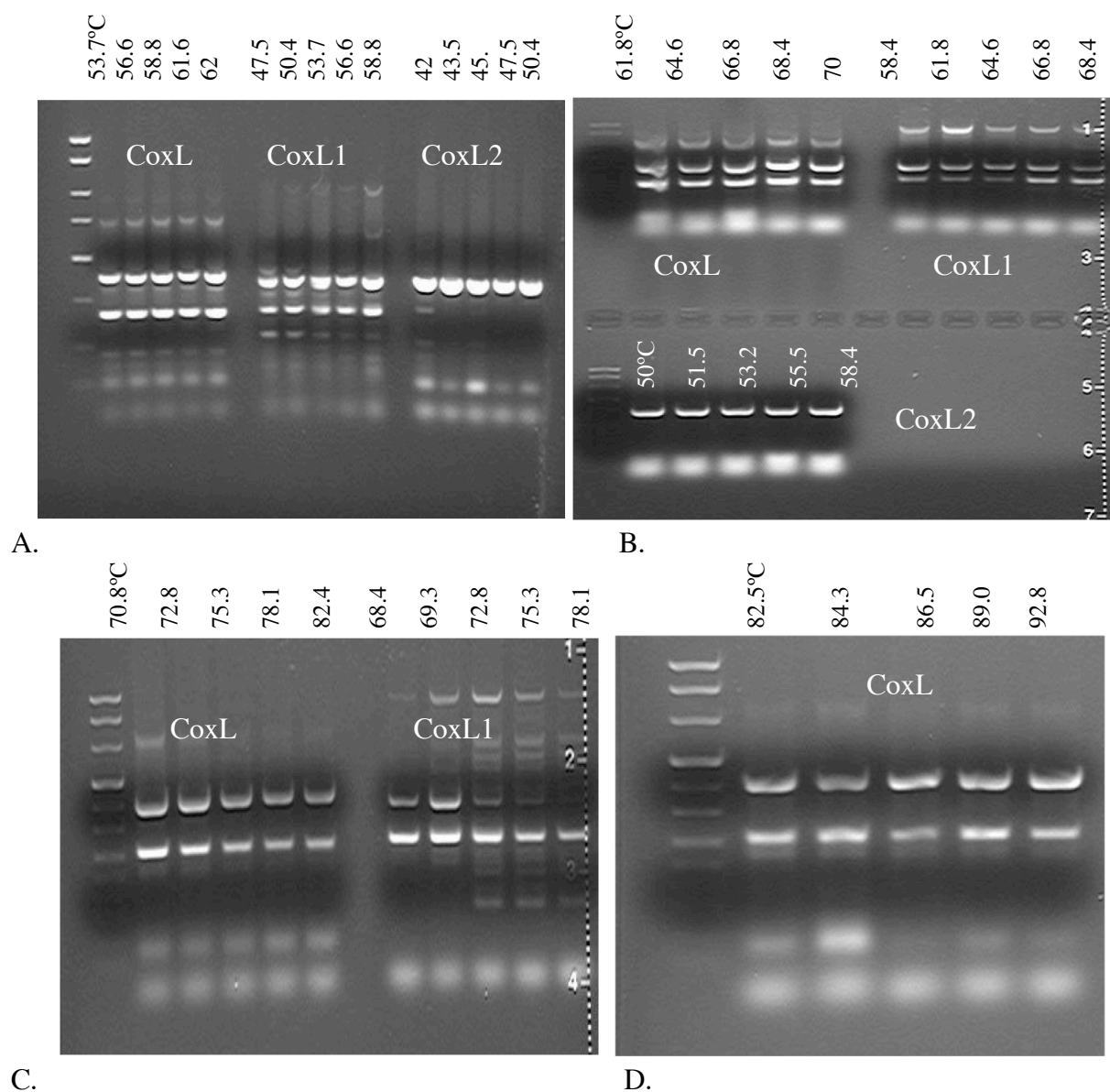


Figure 3.4: Temperature gradients with the first primer sets. A) Each primers set was run at five different temperatures. In this gradient only, the CoxL2 primers were seen to produce single bands at the desired amplicon size. For CoxL the temperature ranged from 53.7-62°C, CoxL1 from 47.5-58.8°C, and CoxL2 from 42-50.4°C. B) Temperature ranges for CoxL from 61.8-70°C, CoxL1 from 58.4-68.4°C, and CoxL2 from 50-58.4°C. C) From left to right CoxL and CoxL1 primer sets run at a temperature range for CoxL from 70.8-82.4°C and for CoxL1 from 68.4-78.1°C. D) CoxL primer set with a temperature range of 82.5-92.8°C.

single amplicon bands at the predicted base pair size on the first temperature gradient range. The optimum temperature for the CoxL2 primer set was found to be 58.4°C. This original primer set for CoxL2 was used throughout the *coxL* gene expression experiments.

New primer sets were redesigned for *coxL* and *coxL1* to find a target region, which produced a single amplicon. Over the new temperature gradients tested, the optimum temperature for the second CoxL primer set (CoxLf and CoxLr) was found to be 65.5°C while the optimum temperature for the second CoxL1 primer set (CoxL1f and CoxL1r) was found to be 63.7°C (Figure 3.5). The primer set for CoxL1 produced two bands for gene expression using *S. pomeroyi* DNA. When further tested using extracted RNA from the reaction kettle CO oxidation experiment, *coxL* gene expression produced only one amplicon band at the predicted base pair length.

### **3.6 *coxL* Gene Expression in *Silicibacter pomeroyi***

Gene expression for the *coxL* gene in *S. pomeroyi* was seen for all [CO] from “CO-free” controls to higher levels of CO (e.g. ~18 nM). The CO-free negative control with no RNA and negative control with no reverse transcription (RT) step showed no *cox* expression (Figure 3.6 and 3.7)

Time point 1 (0 hr.) showed expression present in the negative control with no RT step and in *coxL* at 230 bp, in *coxL1* at 360 bp, and in *coxL2* at 379 bp (Figures 3.6 and 3.7). Time point 2 (0.25 hrs.) also showed expression in all three primer sets at their predicted amplicon size. Time points 3 (0.5 hrs.) and 4 (1 hr.) showed no expression for any primer set. Time point 5 (2 hrs.) showed expression in the negative control with no RT step and all three primer sets.

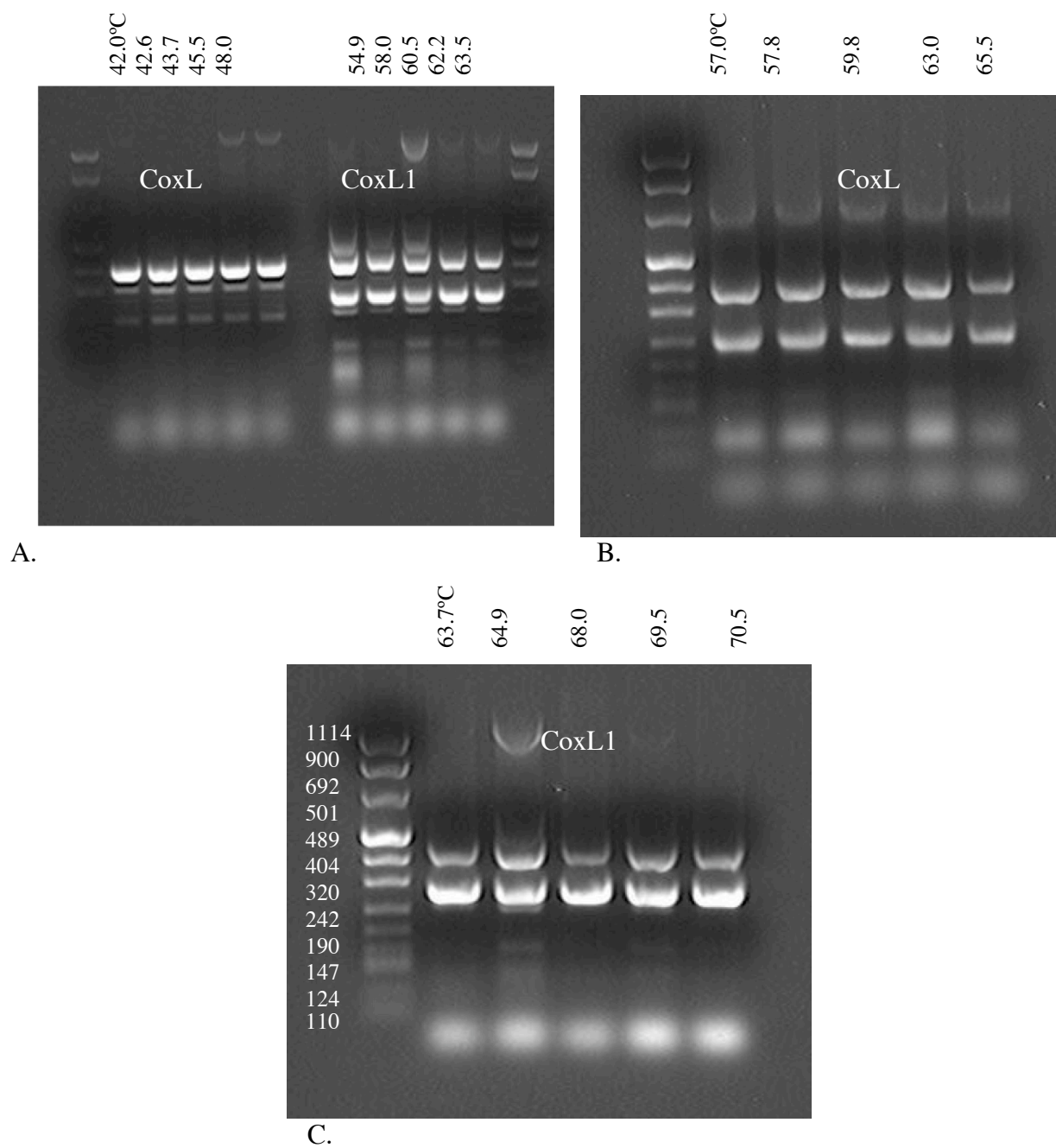
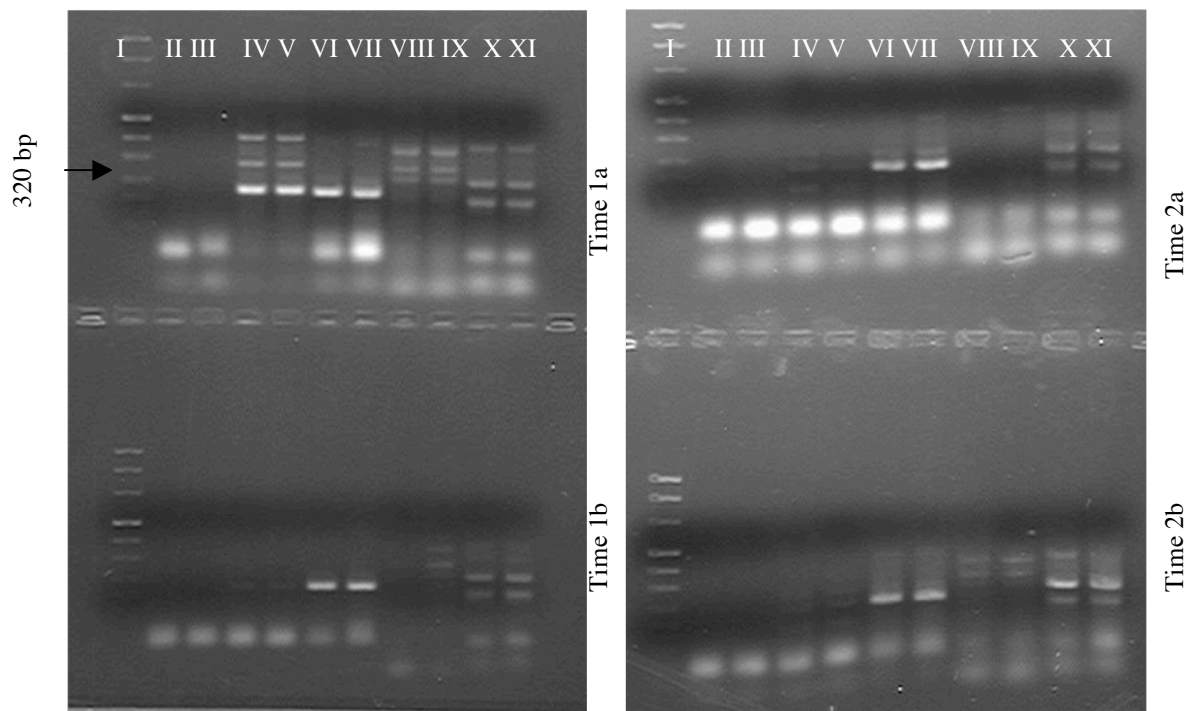


Figure 3.5: Temperature gradient with the newly designed primer sets for CoxL and CoxL1. A) Temperature ranges for CoxL from 42.0-48.0°C and for CoxL1 from 54.9-63.5°C. B) CoxL temperatures ranging from 57.0-65.6°C. C) CoxL1 temperatures ranging from 62.0-72.0°C.



A.

B.

Figure 3.6: Control 1 CO-free air; A) 1a & 1b; B) 2a & 2b. Each gel represents a different time point. The top and bottom of the gel represent the two bacteria samples taken at that time point (a and b). Run from left to right in each gel: lane I, ladder; lanes II and III, negative control no RNA; lanes IV and V, negative control no reverse transcription (RT) step; lanes VI and VII, CoxL; lanes VIII and IX, CoxL1; lanes X and XI, CoxL2. A standard ladder is run in the first well on the left for each gel as a measurement of amplicon base pair size.

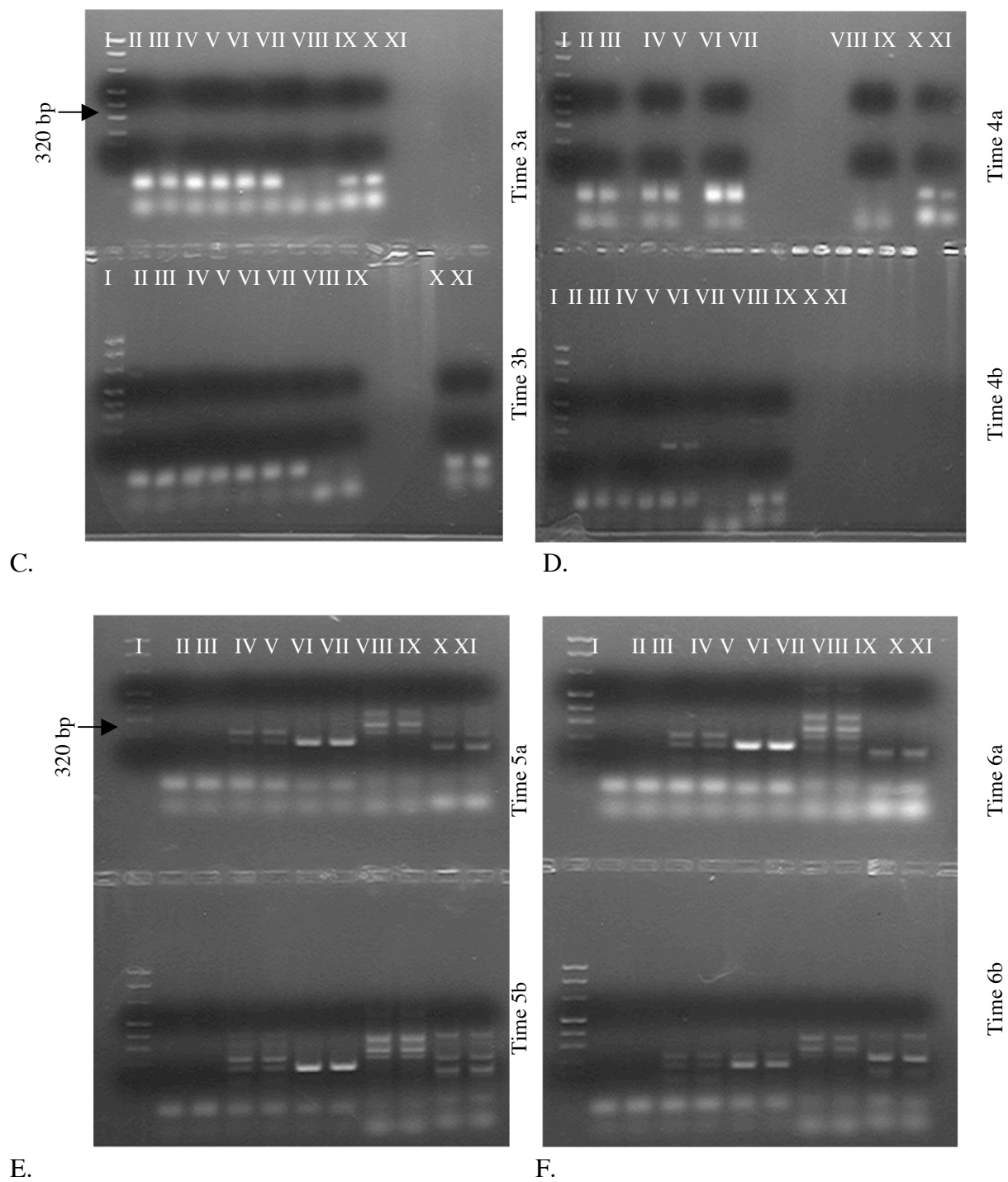
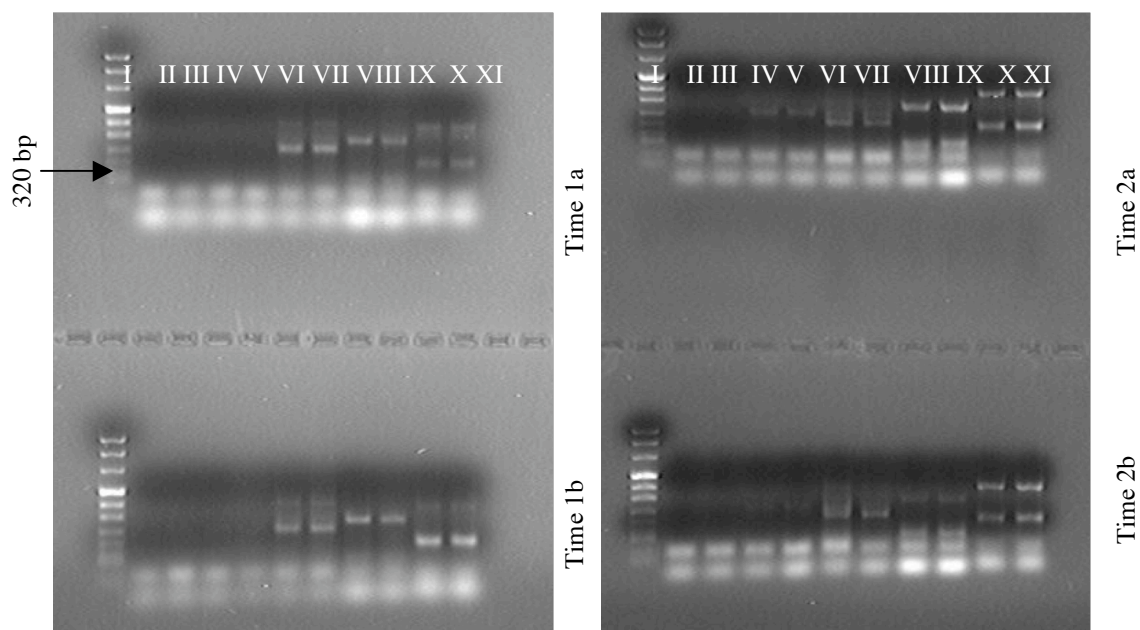


Figure 3.7: Control 1 CO-free air; C) 3a & 3b; D) 4a & 4b; E) 5a & 5b; F) 6a & 6b

Time point 6 (4 hrs.) also showed some expression in the negative control with no RT step and each primer set. A molecular weight marker was placed at 320 bp for a reference. Control 1 was bubbled with CO free Schutze air but never achieved a [CO] below the limit of detection. The samples were analyzed using the first primer sets designed for *coxL*, *coxL1*, and *coxL2*. Examining the gels, even at low levels of CO, below that of the estimated average for open ocean [CO], *S. pomeroyi* still showed *coxL* gene expression at all times. Exceptions were seen in the gels for time points 3 and 4. Here the gel showed no bands for any of the primer sets, most likely due to an unknown error during the RT or PCR process since they were both carried out on the same day. Also, there are some bands present in a few negative controls (such as the gel for time point 1) suggesting RNA contamination in the sample. This contamination may also affect the presence of bands in the subsequent *coxL* primer sets for the time point. In the duplicate sample for time point 1 there is no contamination in the negative control. For the *CoxL2* primer set there are also multiple bands present in the gels. Using the amplicon size and standard marker, the correct band can be picked out on the gel for analysis. The amplicon size for each primer set was 230 bp for *coxL*, 360 bp for *coxL1*, and 379 for *coxL2*.

Control 2 Time point 1 (0 hr.) showed expression for all three primer sets at the predicted amplicon sizes with no expression in any of the negative controls (Figure 3.8). Time point 2 (0.25 hrs.) showed some expression in the negative control with no RT step with a weak band present around 294 bp and expression in all three primer sets. For the double band in *coxL2* the first band on the gel was the predicted amplicon size at 379 bp. Time points 3 (0.5 hrs.) and 4 (1 hr.) also showed expression for all three primer sets and a weak band in the negative control with no RT step (Figure 3.9). Time point 5 (2 hrs.) showed bands for all samples run including both negative controls suggesting contamination of RNA for all samples during the reverse



A.

B.

Figure 3.8: Control 2 CO-free air; A) 1a & 1b; B) 2a & 2b. Each gel represents a different time point. The top and bottom of the gel represent the two bacteria samples taken at that time point (a and b). Run from left to right in each gel: lane I, ladder; lanes II and III, negative control no RNA; lanes IV and V, negative control no reverse transcription (RT) step; lanes VI and VII, CoxL; lanes VIII and IX, CoxL1; lanes X and XI, CoxL2. A standard ladder is run in the first well on the left for each gel as a measurement of amplicon base pair size.

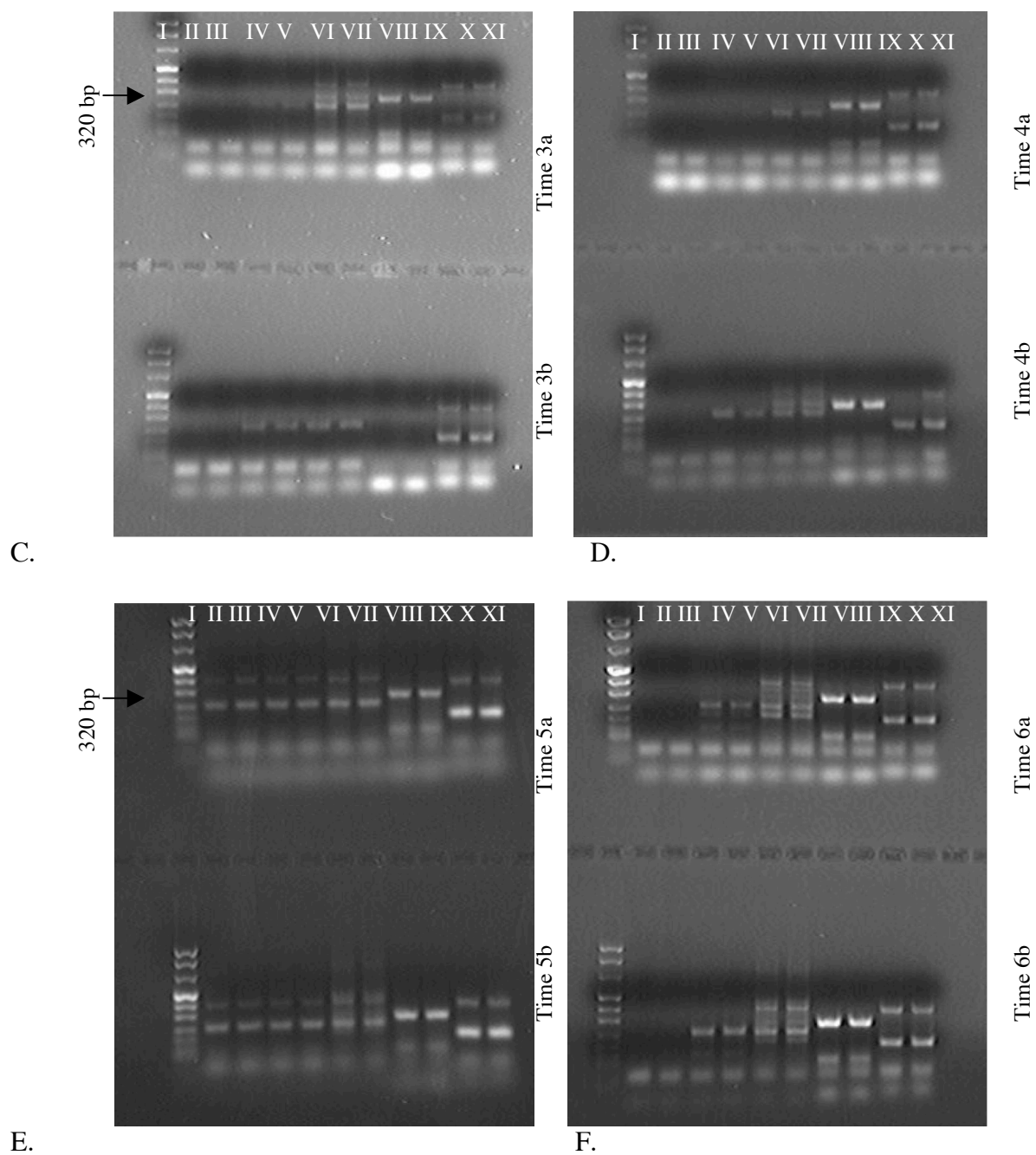
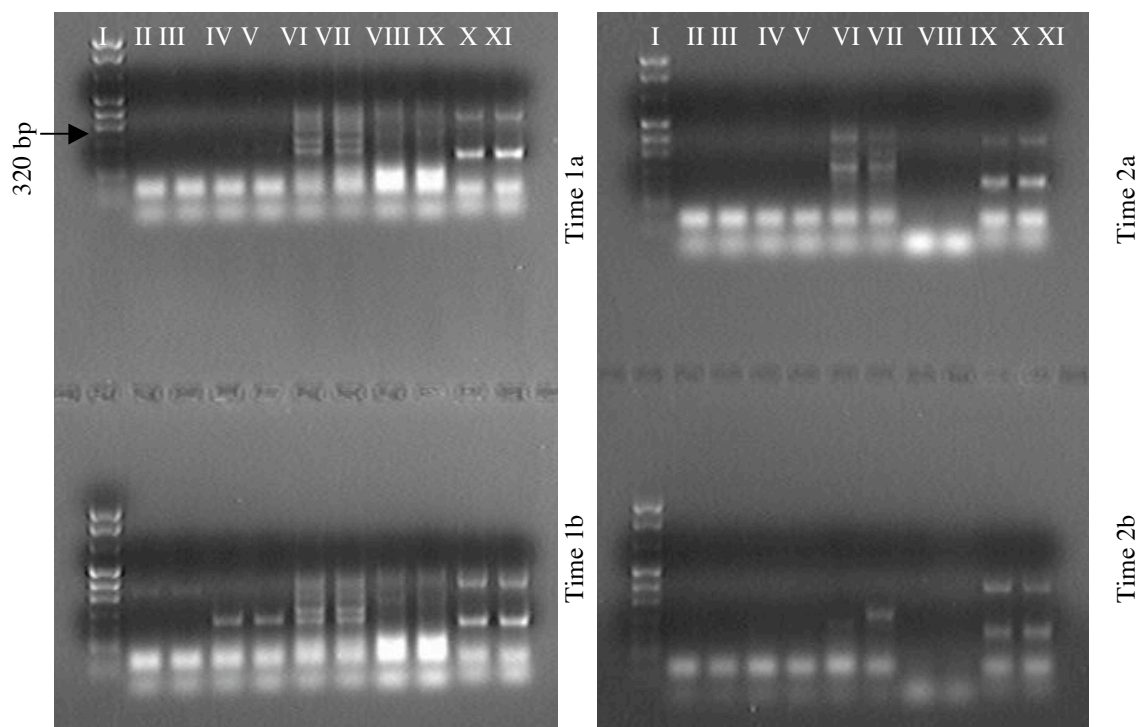


Figure 3.9: Control 2 CO-free air; Each gel represents a different time point. The top and bottom of the gel represent the two bacteria samples taken at that time point (a and b). C) 3a & 3b; D) 4a & 4b; E) 5 a & 5b; F) 6a & 6b

transcription process. Time point 6 (4 hrs.) again showed expression in the negative control with no RT step and for all primer sets of *coxL*. The bands run with the second primer sets were much clearer with fewer multiples than those run with the first primer sets.

Control 2 was run with the improved second primer sets designed for *coxL*. The redesigned primer sets confirm expression for *coxL*, *coxL1*, and *coxL2* at low [CO], although the bands are not always consistent. This, however, does not necessarily mean that the *coxL* genes are not expressed and could simply result from error during any of the steps preceding gel electrophoresis. Double bands were seen again with the CoxL2 primer. This was the same primer set used throughout the research. The gel order for Control 2 was the same as for Control 1. Duplicates were run for negative controls as well as for the samples taken at each time point and for the time point itself (top and bottom of gel). For the second designed primer sets for *coxL* and *coxL1*, the amplicon sizes were 251 and 294 bp. The primer set for *coxL2* was the same as the previous set with an amplicon size of 379 bp. The primer sets were also run at the new optimum temperatures.

Experiment 1 was run with the second primer sets for *coxL* and *coxL1* and the original primer set for *coxL2*. Examining each of the gels run for the time point samples shows clearer bands with less *coxL1* expression compared to those from Controls 1 and 2 (Figures 3.10 and 3.11). There is also less contamination to the samples with only one gel showing expression in one of the negative controls at time point 1. There are still some multiple band amplicons especially seen in the overall CoxL primer set. The CoxL2 primer set shows the most consistent expression over all the time points. Again the order for the gels is the same as shown previously with duplicates run for each negative control, CoxL, CoxL1, and CoxL2. Also, duplicates are run for each time point on the top and bottom of the gel.



A.

B.

Figure 3.10: Experiment 1 with elevated CO; Each gel represents a different time point. The top and bottom of the gel represent the two bacteria samples taken at that time point (a and b). Run from left to right in each gel: lane I, ladder; lanes II and III, negative control no RNA; lanes IV and V, negative control no reverse transcription (RT) step; lanes VI and VII, CoxL; lanes VIII and IX, CoxL1; lanes X and XI, CoxL2. A standard ladder is run in the first well on the left for each gel as a measurement of amplicon base pair size. A) 1a & 1b; B) 2a & 2b

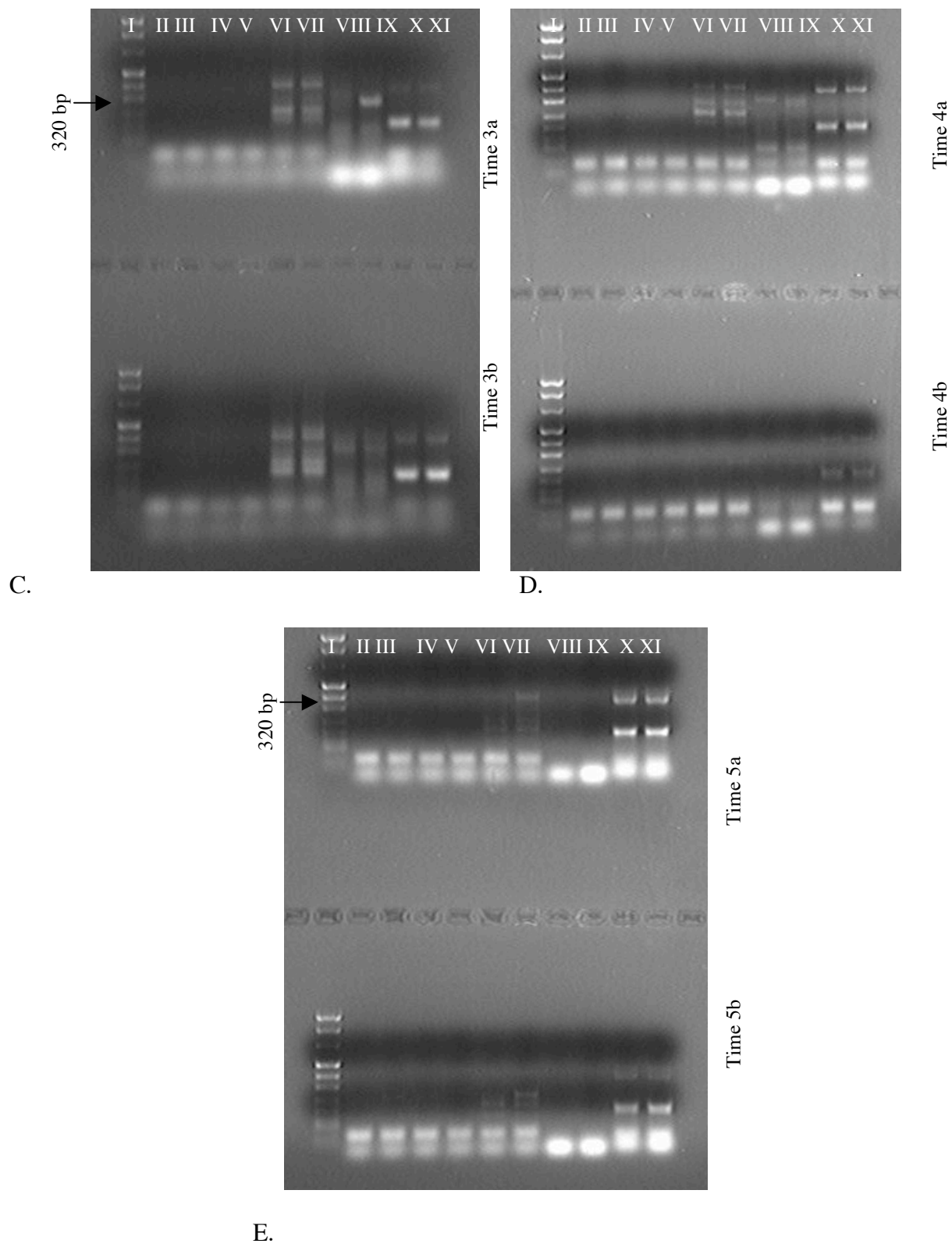


Figure 3.11: Experiment 1 with CO; C) 3a & 3b; D) 4a & 4b; E) 5a & 5b

Time point 1 (0 hr.) showed expression for each primer set with multiple bands for the CoxL and CoxL2 primer sets. Also there was some expression in the negative control (with no RT step) at 251 bp (Figure 3.10). Time point 2 (12 hrs.) showed expression only with the CoxL and CoxL2 primers with fewer multiple bands and also no expression with the CoxL1 primer set. Time point 3 (23 hrs.) again showed expression with all three primer sets with multiple bands in CoxL and CoxL2. Time point 4 (37 hrs.) showed expression with CoxL and CoxL2 with a faint band in CoxL1. Time point 5 (60 hrs.) showed clear expression with CoxL2 only.

After seeing less CoxL1 expression in the Experiment 1 gels, the CoxL1 and CoxL2 primer sets were examined more closely to see if conclusions could be drawn about a difference in expression. The samples for those time points run in Experiment 1 were rerun along with new samples from Experiment 2 that used higher [CO] as a starting point. In the gel for Experiment 2 are time points 1 (0 hr.); 3 (19 hrs.); 5 (43 hrs.); 7 (91 hrs.); & 9 (139 hrs.) In these gels the overall CoxL primer set was not run since it seemed to show expression throughout the previous experiments and controls. Additionally, the question addressed here was the potential difference in expression between the two *coxL* genes.

For this case, positive and negative controls were used to gauge expression for each primer set. The negative controls were the same as in the previous gels with no RNA and no RT step. The positive controls were taken from samples in the control trials that showed consistent *coxL1* and *coxL2* expression. The positive control for *coxL1* and *coxL2* were from time point 5b in Control Trial 2, both showing positive *coxL* gene expression in previous trials.

It is apparent that the CoxL2 primer set showed expression more consistently than the CoxL1 primer set. The bands present for *coxL2* shown on the gel in both experiments reflect this (Figures 3.12 and 3.13). Experiment 1 samples from time points 1-5a showed expression in both

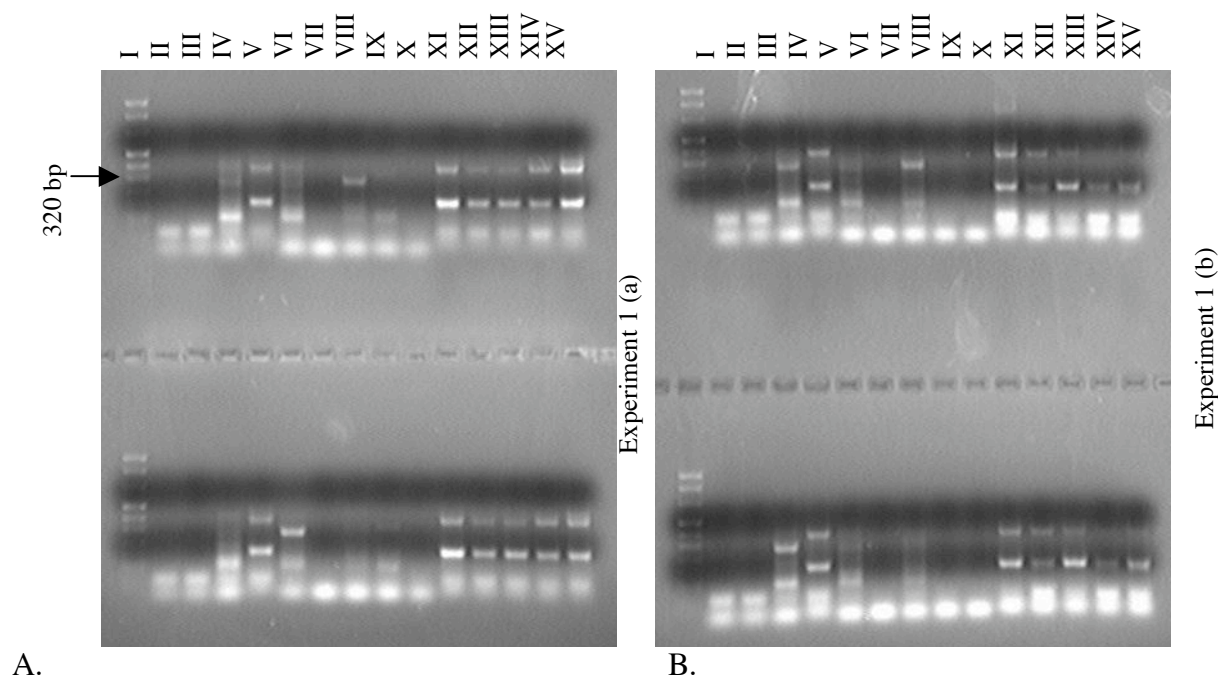


Figure 3.12: Experiment 1 with CO, CoxL1 and CoxL 2; Each gel represents all times points run for a particular trial. The top and bottom represent duplicates of one bacteria sample taken at each time point during a particular trial. Run from left to right in each gel: lane I, standard ladder; lane II, negative control no RNA; lane III, negative control no reverse transcription (RT) step; lane IV, positive control for CoxL1; lane V, positive control for CoxL2; lane VI, CoxL1 for time point 1; lane VII, CoxL1 for time point 2; lane VIII, CoxL1 for time point 3; lane IX, CoxL1 for time point 4; lane X, CoxL1 for time point 5; lane XI, CoxL2 time point 1; lane XII, CoxL2 for time point 2; lane XIII, CoxL2 for time point 3; lane XIV, CoxL2 for time point 4; lane XV, CoxL2 for time point 5. A standard ladder is run in the first well on the left for each gel as a measurement of amplicon base pair size. The RNA extracted at each time point was grouped on the gel so that the primer set for *coxL1* was run for all time points followed by the primer set for *coxL2* for all time points.

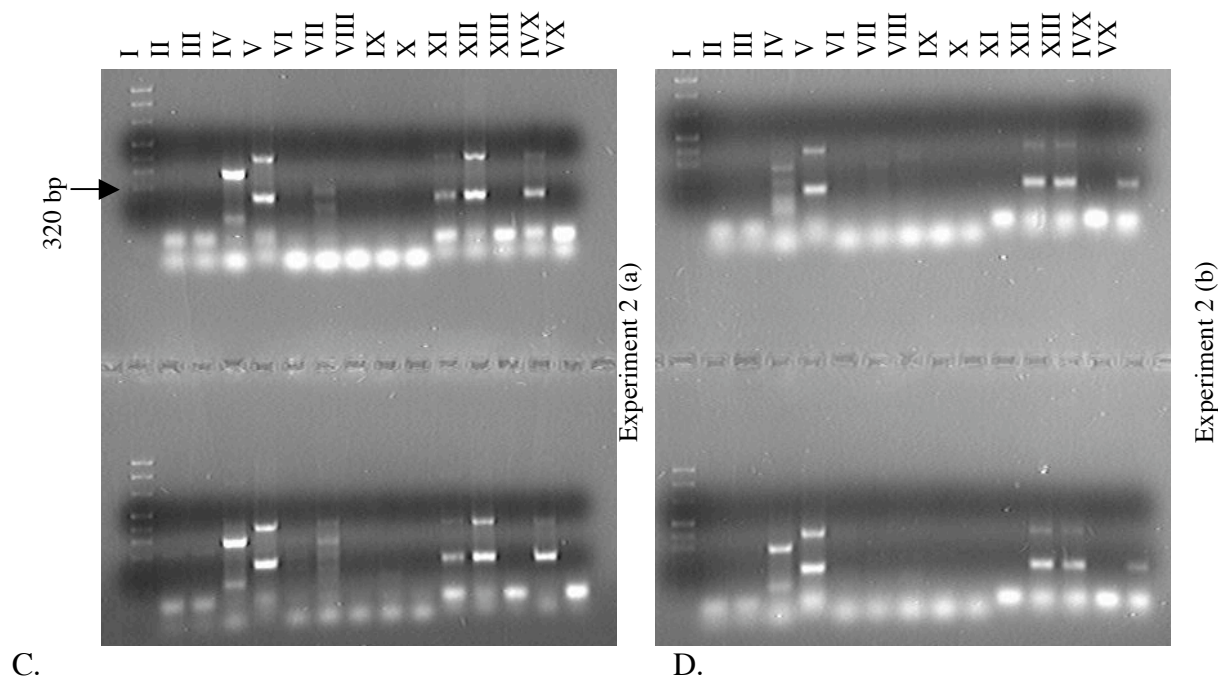


Figure 3.13: Experiment 2 with CO, CoxL1 and CoxL 2; Each gel represents all times points run for a particular trial. The top and bottom represent duplicates of one bacteria sample taken at each time point during a particular trial. Run from left to right in each gel: lane I, standard ladder; lane II, negative control no RNA; lane III, negative control no reverse transcription (RT) step; lane IV, positive control for CoxL1; lane V, positive control for CoxL2; lane VI, CoxL1 for time point 1; lane VII, CoxL1 for time point 3; lane VIII, CoxL1 for time point 5; lane IX, CoxL1 for time point 7; lane X, CoxL1 for time point 9; lane XI, CoxL2 time point 1; lane XII, CoxL2 for time point 3; lane XIII, CoxL2 for time point 5; lane XIV, CoxL2 for time point 7; lane XV, CoxL2 for time point 9. A standard ladder is run in the first well on the left for each gel as a measurement of amplicon base pair size. The RNA extracted at each time point was grouped on the gel so that the primer set for *coxL1* was run for all time points followed by the primer set for *coxL2* for all time points.

positive controls at the appropriate amplicon sizes with some expression seen for CoxL1 in one time point and for CoxL2 at all time points. In Experiment 1 with samples from time points 1-5b, expression was seen in both positive controls, again only one time point for CoxL1, and multiple time points for CoxL2. In Experiment 2, with samples from time points 1,3,5,7, & 9a expression was seen in both positive controls, faintly in one time point for CoxL1, and three time points for CoxL2. In Experiment 2, with samples from time points 1, 3, 5, 7, & 9b, expression was seen in both positive controls, no expression was seen in any of the CoxL1, and only three time points in CoxL2.

### 3.6.1 *coxL* Gene Expression in BMS and OMP Clades

Two clades of marine bacterial protein show *coxL* gene expression, OMP and BMS. *S. pomeroyi* has genes in both clades with two *coxL* genes, 1 & 2. In looking at the gene expression of the overall *coxL* gene (CoxL) and the two *coxL* genes separately (CoxL1 and CoxL2), it was noted that while expression seems to occur at various conditions of [CO] the *coxL1* gene expression was less prevalent. The *coxL2* gene showed expression throughout the experiments both with high and low CO. In the presence of high [CO], however, there was less *coxL1* gene expression relative to *coxL2* gene, with few or no bands in the gels run. The only consistent expression of *coxL1* was in the controls with a very low concentration of CO, those bubbled with CO free air.

### 3.7 Impact of *Silicibacter pomeroyi* on Marine CO Concentration

An estimated impact of *Silicibacter pomeroyi*-like bacteria on coastal CO concentrations was modeled using the determined oxidation rate constant of *Silicibacter* from this study and

yearly average CO photoproduction rates calculated from nine years of remote sensing SeaWiFS data (provided by C. F. Fichot). The CO photoproduction rates were calculated for coastal water off of Sapelo Island, Georgia (80.91°W, 31.181°N) using the CDOM and CO Apparent Quantum Yield spectra shown in Figure 3.14. The CO photoproduction rates were depth integrated over typical mixed layer depths (20 m, 10 m, and 50 m) and converted into concentration values for the water column. These production values were added to a starting CO concentration of 15 nM and the determined oxidation rates by *S. pomeroyi* were subtracted using a 1-hour time step to give the new [CO] within the modeled mix layer. The oxidation rates changed according to available [CO] as in equation 3.6. The resulting values were plotted versus time over 3 sequential 24-hour cycles to give projected daily CO concentrations and quantify the possible drawdown by marine bacteria (Table 3.8 and Figures 3.15 and 3.16). The calculation did not include wind driven gas exchange and it was assumed that the water column was well mixed over the defined mixed layer depth. The following equations were used to generate the plots of [CO]:

$$[\text{CO}]_s + \text{CO}_p = [\text{CO}]_t \quad (3.5)$$

$$[\text{CO}]_c = \frac{d[\text{CO}]}{dt} = (n)([\text{CO}]_t)(k_c) \quad (3.6)$$

$$[\text{CO}]_t - [\text{CO}]_c = [\text{CO}]_f \quad (3.7)$$

where  $[\text{CO}]_s$  is a starting CO concentration (typical for coastal waters),  $\text{CO}_p$  is the photoproduced CO over the time step,  $[\text{CO}]_t$  is the total CO concentration once photoproduced CO is added to the starting concentration,  $n$  the number of bacterial cells per ml,  $k_c$  is the cell normalized CO oxidation rate constant found in this study,  $[\text{CO}]_c$  is the amount of CO consumed over the time step, and  $[\text{CO}]_f$  is the final CO concentration which is plotted (Figures 3.14 and 3.15). This sequence is repeated over each time step to generate a new [CO] for the mixed layer.

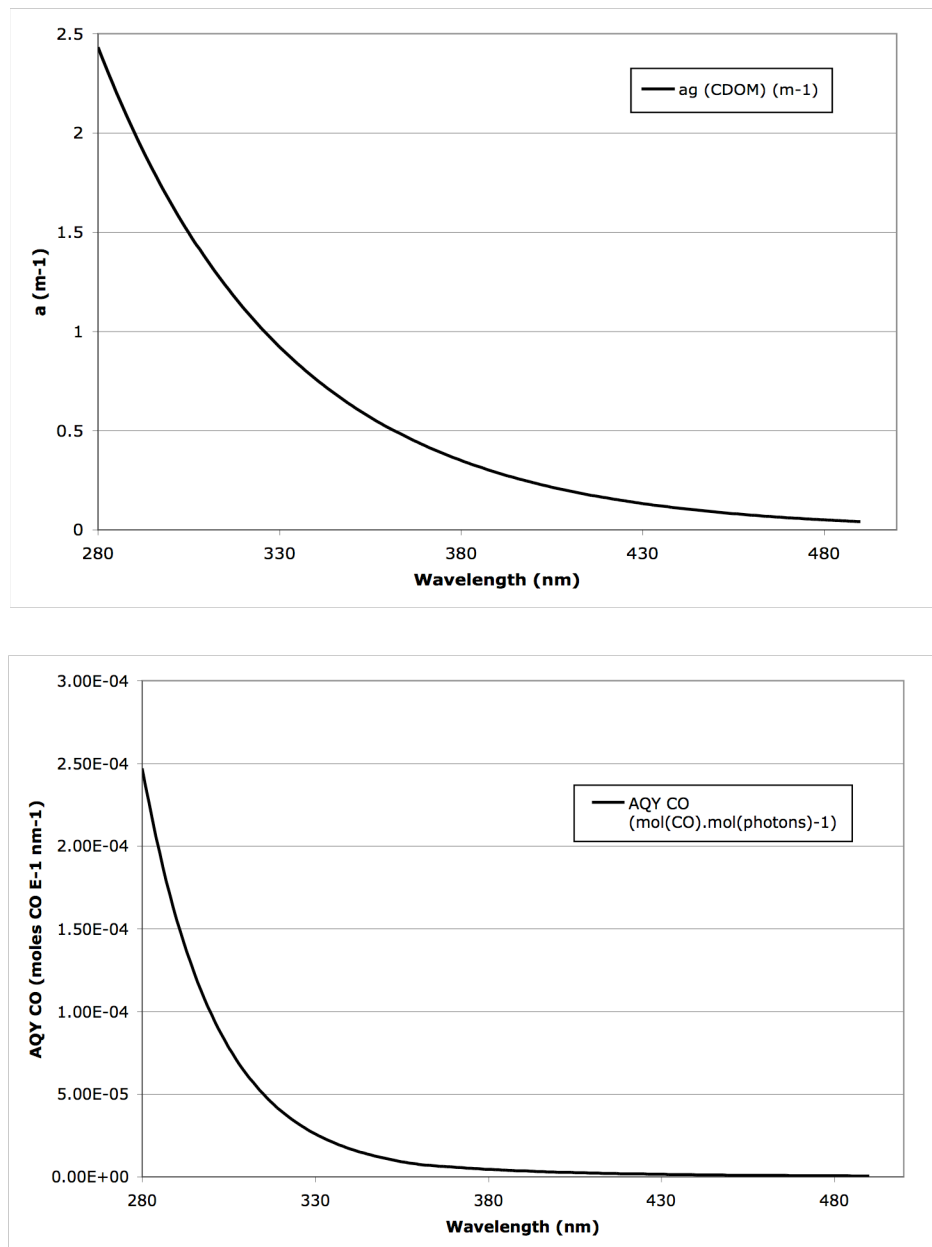
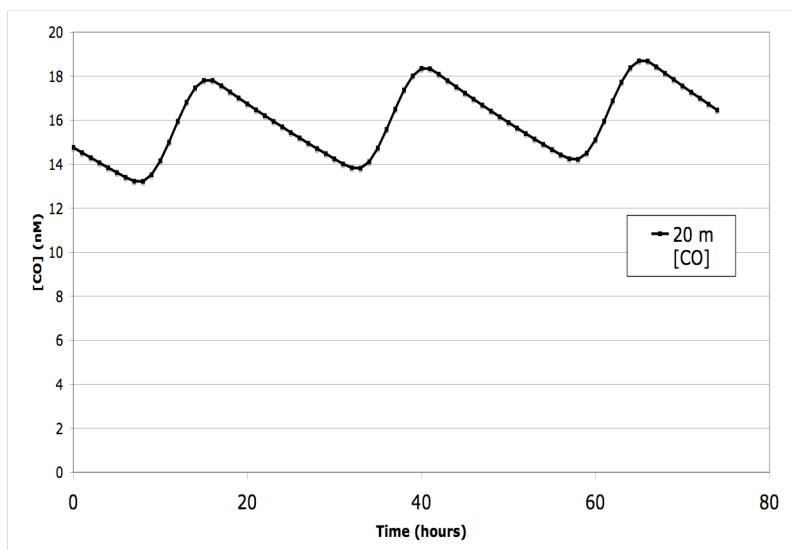


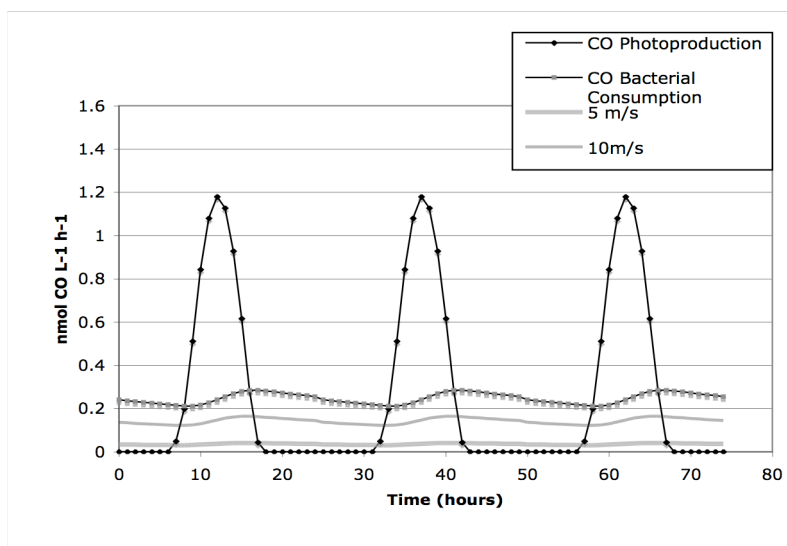
Figure 3.14: Colored dissolved organic matter and apparent quantum yield spectra. The spectra are estimated from 9-years of remote sensing data for coastal water off of Sapelo Island, Georgia ( $80.91^{\circ}\text{W}$ ,  $31.181^{\circ}\text{N}$ ) for the month of January. The CO AQY is based on an average from Zafiriou et al. [2003] and Ziolkowski [2000].

Table 3.8: CO Impact model. CO photoproduction over a 24-hour period is added to an average for coastal CO concentration (20 m depth). Generated bacterial consumptions from CO oxidation rates are subtracted from the total CO concentration to give a predicted impact of *S. pomeroyi* and CO consuming bacteria on overall marine CO concentration.

Time (hours)	CO Photoproduction nmol CO L <sup>-1</sup> h <sup>-1</sup>	[CO]+ photoproduction	CO consumption	Total [CO]-bacterial consumption
0	0	15	0.24	14.76
1	0	14.760	0.236	14.524
2	0	14.524	0.232	14.291
3	0	14.291	0.229	14.063
4	0	14.063	0.225	13.838
5	0	13.838	0.221	13.616
6	0	13.616	0.218	13.399
7	0.0495	13.448	0.214	13.234
8	0.1997	13.433	0.212	13.222
9	0.5119	13.733	0.212	13.522
10	0.8423	14.364	0.216	14.148
11	1.0809	15.229	0.226	15.002
12	1.1798	16.182	0.240	15.942
13	1.1267	17.069	0.255	16.814
14	0.9275	17.741	0.269	17.472
15	0.6165	18.089	0.280	17.809
16	0.2833	18.092	0.285	17.808
17	0.0437	17.851	0.285	17.566
18	0.0001	17.566	0.281	17.285
19	0	17.285	0.277	17.009
20	0	17.009	0.272	16.737
21	0	16.737	0.268	16.469
22	0	16.469	0.264	16.205
23	0	16.205	0.259	15.946
24	0	15.946	0.255	15.691



A.



B.

Figure 3.15: CO Photoproduction vs. Bacterial Consumption. A.) Depth integrated (20 m) rates for CO photoproduction using typical mid-month (15) the climatologies based on 9 years of remote sensing data (Sep 1997 - Aug 2006). The above data was taken for the month of January. Carbon monoxide photoproduction is added to a starting  $[CO]$  of 15 nM at  $t=0$ . B.) Comparative rates for CO production, consumption, and ventilation to the atmosphere at wind speeds of 5 m/s and 10 m/s. Ventilation not included in (A).

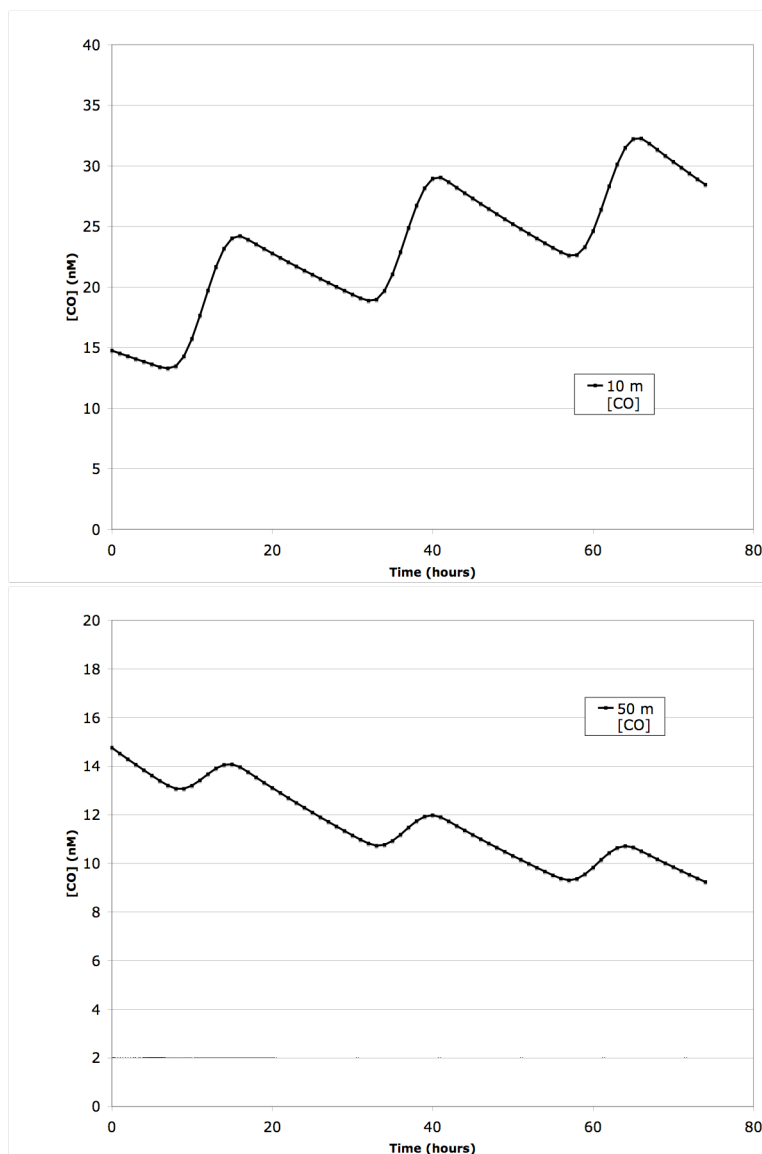


Figure 3.16: CO Photoproduction vs. Bacterial Consumption. Depth integrated (10 m, and 50 m) rates for CO photoproduction typical mid-month (15) the climatologies based on 9 years of remote sensing data (Sep 1997 - Aug 2006). The above data was taken for the month of January. Carbon monoxide photoproduction is added to a starting [CO] of 15 nM.

A population of  $2.5 \times 10^5$  cells  $\text{ml}^{-1}$  was estimated for all CO consuming bacteria using an average value for the total percentage of CO consumers found in coastal waters (Moran and Miller, 2007). This average percentage of CO consuming bacteria was assumed to be 25% of all bacteria in a typical sea water bacterial sample ( $10^6$  cell  $\text{ml}^{-1}$ ). This average population was then assumed to act like *Silicibacter pomeroyi* in terms of the cell normalized oxidation rate constant, giving an oxidation rate constant used together with our cell normalized oxidation rate of  $7.1 \times 10^{-11}$  ml cell $^{-1}$  h $^{-1}$  and oxidation rate constant of  $k_{co}=0.0193$  h $^{-1}$ . Under these conditions, *S. pomeroyi* reduced the steady state concentration of CO on the order of 0.24 nM h $^{-1}$  over the first hour and continued to reduce the [CO] over the 24-hour cycle by an average of 0.25 nM h $^{-1}$ .

While not used in the calculations, a rough estimate of the potential effect of wind driven gas exchange on a 20 m mixed layer was also plotted along with CO photoproduction rates and CO consumption rates for a 24-hr. period (Figure 3.14 B). The CO gas flux to the atmosphere was calculated using a sea-to-air gas exchange equation by Stubbins et al. [2006]:

$$R_f = k_{CO} \Delta CO = k_{CO} (CO_w - \alpha CO_a) \quad (3.8)$$

The gas transfer velocity for CO,  $k_{co}$ , was estimated from  $k_{CO_2}$  values determined by Jähne and Haußecker [1998]. The Schmidt number for CO,  $Sc_{CO}$ , was estimated as 500 (Jähne and Haußecker 1998) and used to calculate  $k_c$  using the equation  $k_{CO}=(Sc_{CO}/600)^{-0.5}$ . The surface water equilibrium ( $\alpha CO_a$ ) was estimated to be 0.14 nmol L $^{-1}$  as determined by Stubbins et al. [2006].

The values plotted for the impact of CO oxidizing bacteria on CO concentration were determined by CO photoproduction rates from the month of January. These rates were typical of all twelve months with slight variation from winter to summer. The summer months represent a greater contribution from photoproduction because of greater solar radiation. The range of total

CO production from January (minimal photoproduction) to July (maximum photoproduction) is on the order of 0.025 nM CO at the height of solar radiation, noon. The plotted values for both January and July follow the same diurnal pattern varying only in degree of added photoproduction to the initial CO concentrations.

## CHAPTER 4

### DISCUSSION

#### **4.1 CO Oxidation by *Silicibacter pomeroyi***

CO was drawn down in an exponential fashion by *Silicibacter pomeroyi* in the kettle reactor for both Experiment 1 and Experiment 2. The higher initial CO concentration for Experiment 2 was just above the average for coastal [CO] and was drawn down by *S. pomeroyi* to just below the average concentration for open ocean CO. In the second experiment with CO, *S. pomeroyi* was introduced after the CO concentration had been raised to  $17.52 \text{ nM} \pm 0.33 \text{ nM}$ . The bacteria were able to draw down the CO concentration over 139 hours to  $1.26 \text{ nM} \pm 0.08 \text{ nM}$ . In the previous experiment, which bubbled CO into a kettle with *S. pomeroyi* already present, *S. pomeroyi* was able to reduce the CO to very low concentrations, on the order of  $0.25 \text{ nM} \pm 0.02 \text{ nM}$ . These results are similar to those of Moran et al. [2004] who found that *S. pomeroyi* was able reduce the overall CO concentration to  $0.11 \text{ nM}$  after 50 hours of incubation ( $0.11 \text{ nM}$  is equivalent to a headspace equilibrium concentration of  $0.13 \pm 0.05 \text{ ppm}$ ).

#### **4.2 CO Oxidation Rate**

For the calculation of oxidation rate, there was little variation in the bacterial growth after the MBM inoculated with *Silicibacter* was taken out of the  $30^\circ\text{C}$  incubator. At room temperature, there was slow bacterial growth over the time period for these experiments bubbled with CO, therefore the bacterial number was averaged over the time period for the oxidation

rates after the initial 8 hours of growth. Our cell normalized CO oxidation rate for *S. pomeroyi* was found to be very similar to that calculated from data collected by Moran et al. (2004). Moran et al. [2004] performed CO drawdown experiments over a period of approximately 75 hours. For comparison, CO concentrations and time were estimated from their Supplementary Figure S2 (Moran et al., 2004) and used to estimate a cell normalized CO oxidation rate of  $2.23 \times 10^{-11}$  ml cell<sup>-1</sup> h<sup>-1</sup>. This was of the same order of magnitude as the cell normalized oxidation rate in this study of  $7.14 \times 10^{-11}$  ml cell<sup>-1</sup> h<sup>-1</sup>. For further details of the calculations of the cell normalized CO oxidation rate from the Moran et al. [2004] data see Appendix E.

#### **4.3 *coxL* Gene Expression in *Silicibacter pomeroyi***

Gene expression for *coxL* was seen at all levels of [CO] present in all experiments, which were all conducted within the [CO] range found in the ocean. This suggests that *S. pomeroyi* is expressing the *coxL* gene at all times in the environment. Consequently, *S. pomeroyi* must always gain some sort of energy benefit by having these genes expressed at all [CO].

In Control 1, most lanes showed some contamination in one of the negative controls, usually the no RT control. This suggests that DNA remained in the sample after RNA extraction. Even though there was contamination in some of the gels, it is clear that there is still expression of the *coxL* gene seen by bands present in all three of the primer sets designed. Two of the gels show absolutely no bands in any of the wells. These RNA samples were all taken through the RT step on the same day and suggest there was an error in the preparation for PCR and gel electrophoresis. The gels for Control 2 were performed with the improved set of primers and showed much clearer bands with fewer multiple band patterns, though *coxL2* was always

seen to have two bands present. After the redesign, there was also less apparent expression in the negative controls and expression in all of the primer sets for *coxL*.

In the elevated CO experiments, only one gel (Experiment 1, time point 1b) shows expression in a negative control with all other gels showing no negative control expression. All time points in Experiment 1 show expression in all three primer sets, confirming gene expression at high and low levels of CO concentration which suggests that *coxL* is expressed constitutively or that CO concentration is not the trigger for expression. Experiment 1 was reanalyzed and Experiment 2 was run for the first time using *coxL1* and *coxL2* to better compare any differences the two genes may have in expression. Expression is still shown, predominantly for *coxL2*, with very little, if any expression for *coxL1*.

Since initial results suggest that *Silicibacter pomeroyi*'s expression of *coxL* may be constitutive, then oxidation may be a continuous process in marine surface waters rather than being regulated by ambient CO concentrations. The impact of constitutive *coxL* gene expression is evident from the overall abundance and importance of marine Roseobacters as CO consumers. *S. pomeroyi* and its relatives in the Roseobacter clade comprise around 10-20% of coastal and oceanic mixed-layer bacterioplankton (Moran et al., 2004).

Although the microbial strains isolated from coastal seawater that oxidize CO at environmental concentrations are phylogenetically diverse, the most active strains are closely related to the Roseobacter clade of alphaproteobacteria (Tolli et al., 2006). Tolli et al. [2006] found that 15% of the environmental CO oxidation occurring off the coast of New England could be attributed to Roseobacter-like organisms. Given the high rates of CO oxidation by some Roseobacter isolates and their abundance *in situ*, Roseobacter organisms are therefore likely to be important contributors to total CO oxidation in coastal waters (Tolli et al., 2006). Given that

*Silicibacter* shows constitutive expression of its *coxL* gene in this study, this contribution may be more important than previously recognized. Microbiological studies to determine the identity, abundance, and phylogenetic relatedness of microorganisms responsible for environmental CO oxidation have the potential to improve our understanding of this component of carbon cycling in natural waters (Tolli and Taylor, 2005).

#### 4.3.1 Differences in *coxL1* and *coxL2* Gene Expression

The original goal of this thesis was to examine the overall *coxL* gene expression but primers were designed also for the two individual *coxL* genes to look at potential differences in expression. In the initial experiments, with low levels of CO, both genes show expression (Control 2 after redesign of primers). However, looking at the expression when the levels of CO were much higher, *coxL1* may not be as consistently expressed. The OMP clade gene, *coxL2*, seems to be the primary gene expressed in this higher CO situation. In the gels of Experiment 2 run with the *CoxL2* primer set, some wells do not show expression, with no amplicon bands present. In this case, it is likely that the RNA has been degraded. The products of PCR are more likely to produce false negatives than false positives.

There is the possibility that each gene has a different affinity for CO. The co-occurrence of BMS and OMP *coxL* sequences raises questions about the expression and physiological and ecological roles of CO dehydrogenases (King 2003). Whether both are expressed in the same organism and under what conditions are not known (King 2003). However, BMS and OMP *coxL* may affect whole cell affinity for CO, since *Aminobacter sp.* strain COX, a high-affinity CO oxidizer, may contain only BMS *coxL* while *O. carboxidovarens*, a low-affinity CO oxidizer, contains only the OMP sequence. The gene expression found for the two *coxL* genes in

*Silicibacter pomeroyi* is consistent with King's [2003] findings. From this study it can be determined that for *Silicibacter pomeroyi*, the *coxL1* gene (BMS clade) is expressed at lower [CO] while the *coxL2* gene (OMP clade) is expressed at higher [CO].

#### 4.4 Modeled Impact of CO Oxidizing Bacteria

From the oxidation rates calculated, a model for CO consumption by *S. pomeroyi*-like CO consuming marine bacteria was generated. This oxidation resulted in an overall diurnal pattern of [CO], ranging from 13 nM to 18 nM. This is a slightly high range for coastal [CO] (average 12 nM; Jones and Amador, 1993). However, wind gas exchange was not considered in this model. Including wind driven gas exchange may account for the additional loss of CO, bringing the [CO] down to measured levels. Based on typical *in situ* data for an estimated population of CO consuming bacteria and an average initial concentration of coastal CO, a curve was produced with peaks of highest CO concentration approximately 3 hours past mid-day. This time peak is similar to that of *in situ* measurements in which surface water [CO] showed a maximum and minimum occurring early in the afternoon and morning (Ohta, 1997). The mid-afternoon peak also argues against the mechanistic findings from Conrad et al. [1982]. In this model, CO photoproduction is instantaneous with no time lag due to a reaction mechanism that creates CO over a period of time. The post-noon maximum is instead a function of the balance of kinetics for CO photoproduction and microbial consumption.

Based on the model for CO photoproduction and bacterial consumption, it is possible that *Silicibacter*-like organisms consume  $0.25 \text{ nM h}^{-1}$  of the coastal CO, oxidizing it into  $\text{CO}_2$ . This translates into an important impact to the overall CO and carbon cycle. It was also found that 89% of CO produced from photochemistry in a 24-hr period is consumed by bacteria under the

assumptions of the model. This compares to the Zafiriou et al. [2003] estimates that marine bacterioplankton are the dominant sink for CO in the surface ocean, consuming around 86% of the CO that is produced photochemically from DOM.

## CHAPTER 5

### CONCLUSION

#### 5.1 Concluding Statements

From this research we concluded that *coxL* gene expression in *Silicibacter pomeroyi* is constitutive at all levels of [CO] present in our experiments, which were conducted within the [CO] range found in the ocean. This suggests that *S. pomeroyi* are expressing the *coxL* gene at all times and for *S. pomeroyi*, it is always energetically beneficial to turn on the *coxL* genes. Within the [CO] tested, carbon monoxide concentration was not a trigger for gene expression. There was a detectable difference in expression observed between the two *coxL* genes, *coxL1* and *coxL2*, with *coxL1* expressed at low [CO] and *coxL2* expressed at both low and high [CO]. A CO oxidation rate and cell normalized rate constant were determined for *Silicibacter pomeroyi* and were used to model an impact of CO consuming bacteria on oceanic [CO]. The simple model determined that under these specific conditions *S. pomeroyi* and other CO consuming bacteria would drawdown CO concentration in coastal waters by an average of 0.25 nM h<sup>-1</sup>. It also projected 89% of CO produced from photochemistry in a 24-hr period is consumed by bacteria under the assumptions of the model. The model also confirms that the cell normalized CO oxidation rates determined for *S. pomeroyi* in the laboratory is roughly suitable for use in oceanic models.

## 5.2 Future Research

This research was able to answer some questions surrounding *Silicibacter pomeroyi* and CO consumption but questions still remain for future research. This study was conducted in the lab on an isolated strain of marine bacteria, *Silicibacter pomeroyi* (DSS-3). The next step in classifying the impact of *S. pomeroyi* on marine CO oxidation is to take the research out of the lab and into the field. With well-designed primer sets for *coxL* based on the known genome of *S. pomeroyi*, the CO gene expression from field bacterial samples can be conducted. These bacteria were isolated off the coast of Georgia, which would be an appropriate field site to carry out future research to see if CO oxidation rates calculated in the lab are representative of environmental rates. Also since *Silicibacter* belongs to the dominant marine Roseobacter clade, which may account for a large percentage of overall CO oxidation, it is possible that it can be used as a proxy for the overall CO oxidizing community for study of oxidation rates and expression patterns.

From this study it was found that CO concentration is not the determining factor for *coxL* gene expression but it is possible that expression may be influenced by another factor. There is a potential for the CO gene to be regulated by light in some Roseobacter organisms. A blue light sensor was found in a relative of *S. pomeroyi*, TM1040 (Moran personal communication). *S. pomeroyi* however does not have the blue light sensing capabilities that TM1040 has so it is unclear if this has any relevance to *S. pomeroyi's coxL* gene expression. Another thought is that regulating *coxL* gene expression might serve as a defensive strategy against reactive oxygen species for these particular bacteria, turning off the gene as a protective mechanism. Any of these possibilities would be tests for future research to narrow down the environmental regulation for genetic expression of *coxL*.

## REFERENCES

- Azam, F. Microbial Control of Oceanic Carbon Flux: The Plot Thickens. *Science*. 280 (5364) 694-696. 1998.
- Bates, T. S. et al. Regional and seasonal variations in the flux of oceanic carbon monoxide to the atmosphere. *Journal of Geophysical Research*. 100 (D11) 23,093-23,101. 1995.
- Bauer, K., R. Conrad, and W. Seiler. Photooxidative Production of Carbon Monoxide by Phototrophic Microorganisms. *Biochimica et Biophysica Acta*. 589: 46-55. 1980.
- Buchan, A., J. M. Gonzalez, and M. A. Moran. Overview of the Marine *Roseobacter* Lineage. *Applied and Environmental Microbiology*. 71 (10) 5665-5677. 2005.
- Conrad, R. and W. Seiler. Photooxidative Production and Microbial Consumption of Carbon Monoxide in Seawater. *FEMS Microbiology Letters*. 9: 61-64. 1980.
- Conrad, R., O. Meyer, and W. Seiler. Role of Carboxydobacteria in Consumption of Atmospheric Carbon Monoxide by Soil. *Applied and Environmental Microbiology*. 42 (2) 211-215. 1981.
- Conrad, R. et al. Carbon Monoxide in Seawater (Atlantic Ocean). *Journal of Geophysical Research*. 87 (C11) 8839-8852. 1982.
- Conrad, R. and W. Seiler. Utilization of Traces of Carbon Monoxide by Aerobic Oligotrophic Microorganisms in Ocean, Lake, and Soil. *Archives of Microbiology*. 132: 41-46. 1982.
- Cooper, W. J. et al. Sunlight-Induced Photochemistry of Humic Substances in Natural Waters: Major Reactive Species. *Advances in Chemistry Series*. 219: 333-361. 1989.
- Diekert, G. B. and R. K. Thauer. Carbon Monoxide Oxidation by *Clostridium thermoaceticum* and *Clostridium formicoaceticum*. *Journal of Bacteriology*. 136 (2) 597-606. 1978.
- Dunfield, K. E. and G. M. King. Molecular Analysis of Carbon Monoxide-Oxidizing Bacteria Associated with Recent Hawaiian Volcanic Deposits. *Applied and Environmental Microbiology*. 70 (7) 4242-4248. 2004.
- Erickson, D. J. Ocean to Atmosphere Carbon Monoxide Flux: Global Inventory and Climate Implications. *Global Biogeochemical Cycles*. 3 (4) 305-314. 1989.

Erickson, D. J. and J. A. Taylor. 3-D Tropospheric CO Modeling: The Possible Influence of the Ocean. *Geophysical Research Letters*. 19 (19) 1955-1958. 1992.

Gnanadesikan, A. Modeling the diurnal cycle of carbon monoxide: Sensitivity to physics, chemistry, biology, and optics. *Journal of Geophysical Research*. 101 (C5) 12,177-12,191. 1996.

Gonzalez, J. M. and M. A. Moran. Numerical Dominance of a Group of Marine Bacteria in the  $\alpha$ -Subclass of the Class *Proteobacteria* in Coastal Seawater. *Applied Environmental Microbiology*. 63 (11) 4237-4242. 1997.

Gonzalez, J. M. et al. *Silicibacter pomeroyi* sp. nov. and *Roseovarius nubinhibens* sp. nov., dimethylsulfoniopropionate-demethylating bacteria from marine environments. *International Journal of Systematic and Evolutionary Microbiology*. 53: 1261-1269. 2003.

Greenberg, A. E., L. S. Clesceri, and A. D. Eaton. *Standard Methods for the Examination of Water and Wastewater*. 18<sup>th</sup> edition. 1992.

Hardy, K. and G. M. King. Enrichment of High-Affinity CO Oxidizers in Maine Forest Soil. *Applied and Environmental Microbiology*. 67 (8) 3671-3676. 2001.

Hirsch et al. Life under the conditions of low nutrient concentrations. *Strategies of microbial life in extreme environments*. Verlag Chemie. 243-260. 1979.

Hobbie, J.E., R.J. Daley, and S. Jasper. Use of Nuclepore Filters for Counting Bacteria by Fluorescence Microscopy. *Applied and Environmental Microbiology*. 1225-1228. 1977.

Jähne, B. and H. Haußecker. Air-Water Gas Exchange. *Annual Review Fluid Mechanics*. 30: 443-68. 1998.

Johnson, J. E. and T. S. Bates. Sources and sinks of carbon monoxide in the mixed layer of the tropical South Pacific Ocean. *Global Biogeochemical Cycles*. 10 (2) 347-359. 1996.

Jones, R. D. and R. Y. Morita. Carbon monoxide oxidation by chemolithotrophic ammonium oxidizers. *Can. Journal of Microbiology*. 29: 1545-1551. 1983.

Jones, R. D. and J. A. Amador. Methane and Carbon Monoxide Production, Oxidation, and Turnover Times in the Caribbean Sea as Influenced by the Orinoco River. *Journal of Geophysical Research*. 98 (C2) 2353-2359. 1993.

Kang, B. S. and Y. M. Kim. Cloning and Molecular Characterization of the Genes for Carbon Monoxide Dehydrogenase and Localization of Molybdopterin, Flavin Adenine Dinucleotide, and Iron-Sulfur Center in the Enzyme of *Hydrogenophaga pseudoflava*. *Journal of Bacteriology*. 181 (18) 5581-5590. 1999.

Kettle, A. J. Diurnal Cycling of Carbon Monoxide (CO) in the Upper Ocean Near Bermuda. *Ocean Modeling*. 8: 337-367. 2005.

Kerby, R. L., S. S. Hong, S. A. Ensign, L. J. Coppoc, P. W. Ludden, and G. P. Roberts. Genetic and Physiological Characterization of the *Rhodospirillum rubrum* Carbon Monoxide Dehydrogenase System. *Journal of Bacteriology*. 174 (16) 5284-5294. 1992.

Khalil, M. A., and R. A. Rasmussen. The Global Cycle of Carbon Monoxide: Trends and Mass Balance. *Chemosphere*. 20 (1-2) 227-242. 1990.

Kieber, D. J., J. McDaniel, and K. Mopper. Photochemical source of biological substrates in sea water: implications for carbon cycling. *Letters to Nature*. 341: 637-639. 1989.

King, G. M. Molecular and Culture-Based Analyses of Aerobic Carbon Monoxide Oxidizer Diversity. *Applied and Environmental Microbiology*. 69 (12) 7257-7265. 2003.

King, G. M. Nitrate-Dependent Anaerobic Carbon Monoxide Oxidation by Aerobic CO-Oxidizing Bacteria. *FEMS Microbiol. Ecol.* 56: 1-7. 2006.

Leifer, A. The kinetics of environmental aquatic photochemistry. American Chemical Society. Chapter 1. 1998.

McConnel, J. C. and M. B. McElroy. Natural Sources of Atmospheric CO. *Nature*. 233: 187-188. 1971.

Miller, W. L. and R. G. Zepp. Photochemical production of dissolved inorganic carbon from terrestrial organic matter: Significance to the oceanic organic carbon cycle. *Geophysical Research Letters*. 22 (4) 417-420. 1995.

Miller, W. L. and M. A. Moran. Interaction of Photochemical and Microbial Processes in the Degradation of Refractory Dissolved Organic Matter from a Coastal Marine Environment. *Limnology and Oceanography*. 42 (6) 1317-1324. 1997.

Miller, W. L. An Overview of Aquatic Photochemistry as it Relates to Microbial Production. *Microbial Biosystems: New Frontiers. Proceedings of the 8<sup>th</sup> International Symposium on Microbial Ecology*. Atlantic Canada Society for Microbial Ecology, Halifax, Canada, 1999.

Mopper, K. and D. J. Kieber. Marine photochemistry and its impact on carbon cycling. The effects of UV radiation in the marine environment. *Cambridge environmental chemistry series*. (10) Chapter 4. 2000.

Moran, M. A. and R. G. Zepp. Role of Photoreactions in the Formation of Biologically Labile Compounds from Dissolved Organic Matter. *Limnology and Oceanography*. 42 (6) 1307-1316. 1997.

Moran, M. A. et al. Genome sequence of *Silicibacter pomeroyi* reveals adaptations to the marine environment. *Letters to Nature*. 432: 910-913. 2004.

Moran, M. A. and W. L. Miller. Carbon Biogeochemistry in the Coastal Ocean — Resourceful Heterotrophs. *Nature Reviews Microbiology* (in press), 2007.

Ohta, K. Diurnal Variations of Carbon Monoxide Concentrations in the Equatorial Pacific Upwelling Region. *Journal of Oceanography*. 53: 173-178. 1997.

Pomeroy, L. R. The Ocean's Food Web, A Changing Paradigm. *BioScience*. 24 (9) 499-504. 1974.

Porter, K.G. and Y.S Feig. The Use of DAPI for Identifying and Counting Aquatic Microflora. *Limnology and Oceanography*. 25 (5) 943-948. 1980

Rivas, R. et al. An effective, rapid and simple method for total RNA extraction from bacteria and yeast. *Journal of Microbiological methods*. 47: 59-63. 2001.

Roberts, G. P., H. Y. Youn, and R. L. Kerby. CO-Sensing Mechanisms. *Microbiology and Molecular Biology Reviews*. 68 (3) 453-473. 2004.

Smith, S. V., and J. T. Hollibaugh. Coastal Metabolism and the Oceanic Organic Carbon Balance. *Reviews of Geophysics*. 31 (1) 75-89. 1993.

Stubbins, A., G. Uher, V. Kitidis, C. S. Law, R. C. Upstill-Goddard, and E. M. S. Woodward. The Open-Ocean Source of Atmospheric Carbon Monoxide. *Deep-Sea Research*. 53: 1685-1694. 2006.

Stumm, W. and J. J. Morgan. *Chemical Equilibria and Rate in Natural Waters*. Environmental Science and Technology. 3<sup>rd</sup> Edition. 64. 1996.

Swingley, W. D. et al. The complete genome sequence of *Roseobacter denitrificans* reveals a mixotrophic as opposed to photosynthetic metabolism. *Journal of Bacteriology*. 189: 683-690. 2007.

Swinnerton, J. W., V. J. Linnenbom, and C. H. Cheek. A Sensitive Gas Chromatographic Method for Determining Carbon Monoxide in Seawater. 193-195.

Swinnerton, J. W., V. J. Linnenbom, and R. A. Lamontagne. The Ocean: A Natural Source of Carbon Monoxide. *Science*. 167: 984-986. 1970.

Tolli, J. D. and C. D. Taylor. Biological CO Oxidation in the Sargasso Sea and in Vineyard Sound, Massachusetts. *Limnology and Oceanography*. 50 (4) 1205-1212. 2005.

- Tolli, J. D., S. M. Sievert, and C. D. Taylor. Unexpected Diversity of Bacteria Capable of Carbon Monoxide Oxidation in a Coastal Marine Environment, and Contribution of the *Roseobacter*-Associated Clade to Total CO Oxidation. *Applied Environmental Microbiology*. 72 (3) 1966-1973. 2006.
- Valentine, R. and R. Zepp. Formation of Carbon Monoxide from the Photodegradation of Terrestrial Dissolved Organic Carbon in Natural Waters. *Environ. Sci. Technol.* 27: 409-412. 1993.
- Wiesenburg, D. A. and N. L. Guinasso Jr. Equilibrium Solubilities of Methane, Carbon Monoxide, and Hydrogen in Water and Sea Water. *Journal of Chemical and Engineering Data*. 24 (4) 356-360. 1979.
- Wilson, D. F., J. W. Swinnerton, and R. A. Lamontagne. Production of Carbon Monoxide and Gaseous Hydrocarbons in Seawater: Relation to Dissolved Organic Carbon. *Science*. 168: 1577-1579. 1970.
- Xie, H. et al. A Simple Automated Continuous-Flow-Equilibration Method for Measuring Carbon Monoxide in Seawater. *Environmental Science Technology*. 35: 1475-1480. 2001.
- Xie, H. et al. Validated methods for sampling and headspace analysis of carbon monoxide in seawater. *Marine Chemistry*. 77: 93-108. 2002.
- Xie, H. et al. Biological consumption of carbon monoxide in Delaware Bay, NW Atlantic and Beaufort Sea. *Marine Ecology Progress Series*. 290: 1-14. 2005.
- Zafiriou, O. C., S. S. Andrews, and W. Wang. Concordant Estimates of Oceanic Carbon Monoxide Source and Sink Processes in the Pacific Yield a Balanced Global "Blue-Water" CO Budget. *Global Biogeochemical Cycles*. 17 (1) 15-1-15-13. 2003.
- Zepp, R. G., T. V. Callaghan, and D. J. Erickson. Effects of Enhanced Solar Ultraviolet Radiation on Biogeochemical Cycles. *Journal of Photochemistry and Photobiology*. 46: 69-82. 1998.
- Ziolkowski, L. A. Marine Photochemical Production of Carbon Monoxide. M. Sc. Thesis, Dalhousie University, Halifax, NS, Canada, 121 pp. 2000.
- Zuo, Y. and R. D. Jones. Formation of Carbon Monoxide by Photolysis of Dissolved Marine Organic Material and Its Significance in the Carbon Cycling of the Oceans. *Naturwissenschaften*. 82: 472-474. 1995.

## APPENDICES

### **Appendix A: Extended Methods**

#### **2.2 Bacterial Growth**

##### *2.2.1 Preparing Agar Plates with ½ YTSS Growth Medium*

In a 1000 ml media bottle 1.25g of tryptone, 2g of yeast extract, 10g of sea salts, and 7.5-9g of agar were weighed and combined. The bottle was filled half way with 500 ml of DI water. The bottle was capped loosely and marked with autoclave tape. The mixture was then autoclaved for about an hour at 15 psi on the long liquid cycle. The medium was removed from the autoclave and swirled to distribute the agar thoroughly. The ½ YTSS medium was cooled in a water bath around 50-60°C. The plates were poured directly from the bottle on an ethanol sterilized bench so that the bottom of each plate was covered with medium, ~30-35 ml of medium per 90 mm plate. The medium was allowed to harden over night. After hardening the plates were inverted and stored at 4°C for later use.

##### *2.2.2 Inoculation*

The plates were removed from the 4°C storage and allowed to reach room temperature. They were inoculated with the isolate bacteria *Silicibacter pomeroyi* (DSS-3) by streaking a small amount with a sterile inoculation loop. The bacteria was spread out from the initial inoculation site in one line and streaked across the plate in a zigzag pattern. The loop was sterilized, passed through one of the first streaks, and spread out again. This was repeated twice

turning the plate so that it had three streaked sites. Once inoculated and streaked the plates were incubated at 30°C for 2-3 days until a cultured colony could be seen. The incubated plates were then removed and stored at 4°C to stop bacterial growth.

### *2.2.3 ½ YTSS Liquid Growth Medium*

In a 1000 ml media bottle 1.25g of tryptone, 2g of yeast extract, and 10g of sea salts were weighed and combined. The bottle was filled half way with 500 ml of DI water. The bottle was capped loosely and marked with autoclave tape. The mixture was then autoclaved for about an hour at 15 psi on the long liquid cycle. The ½ YTSS Liquid medium was removed from the autoclave. The medium was cooled in a water bath around 50- 60°C and stored at 4°C. For inoculation a single DSS-3 cell was added to 10 ml of ½ Liquid YTSS and incubated over night.

### *2.2.4 Marine Basal Media*

The Marine Basal Media (MBM) was prepared in three separate containers and combined after autoclaving and sterile filtrating. The FeEDTA Stock Solution was prepared with 50 mg FeEDTA (Ethylenediamine tetraacetic acid; ferric-sodium salt) and 100 ml DI H<sub>2</sub>O and autoclaved. The Basal Media was prepared with 150 ml 1M Tris HCL (pH 7.5), 87 mg K<sub>2</sub>HPO<sub>4</sub>, 1.5 g NH<sub>4</sub>Cl, and 375 ml DI H<sub>2</sub>O. This was autoclaved and stored at room temperature. For the Marine Basal Media (per L) 20 g of Sea Salts were combined with 700 ml DI H<sub>2</sub>O. This solution was autoclaved and 250 ml Basal Media, 50 ml FeEDTA, carbon substrates (1 µM glucose), and an optional 0.1% vitamin supplement were added post-autoclaving once the media had cooled to ~50°C. The glucose was added by sterile filtration. The three separate solutions

were combined for a final volume of 1000 ml of Marine Basal Media. For inoculation of the MBM 10 ml of ½ liquid YTSS/DSS-3 were added and incubated over night, shaken at 30°C.

## **2.3 CO Kettle Incubations**

### *2.3.1 CO Drawdown*

Carbon monoxide drawdown was examined using a sealed 2000 ml Pyrex® glass reaction kettle. Its interchangeable cover had four openings that accommodated three 24/40 joints and one 34/45 joint in the middle. The openings and joints held a thermometer, repipet dispenser, bubbling stick, and CO free air vent. Cover and kettle were clamped to form a tight seal. Room air was pumped through polyethelene drying tubes filled with Schutze Reagent to create CO free air using a Masterflex pump. Pumped air was driven through a three-valve flowmeter connected to the Masterflex pump and a 51.8 ppm ± 5% Scotty Specialty Gases CO tank. The three-valve flowmeter was used to adjust the flow rate of the CO free air and the CO standard gas. Gas running out of the flowmeter was directed through a DI water humidifier flask and into the reaction kettle.

The reaction kettles were allowed to reach equilibrium and set up either with or without inoculated cultures of *Silicibacter pomeroyi* in marine basal media, a liquid growth medium and a seawater environment (Figure 2.1). The kettles were bubbled with or without [CO]. In those kettles bubbled with [CO]-free air, room air was drawn through Schutze® reagent (a chemical CO oxidizer). The question of CO gene expression was answered for each condition. Gas samples were analyzed over a time course and [CO] were measured using a reduced gas, gas

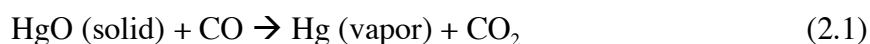
chromatograph. Microbial samples were taken from the media in correlation with the gas time points. RNA was extracted from the microbial samples and CoxL gene expression was measured with PCR.

*Silicibacter pomeroyi* (DSS3) was grown in 1/2 YTSS incubated 2-3 days at 30°C until colonies were present. A single colony was then transferred to 10ml of 1/2 Liquid YTSS and incubated overnight at 30°C shaken. The 10ml of 1/2 Liquid YTSS was added at a 1:100 dilution into 1000 ml of Marine Basal Media (MBM) and incubated overnight at 30°C shaken. The OD was found to be 0.056 suggesting that DSS3 was in a log growth phase. The MBM was added to a kettle and bubbled with a CO/CO free mixture to attain a desired [CO]. To attain a zero [CO] in the MBM CO free air was bubbled through a humidifier flask for at least 10-15 minutes to degas the CO from the DI water in the flask. The humidifier flask was connected to the bubble stick in the kettle and CO free air was allowed to bubble through the kettle for at least 90 minutes to degas the 1000ml kettle and MBM solution.

## **2.4 Gas Chromatography**

To measure [CO] in the headspace, measurements were taken from seawater samples and injected into a gas chromatograph (Figure 2.2). A known volume of seawater (90 ml) was extracted via a gas tight syringe at various time points. CO free air was pulled into the syringe Schutze Reagent to create a known volume of headspace (10 ml) and the syringe was shaken vigorously to equilibrate the headspace and seawater. The syringe was shaken by hand for approximately 30 s to 1 minute, which was found to be sufficient for the two phases in the glass bottle to equilibrate (Conrad, R. et al., 1982). The headspace was injected into a 1 ml stainless steel sample loop of a Reduced Gas Detector Gas Chromatograph (GC) (Figures 2.3 and 2.4).

The GC's temperature and pressure settings remained constant: nitrogen carrier gas, 20 psi; valve, 35 psi; reactor cell, 290°C; reduced gas detector cell, 170°C; column oven, 110°C. The sample loop was designed to load and inject gas samples through a specific path of columns. Passing the sample through a 30'' Unibeads® 1S 60/80 column followed by a 30'' molecular sieve 5A column separated the CO. The CO then passed through a heated mercuric oxide (HgO) reactor, reducing the mercuric oxide to mercury vapor as the CO was oxidized. The CO concentration was detected using the mercury oxide to mercury vapor conversion:



The mercury vapor passed by an ultraviolet (UV) lamp, which sent a voltage signal to a computer. The CO concentration was calculated as a peak area through Peak Simple computer analysis. The resultant peak areas were compared to 1ppm CO standard peaks used to create a standard curve (Table 2.1, Figure 2.5). To calculate the CO concentration in the aqueous solution a two-part calculation was used that accounted for salinity, air to volume ratio in the syringe, and the water temperature. Using the two part equation for calculating CO concentration in an aqueous solution with the Bunsen solubility coefficient the concentration of CO could be measured.

#### *2.4.1 Calculating CO Concentration in an Aqueous Solution*

The Peak Simple program was used to generate peak areas (millivolts) of CO from headspace samples. The peak areas were converted into CO concentration in an aqueous solution (nmol). Using a set of equations by Xie et al, [2002] the CO concentration where calculated in ppmv (part per million by volume) using a set of equations (Appendix A):

$$\{CO\}_w = 10^{-6} \beta m_a p \quad (2.2)$$

$$m_a(\text{ppmv}) = \frac{PA * \text{std}(\text{ppm})}{\text{std}PA} \quad (2.3)$$

$$\{CO\}_{aq} = (\{CO\}_w V_w + 10^{-6} m_a V_a) / V_w \quad (2.4)$$

$$\{CO\}_{aq} = 10^{-6} m_a (\beta p V_w + V_a) / V_w \quad (2.5)$$

$$[CO]_{aq} = \frac{10^9 * p\{CO\}_{aq}}{(RT)} \quad (2.6)$$

### 2.4.2 Limit of Detection

The limit of detection (LOD) of the gas chromatograph was determined from a number of standard curves (Table 2.2). “Schutze Air” produced no measurable peak from the GC therefore the LOD was calculated as where the standard curve crossed the x-axis when a linear best fit line was not constrained to pass through the origin. This value was equated to a carbon monoxide concentration. The standard curve x-intercept values were averaged and standard deviations were calculated. The lower limit of detection (LLD) was determined by multiplying the standard deviation of twelve standard curve x-intercept values by 3.290. This was then defined as the LOD and measured in parts per million (ppm) (Greenberg A.E. et al., 1992).

$$\begin{aligned} y &= mx + b \\ 0 &= mx + b \\ \frac{-b}{m} &= x \\ |x| &= [CO_{LOD}] \end{aligned} \quad (2.7)$$

## 2.5 Preparing RNA for Gene Expression Analysis

### 2.5.1 RNA Extraction

Bacteria samples were collected for RNA extraction at time points in conjunction with the headspace analysis of [CO] in the kettle. To obtain the desired  $2 \times 10^9$  cells concentration of

gram-negative bacteria, 1.5 ml of culture was added to 2.0ml centrifuge tubes. 10% (150  $\mu$ L) phenol ethanol was added to the tubes to maintain the expression for the desired time point, this was called a stop solution because it stopped the RNA expression. This was centrifuged for 10 minutes at 4°C, 5000 rpm. The supernatant was decanted and the pellet stored at -80°C until RNA extraction.

The RNA was extracted using an RNA extraction protocol (RiboPure™-Bacteria Kit) explained briefly as follows. To the pellet 300  $\mu$ L of Lysis/Binding Solution was added and vortexed vigorously. 300  $\mu$ L of 64% ethanol was added to the lysate and mixed by vortex. This lysate/ethanol mixture was added to a filter cartridge and placed in a collection tube. The tube was centrifuged for ~15 sec- 1 min at 10,000-15,000 x g (10,000-14,000 rpm) to pull the fluid through the filter. The flow through was discarded. To the filter 700  $\mu$ L of Wash Solution #1 was added and centrifuged as described previously. The flow through was discarded. Wash Solution #2/3 was added at 500  $\mu$ L to the filter, centrifuged as described, and flow through discarded. This step was repeated once and centrifuged again to pull all fluid through the filter. The filter cartridge was placed into a fresh collection tube of 60  $\mu$ L of warmed Elution Solution (70-80°C) and was pipetted onto the center of the filter. This was centrifuged for ~30 sec at 10,000-15,000 x g (10,000-14,000 rpm) at room temperature to elute the RNA. Another 30  $\mu$ L of warmed Elution Solution was added to the center of the filter and centrifuged as described previously. The flow through was kept and stored at -20°C. The 260/280 was check on the nanodrop for RNA purity.

### 2.5.2 DNA-Free

The extracted RNA was treated with Turbo DNA-free®, removing any DNA before the reverse transcription step. The RNA (90 µL) was thawed on ice. To the extracted RNA, 9 µL of 10x Turbo DNase Buffer and 3 µL of DNase I were added. This was incubated at 37°C for 20 minutes. An additional 3 µL of DNase I was added to the reaction and incubated at 37°C for another 20 minutes. To the reaction 20 µL of DNase Inactivation Reagent was added and incubated at room temperature for 2 minutes, vortexing a few times. The Inactivation Reagent was pelleted by centrifuging at 10,000 x g for 1.5 minutes and the supernatant was transferred to a fresh tube. The nanodrop was used to determine quality and quantity of the RNA and the tubes were stored at -80°C.

### 2.5.3 Primer Design

Primers were designed specifically for the *coxL* gene in *Silicibacter pomeroyi*. Three different primers were designed based on the two known CO oxidizing clades, OMP and BMS (Table 2.3). These clades refer to two specific *coxL* genes within the *S. pomeroyi* genome. When referring to the gene, *coxL* is lowercase and italicized. When referring to the primer sets CoxL, CoxL1, and CoxL2 are uppercase and not italicized. The primers targeted the *coxL1* and *coxL2* genes individually as well as an overall CoxL primer designed to target both. The *coxL1* & *coxL2* genes were sequenced from Roseobase. These two gene sequences were aligned using BioEdit®. For the overall CoxL primer the two gene sequences, *coxL1* and *coxL2*, were aligned through their conserved regions. Conserved regions of around 20 bp were selected for the forward and reverse primers for CoxL. To find primer sets for CoxL1 and CoxL2 the gene sequences were manually searched for areas of conservation for each gene that was not in the

other gene. Degeneracies were used for base pairs specifically in the CoxL primer set that when aligned did not share the same base pair (Table 2.4). All three primer sets were checked for primer dimmers and hairpins in AutoDimer and BLASTed to make sure they did not amplify with any other than *S. pomeroyi*.

After the initial primers sets were designed multiple amplicon bands were detected in the temperature gradients using gel electrophoresis. Specifically double bands were present in the primer sets for the overall CoxL and individual CoxL1. The initial sets designed for *coxL2* did not produce multiple bands in the temperature gradients. New primer sets were designed for the overall *coxL* and *coxL1* genes. The primer sets for the *coxL2* gene remained the same as the initial design.

#### 2.5.4 Reconstitution

Primers were reconstituted into a stock solution and distributed into working solutions for further gene expression analysis using PCR. Adding the correct amount of DEPC (diethylprocarbonate) water a 100  $\mu\text{M}$  concentration stock solution was made. The original oligonucleotide was in nM to get to 100  $\mu\text{M}$  the conversion is  $\text{M}=\text{moles/L}$ , or  $57.20 \text{ nM} = 572 \mu\text{l}$  of added DEPC water. From the stock primer working solutions were made of 100  $\mu\text{L}$  (10 $\mu\text{M}$ ) in 0.5 ml microcentrifuge tubes. Working solutions were made for each primer set used.

#### 2.5.5 Optimizing Primers

The primer sets were optimized to find the best melting temperature ( $T_m$ ) for the set. The optimization temperature range was calculated from the lowest  $T_m$  in the primer set, then subtracting 8°C from the lower range and adding 2°C to the upper range so that the gradient

ranges over 10°C. (ex: CoxL f=59.7, CoxL r=65.4 so the range is from 52-62°C). The PCR was set up for a gradient of temperatures and approximately five temperatures were picked for each primer set. Each of the 12 columns in the gradient PCR was designated with a specific temperature. The temperatures for each primer set were recorded and the final PCR was run on a gel to look for the optimum temperature. The optimum temperature for each primer set was determined by the best presence of the amplicon bands run on the gel.

### *2.5.6 Reverse Transcription*

The SuperScript™ III RT protocol was followed for reverse transcription creating cDNA for PCR analysis. 1 µL of reverse primer, 10 µL of RNA, and 1 µL of dNTP mix were added to a nuclease-free microcentrifuge and heated to 65°C for 5 minutes and then chilled on ice. The contents of the tube were collected by centrifugation. Added to the tube were 4 µL of 5x First-Strand Buffer, 2 µL of 0.1 M DTT, and 1 µL of RnaseOut™. The tubes were mixed gently and incubated at 42°C for 2 minutes. 1 µL of SuperScript™ III RT was added to the tube and mixed by pipetting up and down. This mixture was then incubated at 42°C for 50 minutes and the reaction was inactivated by heating to 70°C for 15 minutes. Two negative controls were carried out, one with no RNA added to the mixture and the other with no RT step carried out to check for DNA contamination. For the negative control with no RT step, the reaction was heated to 70°C for 15 minutes initially and then to 42°C for 50 minutes.

## **2.6 Polymerase Chain Reaction**

A puReTaq Ready-To-GO PCR bead was used for PCR analysis. The room temperature stable bead contained the following components: stabilizers, BSA, dATP, dCTP, dGTP, dTTP,

~2.4 units of puReTaq DAN polymerase and reaction buffer. In a master mix the primer pairs for CoxL, CoxL1, and CoxL2 were added along with the cDNA (RT) and water. For each reaction 1 $\mu$ L of the corresponding forward and reverse primers, 1 $\mu$ L of cDNA, and 22 $\mu$ L of sterile high-quality water were added to a microcentrifuge tube. This mixture was the master mix from which it was divided into the PCR bead tubes at 25 $\mu$ L. The cDNA (DSS3) was run through PCR using a standard protocol; Run 1 at 95.0°C for 3:00 minutes, Run 2 at 95.0°C for 0:30 seconds, Run 3 at the optimum temperature for the primer for 0:30 seconds, Run 4 at 72.0°C for 0:30 seconds, Run 5 at Go to step 2 for 35 times, Run 6 72.0°C for 10:00 minutes, and Run 7 at 4.0°C for ever. The final PCR products were run on a gel to look for the presence/absence of CoxL gene expression.

## **2.7 Gel Electrophoresis**

When running a large number of samples (~20 wells per comb), a large gel was prepared. In a glass flask, 100 ml of 1x TAE buffer and 2.0 g of agarose were added to make a 2% agarose gel. This solution was microwaved until it boiled (~1-2minutes) or until the agarose was dissolved. Three drops of ethidium bromide were added to the agarose/buffer solution and swirled. The solution was poured to set the gel (~10-15 minutes) with two a well combs inserted.

When running a small number of samples (~12 wells per comb), a small gel was prepared. In a glass flask 40 ml of 1 x TAE buffer and 0.8 g of agarose were added to make a 2% agarose gel. The solution was microwaved until all agarose was dissolved ~1 minute. Two drops of ethidium bromide were added to the agarose/buffer solution and swirled. The solution was poured to set the gel with an inserted well comb.

From the PCR ~5  $\mu\text{L}$  of loading dye was added to each sample (for ~25  $\mu\text{L}$  of sample). The samples were loaded into the gel wells (~15  $\mu\text{L}$ ). An appropriate ladder was also run in the gel (~10  $\mu\text{L}$ ) that was within the base pair range for the amplicon. The gel was run at 100 volts for 60 minutes for the large gel and 100 volts for 40 minutes for the small gel. Photographs were taken in a UV chamber to see the bands on the gel. The presence or absence of bands and the desired amplicon size was analyzed for gene expression.

## **2.8 Bacterial Counts Using DAPI**

Samples were taken of *S. pomeroyi* (DSS-3) in MBM from the kettle incubation to obtain direct counts of bacterial cell numbers for determination of CO drawdown rates per cell. At time points corresponding to samples taken for [CO] and RNA extraction, 5 ml of MBM with *Silicibacter pomeroyi* (DSS-3) was preserved in 6% buffered formalin. The buffered formalin was prepared by adding borate to formaldehyde until it became supersaturated. This solution was filtered into a dark glass bottle and stored at room temperature in the dark. The samples of culture and formalin were stored in the dark at 4°C.

The cells were later filtered and stained with DAPI for counting. A 16 mm filtration column was used to vacuum filter the appropriate volume of diluted culture onto a 0.2  $\mu\text{m}$  pore size, black membrane Poretics polycarbonate filter. The filter was kept on the filter holder while a working DAPI solution was added at a volume enough to cover the cells. A working DAPI solution was prepared by adding 25  $\mu\text{L}$  of the stock solution at 5 mg/ml to 50 ml of filtered DI water giving a final concentration of 2.5  $\mu\text{g/ml}$ . The tower was covered with aluminum foil and the cells incubated with DAPI for 5 minutes. The remaining liquid was pulled through the filter column by vacuum and the column rinsed to filter excess DAPI and loose cells with filtered DI

water. The column was stored in alcohol for later use. The filter was placed onto a slide, a drop of immersion oil was added, and covered with a coverslip. The slides were stored in the dark at 4° for immediate counting or -20°C for a more permanent storage of the samples.

A fluorescence microscope was used to count the cells and allowed to warm up for 15 minutes. A drop of immersion oil was placed onto the coverslip of the slide. The cells were examined under the highest magnification (100x) with a DAPI light filter. The cells were counted in the entire grid for at least 10 fields of view. The number of cells counted in each sample was then extrapolated to a spreadsheet and with the volume of the column and volume of sample added the bacterial concentration was determined.

## Appendix B: Calculating the Carbon Monoxide Concentration in Water

The peak areas (millions of volts) of CO in the headspace were converted to carbon monoxide concentration in the water (nmol/l) using a multi-part calculation. First the CO concentration in the headspace (ppmv) was calculated:

$$\{CO\}_w = 10^{-6} \beta m_a p$$

$$m_a = \frac{PA * std(ppm)}{stdPA}$$

where  $\{CO\}_w$  is the dissolved CO concentration in ml CO/ml H<sub>2</sub>O,  $\beta$  is the Bunsen solubility coefficient of CO, and  $p$  is atmospheric pressure (atm) of dry air.  $PA$  is the peak area measured for a sample,  $std(ppm)$  is the CO concentration of the standard (ppmv),  $stdPA$  is the measured standard peak area (millions of counts). The CO concentration was then converted to units of nM CO in the water using the following equations:

$$\{CO\}_{aq} = (\{CO\}_w V_w + 10^{-6} m_a V_a) / V_w$$

$$\{CO\}_{aq} = 10^{-6} m_a (\beta p V_w + V_a) / V_w$$

$$[CO]_{aq} = \frac{10^9 * p \{CO\}_{aq}}{(RT)}$$

where  $\{CO\}_{aq}$  is the initial concentration of CO in seawater in ml CO/ml H<sub>2</sub>O,  $V_w$  is the water sample volume (ml),  $V_a$  is the volume of headspace air (ml),  $[CO]_{aq}$  is the concentration of CO in seawater in nM,  $R$  is the gas constant (0.08206 atm 1 mol<sup>-1</sup> K<sup>-1</sup>), and  $T$  is temperature (K). The atmospheric pressure ( $p$ ) was assumed to remain constant at 1 atmosphere (Xie et al., 2002). The Bunsen solubility coefficient ( $\beta$ , dimensionless) is a function of temperature and salinity

according to the equation in Appendix C. For the purpose of these calculations the Bunsen coefficient ranged in accordance with changes in both the salinity and temperature. The Weisenburg and Guinasso [1979] equation was extrapolated to fit salinity and temperatures used over this experiment.

### Appendix C: Calculating the Bunsen Coefficient for Carbon Monoxide

Bunsen Coefficient: (Weisenburg and Guinasso, 1979).

$$\ln\beta = A_1 + A_2(100/T) + A_3 \ln(T/100) + S[B_1 + B_2(T/100) + B_3(T/100)^2]$$

Temp	Salinity parts per thousand									
	0	10	20	22	24	26	28	30	32	34
-2	0.03748	0.03524	0.03313	0.03272	0.03232	0.03193	0.03154	0.03115	0.03077	0.03039
-1	0.03654	0.03437	0.03232	0.03193	0.03154	0.03115	0.03077	0.03040	0.03002	0.02966
0	0.03565	0.03353	0.03154	0.03116	0.03078	0.03041	0.03004	0.02967	0.02931	0.02896
1	0.03479	0.03273	0.03080	0.03043	0.03006	0.02970	0.02934	0.02898	0.02863	0.02829
2	0.03396	0.03197	0.03009	0.02973	0.02937	0.02902	0.02867	0.02832	0.02798	0.02765
3	0.03317	0.03123	0.02941	0.02906	0.02871	0.02837	0.02803	0.02769	0.02736	0.02703
4	0.03241	0.03053	0.02876	0.02841	0.02807	0.02774	0.02741	0.02708	0.02676	0.02644
5	0.03168	0.02985	0.02813	0.02780	0.02747	0.02714	0.02682	0.02650	0.02619	0.02588
6	0.03098	0.02921	0.02753	0.02720	0.02688	0.02657	0.02626	0.02595	0.02564	0.02534
8	0.02967	0.02798	0.02640	0.02609	0.02579	0.02549	0.02519	0.02490	0.02461	0.02433
10	0.02845	0.02686	0.02536	0.02507	0.02478	0.02450	0.02422	0.02394	0.02367	0.02340
12	0.02732	0.02582	0.02440	0.02412	0.02385	0.02358	0.02332	0.02306	0.02280	0.02254
14	0.02628	0.02486	0.02351	0.02325	0.02300	0.02274	0.02249	0.02224	0.02199	0.02175
16	0.02531	0.02397	0.02270	0.02245	0.02221	0.02196	0.02173	0.02149	0.02126	0.02103
18	0.02442	0.02315	0.02194	0.02171	0.02148	0.02125	0.02102	0.02080	0.02058	0.02036
20	0.02359	0.02238	0.02124	0.02102	0.02080	0.02058	0.02037	0.02016	0.01995	0.01974
22	0.02281	0.02168	0.02060	0.02039	0.02018	0.01997	0.01977	0.01957	0.01937	0.01917
24	0.02209	0.02102	0.02000	0.01980	0.01960	0.01941	0.01922	0.01903	0.01884	0.01865
26	0.02142	0.02041	0.01944	0.01926	0.01907	0.01889	0.01870	0.01852	0.01835	0.01817
28	0.02080	0.01984	0.01893	0.01875	0.01858	0.01841	0.01823	0.01806	0.01789	0.01773
30	0.02022	0.01932	0.01846	0.01829	0.01812	0.01796	0.01780	0.01764	0.01748	0.01732
32	0.01968	0.01883	0.01802	0.01786	0.01771	0.01755	0.01740	0.01724	0.01709	0.01694
34	0.01917	0.01838	0.01761	0.01747	0.01732	0.01717	0.01703	0.01688	0.01674	0.01660
36	0.01870	0.01796	0.01724	0.01710	0.01696	0.01682	0.01669	0.01655	0.01642	0.01628

The Bunsen Coefficient was taken from Weisenburg and Guinasso [1979] and expanded for the temperature and salinity ranges used in this paper. Temperature and salinity were narrowed to more specific values than those found for CO calculations by Weisenburg and Guinasso [1979]. As seen from the table large changes in salinity seem to not affect the Bunsen Coefficient as much as changes down the columns in temperature. The Bunsen Coefficients used in the calculation of CO in seawater media in the range of 22-24°C for temperature and range of 25-28‰ for salinity.

**Appendix D: Calculating Bacterial Cells from DAPI Counts**

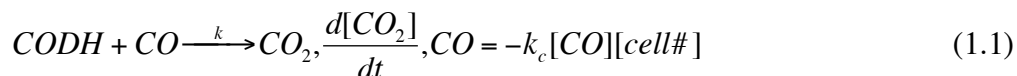
The number of bacteria cells were counted using the fluorescent stain 4',6-diamidino-2-phenylindole (DAPI) and a fluorescence microscope. The total number of *Silicibacter pomeroyi* cells in a given volume was calculated with the following equation:

$$(\bar{N} * (\Pi r^2)) / (9900 * V)$$

Where N is equal to the average number of bacteria counted in the grid, the radius is the area of filtered material found from the tower diameter in  $\mu\text{m}^2$  multiplied by the magnification (100x), and V is equal to the sample volume measured in ml.

### Appendix E: Calculating the Cell Normalized CO Oxidation Rate

The cell normalized CO oxidation rate was calculated by plotting against time the natural log of [CO] at time  $t$  divided by [CO] at time zero. This calculation was carried out for each approximated time point for Supplementary Figure S2 (Moran et al., 2004). Solving equation 3.3 for  $k$  to determine the oxidation rate constant results in:



$$\frac{d[CO]}{dt} = -k[CO] \quad (1.2)$$

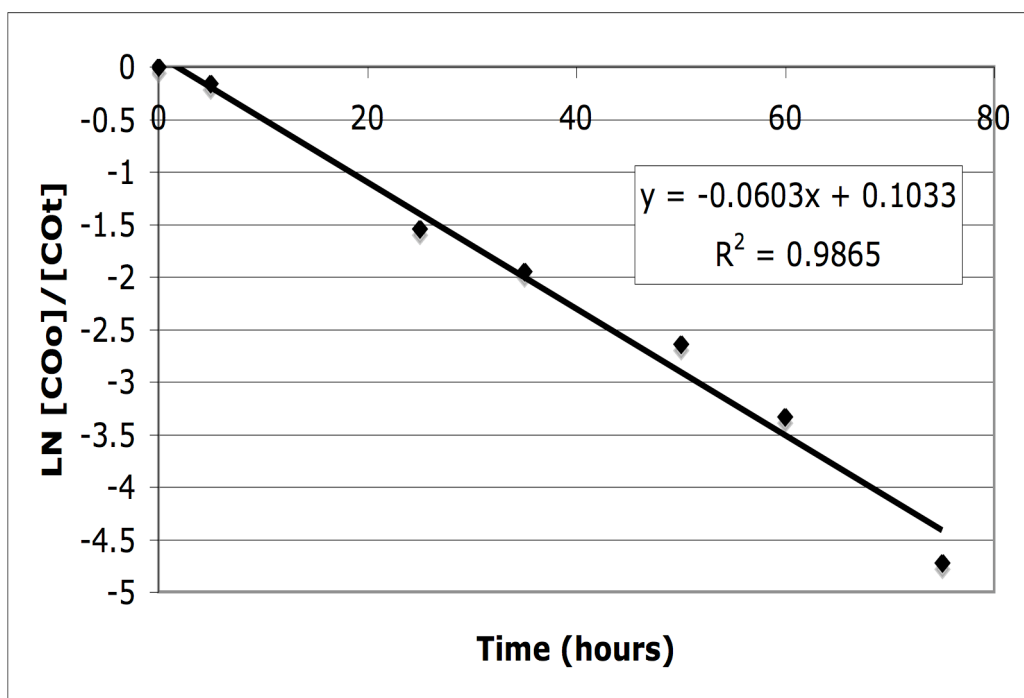
$$[CO]_t = -k[CO]_0 e^{-kt} \quad (1.3)$$

$$\ln \left[ \frac{CO_t}{CO_o} \right] = -kt \quad (1.4)$$

Where A is the changing variable, for this study CO,  $k$  is the rate constant, P is the product, and  $t$  is time. This equation was then plotted as CO concentration versus time. The oxidation rate constant  $k$  was then determined from the slope of the best linear fit to the data and it was then divided by the average number of bacterial cells counted per ml, giving a cell normalized CO oxidation rate in units of milliliters per cell per hour. The OD was 1 at 600 nm absorbance, 100 times as much as the OD for the bacterial counts in this study. A bacterial cell population was then estimated assuming the cell population in Moran et al. [2004] was 100 times large than the cell population counted in Experiment 2 ( $2.7 \times 10^9$ ). The rate constant was found to be  $0.0603 \text{ h}^{-1}$ . Dividing the CO oxidation rate constant by *S. pomeroyi* the cell normalized oxidation rate found to be  $2.23 \times 10^{-11} \text{ ml cell}^{-1} \text{ h}^{-1}$ .

Appendix E, Table 1.1: Carbon monoxide oxidation rate by *S. pomeroyi*.

<b>Time (hours)</b>	<b>Average Estimated [CO]</b>	<b>LN [Co<sub>t</sub>]/[CO<sub>0</sub>]</b>
0	11.22	0
5	9.61	-0.1549
25	2.4	-1.5423
35	1.6	-1.9477
50	0.8	-2.6408
60	0.4	-3.3340
75	0.1	-4.7203



Appendix E, Figure 1.1: Carbon monoxide oxidation rate by *S. pomeroyi*. The rate constant  $k$  was found for Supplementary Figure S2 (Moran et al., 2004) to be the slope of the line,  $k=0.0603$ .